AD-A134 312 FORECASTERS HANDBOOK FOR THE MIDDLE EAST/ARABIAN SEA (U) OCEAN DATA SYSTEMS INC MONTEREY CALIF W E HUBERT ET AL. JUN 83 NEPRF-CR-83-06 1/3

UNCLASSIFIED N00228-82-C-6433 F/G 4/2 NL

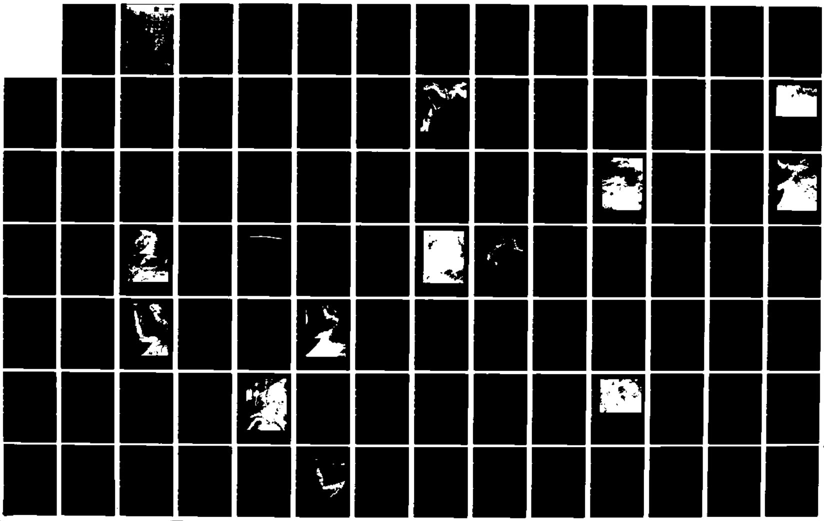

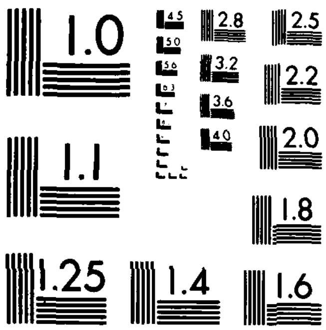

MICROCOPY RESOLUTION TEST CHART
NATIONAL BUREAU OF STANDARDS-1963-A

NAVENVPREDRSCHFAC
CONTRACTOR REPORT
CR 83-06

FORECASTERS HANDBOOK FOR THE MIDDLE EAST/ARABIAN SEA

Prepared By:

W.E. Hubert, A.N. Hull and D.R. Morford
Ocean Data Systems, Inc.
Monterey, California 93940

and

R.E. Englebretson
Science Applications, Inc.
Monterey, California 93940

Contract No. N00228-82-C-[illegible]

JUNE 1983

UNCLASSIFIED

SECURITY CLASSIFICATION OF THIS PAGE (When Data Entered)

(12)

REPORT DOCUMENTATION PAGE

READ INSTRUCTIONS BEFORE COMPLETING FORM

1. REPORT NUMBER NAVENVPREDRSCHFAC Contractor Report CR 83-06	2. GOVT ACCESSION NO. A134312	3. RECIPIENT'S CATALOG NUMBER
4. TITLE (and Subtitle) FORECASTERS HANDBOOK FOR THE MIDDLE EAST/ARABIAN SEA		5. TYPE OF REPORT & PERIOD COVERED Final
		6. PERFORMING ORG. REPORT NUMBER
7. AUTHOR(s) W.E. Hubert, A.N. Hull, D.R. Morford* R.E. Englebretson**		8. CONTRACT OR GRANT NUMBER(s) N00228-82-C-6433
9. PERFORMING ORGANIZATION NAME AND ADDRESS Ocean Data Systems, Inc. (ODSI) 2400 Garden Road Monterey, California 93940		10. PROGRAM ELEMENT, PROJECT, TASK AREA & WORK UNIT NUMBERS O,M, & N-1
11. CONTROLLING OFFICE NAME AND ADDRESS Naval Oceanography Command NSTL Station Bay St. Louis, MS 39529		12. REPORT DATE June 1983
		13. NUMBER OF PAGES 226
14. MONITORING AGENCY NAME & ADDRESS(if different from Controlling Office) Naval Environmental Prediction Research Facility Monterey, California 93940		15. SECURITY CLASS. (of this report) UNCLASSIFIED
		15a. DECLASSIFICATION/DOWNGRADING SCHEDULE

16. DISTRIBUTION STATEMENT (of this Report)

Approved for public release; distribution unlimited.

17. DISTRIBUTION STATEMENT (of the abstract entered in Block 20, if different from Report)

18. SUPPLEMENTARY NOTES

Affiliations: *ODSI, Monterey, CA 93940
**Science Applications, Inc. (SAI), Monterey, CA 93940

(See Reverse)

19. KEY WORDS (Continue on reverse side if necessary and identify by block number)

Tropical meteorology	Arabian Sea	Arabian Peninsula	Forecasting
Monsoon meteorology	Red Sea	Somali Jet	Northeast monsoon
Satellite meteorology	Persian Gulf	Shamal	Onset vortex
Marine meteorology	Gulf of Oman	Tropical Easterly Jet	Monsoon surge
Indian Ocean	Gulf of Aden	Southwest monsoon	Tropical cyclone
			Upwelling

20. ABSTRACT (Continue on reverse side if necessary and identify by block number)

A literature search was conducted with the objective of assimilating information from widely diverse sources to provide the operational Navy forecaster with a single reference text for the Arabian Sea area and the approaches thereto. Navy forecasters were interviewed to determine typical problems and deficiencies in support, and to obtain forecasting RULES/AIDS developed through experience.

(See Reverse)

DD FORM 1 JAN 73 1473 EDITION OF 1 NOV 65 IS OBSOLETE

S/N 0102-014-6601

UNCLASSIFIED

SECURITY CLASSIFICATION OF THIS PAGE (When Data Entered)

18. SUPPLEMENTARY NOTES (Continued)

Qualified requestors may obtain additional copies from the Defense Technical Information Center (DTIC); others apply to National Technical Information Service (NTIS).

20. ABSTRACT (Continued)

The approach adopted has been to describe and discuss the weather patterns which are typical of the two monsoon seasons and the transition seasons between the monsoons. Significant severe weather events are described in the section treating the season in which they are most common. A final section which addresses the effects of the regional weather on specific military evolutions is included. Satellite imagery, selected climatology and illustrative graphics augment the text. Satellite data interpretation techniques applicable to the region are discussed in an appendix.

TABLE OF CONTENTS

LIST OF FIGURES

LIST OF FIGURES (continued)

LIST OF FIGURES (continued)

LIST OF FIGURES (continued)

LIST OF FIGURES (continued)

LIST OF TABLES

FOREWORD

This Forecasters Handbook for the Middle East/Arabian Sea was developed under the Naval Environmental Prediction Research Facility's continuing effort to improve the quality of naval environmental support in all parts of the world.

Several excellent handbooks have been written covering portions of this vital area of interest; the purpose here is to present the most pertinent information available from many sources in a format suitable for use by Fleet forecasters who are unfamiliar with this region. Considerable emphasis is placed on operationally-oriented forecast rules/aids and climatological charts containing parameters related directly to operational decision-making. Wherever possible, satellite imagery is used to demonstrate and clarify key points.

It is intended that this document be responsive to current requirements of U.S. Navy operating forces; it has therefore been assembled in loose-leaf form. Users are urged to submit to this Command their comments and suggestions regarding contents and changes thereto.

The Forecasters Handbook for the Middle East/Arabian Sea was prepared by CAPT William E. Hubert (USN, Ret.), Dr. Arthur N. Hull, and CAPT Dean R. Morford (USN, Ret.), of Global Weather Dynamics, Inc. and LCDR Ronald E. Englebretson (USN, Ret.) of Science Applications, Inc. Mr. Samson Brand of the NAVENVPREDRSCHFAC staff served as Project Coordinator. The Handbook was tasked and funded by the Commander, Naval Oceanography Command, to meet fleet requirements.

Kenneth L. Van Sickle
Captain, U.S. Navy
Commanding Officer

PREFACE

The Middle East is a major source of the world's petroleum supply and the Arabian Sea encompasses the shipping routes used to distribute most of this critical resource. The future status of this vital source of fuel is uncertain because of political unrest in the region. For this reason it is likely that the U.S. Navy will maintain a presence here for some time and that naval forces will require the best possible environmental forecast support to maximize operational effectiveness.

Environmental forecasting in the Middle East/Arabian Sea area is a demanding task even for the most experienced forecaster. Global products from the new NOGAPS model being run at the Fleet Numerical Oceanography Center (FNOC) in Monterey promise to improve basic guidance in this region; however, the Fleet forecaster still has ultimate responsibility for the detailed prediction needed to support specific evolutions. Unfortunately, many Navy meteorologists faced with this important responsibility are serving their first tour in this environmentally unique region. Their problems are further complicated by a relative scarcity of good synoptic observations -- particularly at upper levels in the atmosphere.

This Handbook is written for both "first time" and "old hand" Middle East/Arabian Sea forecasters and is designed to serve, as nearly as possible, as a reference text for support of naval operations anywhere within the area of interest. Since many Navy units now have (or are scheduled to receive) satellite readout and display equipment, considerable attention is devoted to interpretation of satellite data as they apply to a particular phenomenon.

No original meteorological/oceanographic research was involved in preparation of this Handbook; however, climatological information is presented in formats which may be new to the user. Furthermore, the authors' wide experience in Fleet environmental services has been used to translate works from many researchers into operationally-oriented forecast rules and aids.

1.0 GENERAL INTRODUCTION

1.1 Objectives

The objectives of this Handbook are to:

a. Provide operational forecasters with a single reference text of information on the Middle East/Arabian Sea.

b. Organize the material for easy access to self-contained sections dealing with a particular season of the year, location and weather phenomenon.

c. Include unique, seasonal climatological charts containing operationally meaningful parameters.

d. Employ satellite imagery and graphics to illustrate discussions of operationally important phenomena.

e. List FORECAST RULES/AIDS which have direct application to naval operational planning, tactics and daily operations.

f. Identify pertinent and more detailed sources of information in the References Section.

g. Attach supplemental data/information from various sources as Appendices.

1.2 Approach

The following stepwise approach was used to develop this Handbook:

a. Pertinent reference material was assembled from all available U.S. and Middle East Sources.

b. Naval Oceanographic Command personnel who have had recent Middle East/Arabian Sea experience were interviewed to determine realistic requirements for Handbook content.

c. Task Force "cruise reports" were reviewed to determine major problems encountered during Middle East/Arabian Sea deployments.

d. An operationally-oriented outline was stratified by: (1) Monsoon Regime (Season), (2) Geographical Area and (3) Meteorological/ Oceanographic Phenomenon.

e. Satellite images and graphics were carefully selected to illustrate/amplify key phenomena.

f. FORECAST RULES/AIDS which have proven application to identifiable situations were compiled at the end of each Section.

g. Clear and concise text was produced to relate rules, illustrations, data and reference material to current forecasting requirements.

Concurrently with the writing of this Handbook, the Naval Environmental Prediction Research Facility (NAVENVPREDRSCHFAC or NEPRF) is preparing a detailed analysis of the relationship between features appearing in satellite imagery and specific weather phenomena in the Middle East region (Fett et al., 1983); it will be published as Volume 5 of the Navy Tactical Applications Guide series. A determined effort was made to extract valuable new information contained in this specialized NEPRF document and to adapt it to the format and purpose of this Handbook without undue duplication. The authors' goal throughout has been to include only material WHICH TELLS THE OPERATIONAL FORECASTER SOMETHING HE NEEDS TO KNOW.

1.3 Data Sources

Primary data sources were the large technical libraries maintained by NEPRF and the Naval Postgraduate School in Monterey, California. Of particular importance were publications produced by NEPRF, the Naval Oceanography Command and their organizational predecessors.

Two additional data sources were used to obtain reference material for this Handbook:

a. U.S. civilian marine forecasters working in Saudi Arabia under contract to the Meteorology and Environmental Protection Administration (MEPA) collected pertinent documents from local offices.

b. The Saudi Arabian Center for Science and Technology conducted an on-line computer search of U.S. and Saudi Arabian data bases. (Fifty-two unique references were identified.)

Finally, satellite photos were obtained from files maintained at NEPRF. Whenever possible, Defense Meteorological Satellite Program (DMSP) imagery was used because of its superior quality.

1.4. Organization and Content

This Handbook was organized so that the user can refer directly to the season(s) applicable to his deployment without reading the entire document. Because monsoonal flow dominates most of the region, four typical seasons of unequal duration were selected: Southwest Monsoon Regime (Jun - Sep), Fall Transition (Oct - Nov), Northeast Monsoon Regime (Dec - Mar) and Spring Transition (Apr - May). A separate section is devoted to each of these seasons.

At the request of Navy meteorological personnel, Section 7 entitled SPECIAL FORECAST RULES/AIDS presents material of interest to specific Navy operations of a special nature.

Since interviews revealed that some naval units did not have a good initial outfitting of documents on board, and some were unaware of broadcast sources in this area, a recommended list of publications and basic broadcast sources are contained in the Appendices. Satellite imagery interpretation guidance pertinent to the area of interest constitutes the final Appendix (C).

In order to increase the usefulness of this Handbook, it is recommended that users insert supplementary material acquired through experience which amplifies, updates or corrects the information contained herein.

2.0 CHARACTERISTICS OF THE REGION

2.1 Geography

Figure 2-1 is a locator map showing major political and geographical features referred to in this document. The only geographical areas discussed in the text not shown in this figure are the "Atlantic Approaches" around South Africa, the eastern portion of the Bay of Bengal and the "Pacific Approaches" from the South China Sea and Australia. The water areas of the North Indian Ocean are arbitrarily divided into zones for purposes of identification. The names assigned to these zones are used throughout the Handbook when describing the specific weather and oceanographic phenomena. Figure 2-2 shows the locations of cities and small geographical features used as reference points in the text.

2.2 Topography

Figure 2-3 shows a simplified picture of the land elevations which characterize the region covered by this Handbook. The orography is very complex with massive ranges to the north and west (Caucasus, Zagros and Himalayan mountains in Asia and Ethiopian/Kenya Highlands in Africa), a major coastal range northeast of the Red Sea and north of the Gulf of Aden (Hejaz Asia), coastal ranges along both shores of the Gulf of Oman (Hajar and Makran Mountains), a significant range along the west coast of India (Western Ghats) and major desert areas in India, Iran, Iraq, the Arabian Peninsula and North Africa. Various satellite photos contained in the body of the Handbook show different geographic features on relatively clear days. These photos illustrate the complexity of land/sea boundaries and differences in reflectivity between deserts and mountains.

2.3 Bathymetry

Figure 2-4 shows representative contours of water depths within the Red Sea and Persian Gulf. Of particular interest to naval operations are: (a) the deep canyons along the central axis of the Red Sea, and (b) the extremely shallow

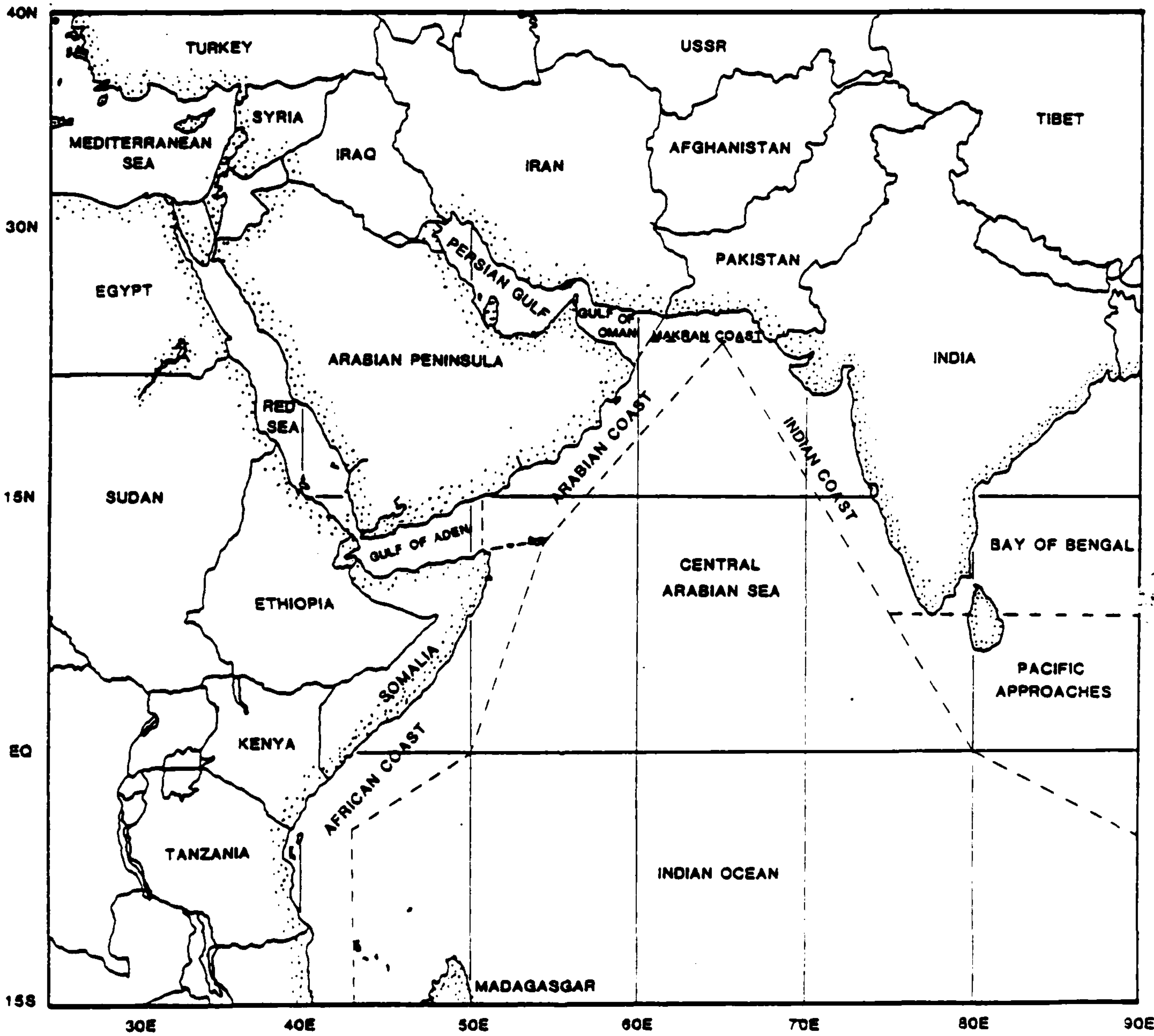

Figure 2-1. Major political and geographical boundaries of the region. Dotted boundaries over water identify zones referenced in this Handbook.

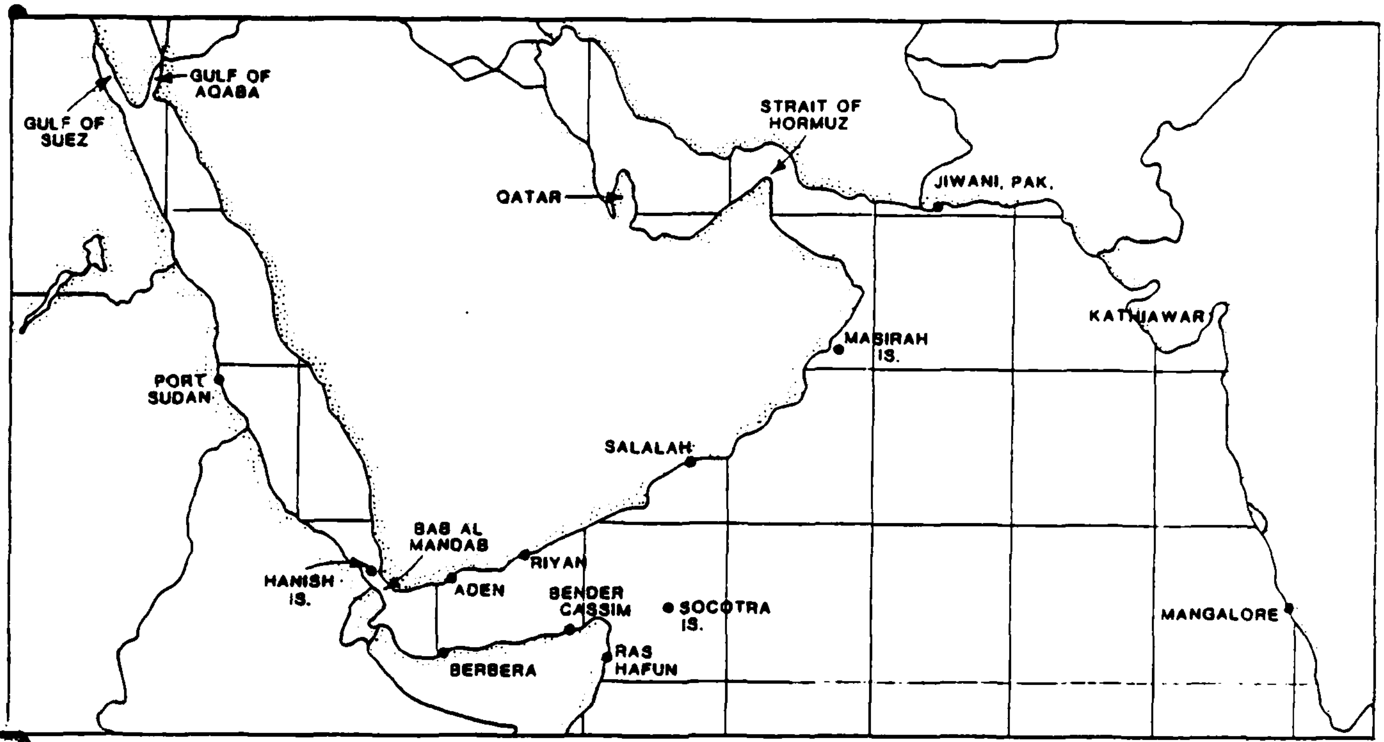

Figure 2-2. Locations of cities and geographical features referenced in the text.

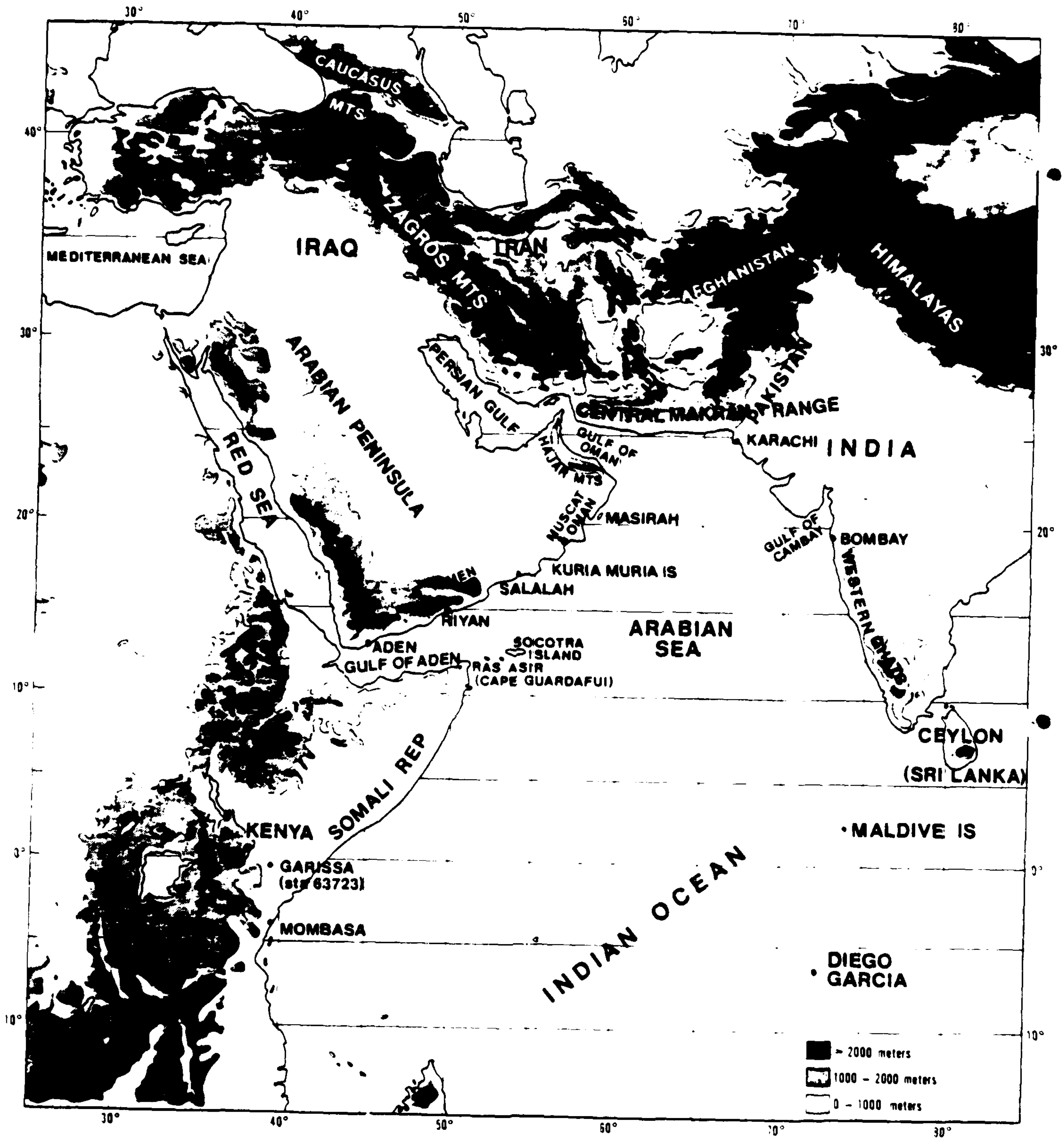

Figure 2-3. Major topographical features of the region. Several islands and cities referenced in the Handbook are also shown (from Brody, 1977).

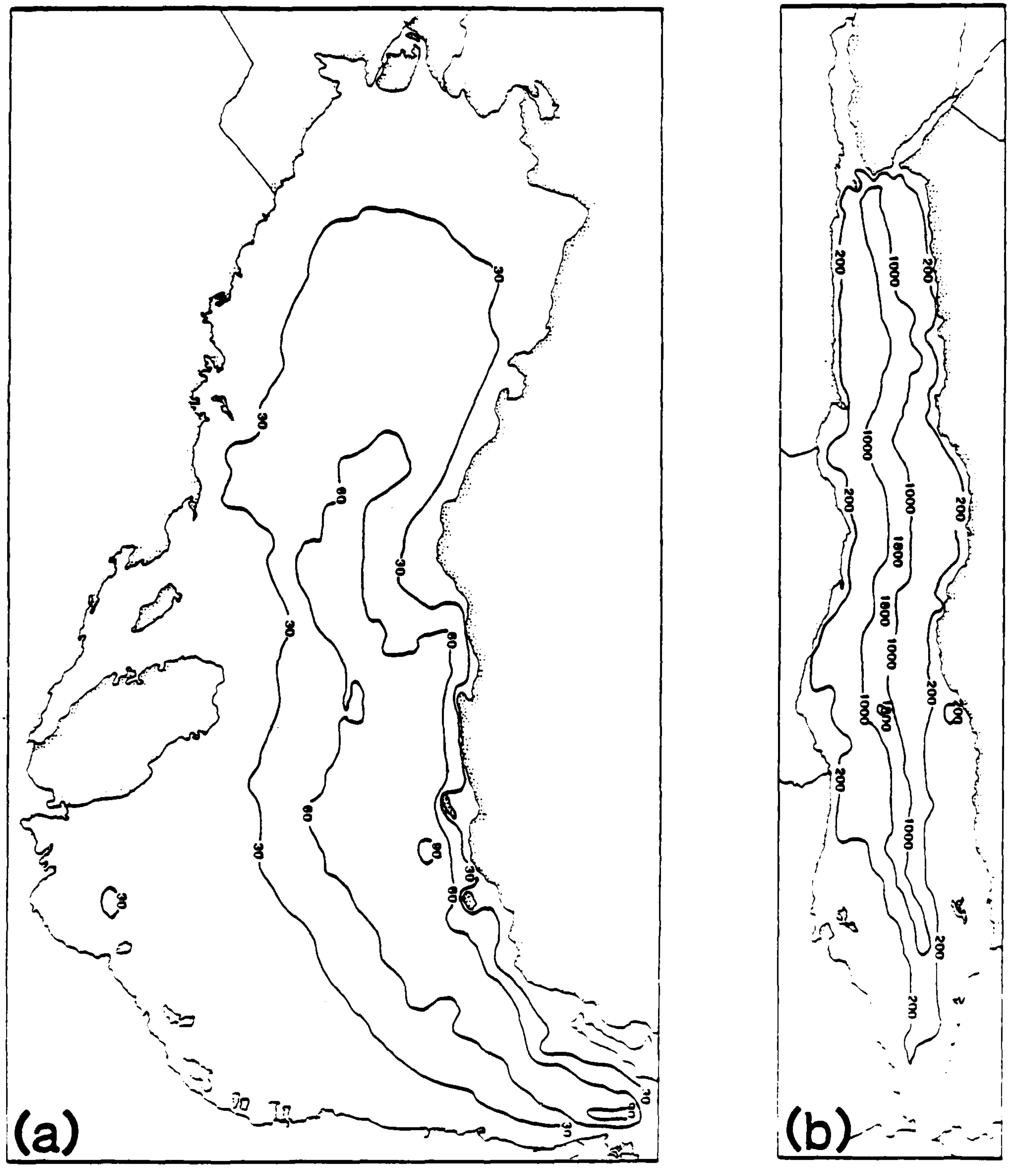

Figure 2-4. Bathymetry of the Persian Gulf (a) and the Red Sea (b). Contours indicate depth in meters.

water found throughout the Persian Gulf. Water depths in the Persian Gulf not only cause abnormal sound speed profiles but also affect wave growth/propagation due to bottom friction. The fact that the Red Sea and Persian Gulf are nearly enclosed bodies of water reduces astronomical tidal variations in these areas but increases the wind stress effect known as "water pileup" (analogous to "storm surge" along open coasts).

2.4 Monsoon Regimes

A set of criteria to determine whether the flow over a region is "monsoonal" has been given by Ramage (1971), who defines the monsoon area as encompassing those locations with January and July surface circulations in which:

a. The prevailing wind direction shifts by at least 120° between January and July;

b. The average frequency of occurrence of prevailing wind directions in both January and July exceeds 40%;

c. The mean resultant wind speeds in at least one of these two months exceed 3 m/s (6 kt);

d. Fewer than one cyclone/anticyclone alternation occurs every two years in either January or July in any 5° latitude/longitude rectangle. (This last criterion excludes areas in which the seasonal wind shift only reflects a change in the mean tracks of moving synoptic systems.)

Since most of the area covered by this document satisfies Ramage's criteria, this Handbook is organized on the basis of Monsoon Regimes and Transition Periods between regimes.

The fundamental cause of seasonal variations in monsoonal flow is strong temperature differences between land and sea. In summer, intense heat lows develop over the land masses surrounding the Arabian Sea. Since the air over the water is cooler than that over land, a pressure gradient is established which causes a low-level flow from water toward land. The result is the Southwest Monsoon at the surface. Upper level flow is strong from the east. In summer, the polar front jet stream is mostly at higher latitudes and the Caucasus/Zagros/Himalayan mountain chain effectively blocks outbreaks of shallow, colder

air masses from northerly sources. Topographic features thus augment intensification of the heat lows and the intensity of the Southwest Monsoon.

In winter, the surface air over the surrounding land masses (particularly in the northern part of the area) is generally colder than that over the Arabian Sea. As a result, a low-level pressure gradient is established which causes surface air to flow from land to sea; this results in the Northeast Monsoon. Upper level flow is generally westerly. Although deeper cold air masses from northerly latitudes do sometimes influence this area in winter, the mountain barriers block most invasions, thereby causing the land/sea temperature differences to be weaker than in summer. As a result, Northeast Monsoon winds are weaker than those during the Southwest Monsoon.

There are basically four seasons associated with the monsoonal flow patterns over the Middle East/Arabian Sea (see Fett et al., 1983, for discussion):

a. The Southwest Monsoon Regime (June through September)
b. The Fall Transition Period (October and November)
c. The Northeast Monsoon Regime (December through March)
d. The Spring Transition Period (April and May)

It should be realized that the periods of time shown for these seasons represent average conditions. The onset and duration of the seasons may vary considerably from year to year, but this breakdown is used to structure this Handbook so that the user may refer only to those chapters pertinent to the season(s) covered by his particular deployment.

3.0 SOUTHWEST MONSOON REGIME (JUN-SEP)

3.1 General Description

The Southwest (summer) Monsoon in our area of interest is characterized by strong surface heat troughs over the surrounding land areas -- particularly over India, Pakistan, Iran and Saudi Arabia.

From the standpoint of surface wind direction over the Arabian Sea, the Southwest Monsoon is typically well established by June; however, the rainy season along the west coast of India does not normally commence until somewhat later (as early as June 1 in southernmost India but as late as July 2 in Karachi). Surface winds reach a maximum in July with the highest speeds (up to 50-60 kt) reported northeast of Socotra Island where winds greater than 33 kt occur more than 30 % of the time.[1] As a result of these consistently strong winds, sea heights of 8 ft or higher persist over more than half of the Arabian Sea during this season.[2]

Upper level winds (above 400 mb) over our area of interest are easterly during the Southwest Monsoon. The Himalayan mountains help to produce and anchor an intense upper anticyclone near 30°N and 85°E (Sadler, 1975). Between this anticyclone and the subtropical ridge of the Southern Hemisphere exist the most extensive and strongest upper tropospheric easterlies within the tropics.

Figure 3-1 is a mosaic of satellite visual images showing a broad area enclosing the Indian Ocean during the Southwest Monsoon regime. Cloud patterns clearly show the directions of the low-level and high-level wind flow in the Arabian Sea, the heavy convective activity over India and a procession of cold surges in the Southern Hemisphere.

There is considerable variability in the time of onset of the Southwest Monsoon, in its intensity once established and in the time at which it ends. At either end of this season, the southwest winds are not persistent; they occur in periods separated by variable or even northeasterly winds. Fluctuations in surface wind intensity during the heart of this monsoon regime are <u>not</u> correlated with the central pressure of the surface heat troughs over land but rather, with the distribution of the pressure gradient over the Arabian Sea. Details concerning the onset of the Southwest Monsoon and breaks within this monsoon regime are presented in Sections 3.2.3 and 3.2.5 respectively.

1. Naval Weather Service Detachment, Asheville, 1974.
2. Ibid.

Figure 3-1. This mosaic is representative of a moderately active Southwest Monsoon situation. The west coast of India and the Central Arabian Sea are cloudy while generally cloud-free conditions prevail over the Red Sea, Gulf of Aden, Persian Gulf, Gulf of Oman, and the Arabian Peninsula. In the typical Southwest Monsoon flow, cloud amounts and the vertical extent of clouds increase from west to east across the Arabian Sea, and the low-level cloud lines parallel the near-surface wind flow. In this example, a thick dust cloud covers the northwestern part of the Persian Gulf and a thin dust veil extends southeastward almost to the Strait of Hormuz (the narrow passage between the Persian Gulf and the Gulf of Oman). Cirrus streamers clearly indicate the direction of the upper-level easterlies. Outside of our particular area of interest, there is a monsoon depression over the western Bay of Bengal and a series of cold-frontal bands forming a procession of cold surges in the Southern Hemisphere. (The northeastern Arabian Sea is shown in greater detail in Figure 3-6, which was recorded on the same date.)

Figure 3-1. NOAA visual mosaic image produced from data recorded on June 23, 1979.

3.2 Large-Scale Circulation Features

The Asian-African monsoon climate results from the unique geography of the Eastern Hemisphere. The nearly continuous east-west mountain range barrier (see Figure 2-3) greatly inhibi s normal low tropospheric air flow and meridional heat exchange. In summer, the resultant heat surplus creates intense surface heat lows over land capped by an intense high pressure ridge along the southern edge of the barrier.

3.2.1 Climatology

Naval Oceanography Command climatological publications (see Appendix A) contain monthly or seasonal data for several operationally significant parameters. It is not the purpose of this Handbook to duplicate existing publications; however, for ready reference and to illustrate the discussion which follows, Figures 3-2a through e provide pertinent climatological data which are representative of the Southwest Monsoon regime. The data from which the figures are derived were not uniformly distributed over the region. In particular, Figure 3-2c, d and e are biased by observations from coastal and island stations; therefore, detail and reliability are reduced over the open ocean. In spite of these limitations, the following climatological charts provide a summary of pertinent parameters and a baseline for the application of the material in this Handbook to daily forecasting problems.

3.2.2 Heat Low and Monsoon Trough

Terms applied to weather phenomena, particularly in tropical regions, tend to defy standardization. In this Handbook, the following definitions apply:

a. Heat Low (or Thermal Low): "An area of low atmospheric pressure due to high temperatures caused by intensive heating at the earth's surface. Thermal lows are common to the continental subtropics in summer; they remain stationary over the area that produces them; their cyclonic circulation is generally weak and diffuse; they are non-frontal." (Huschke, 1959)

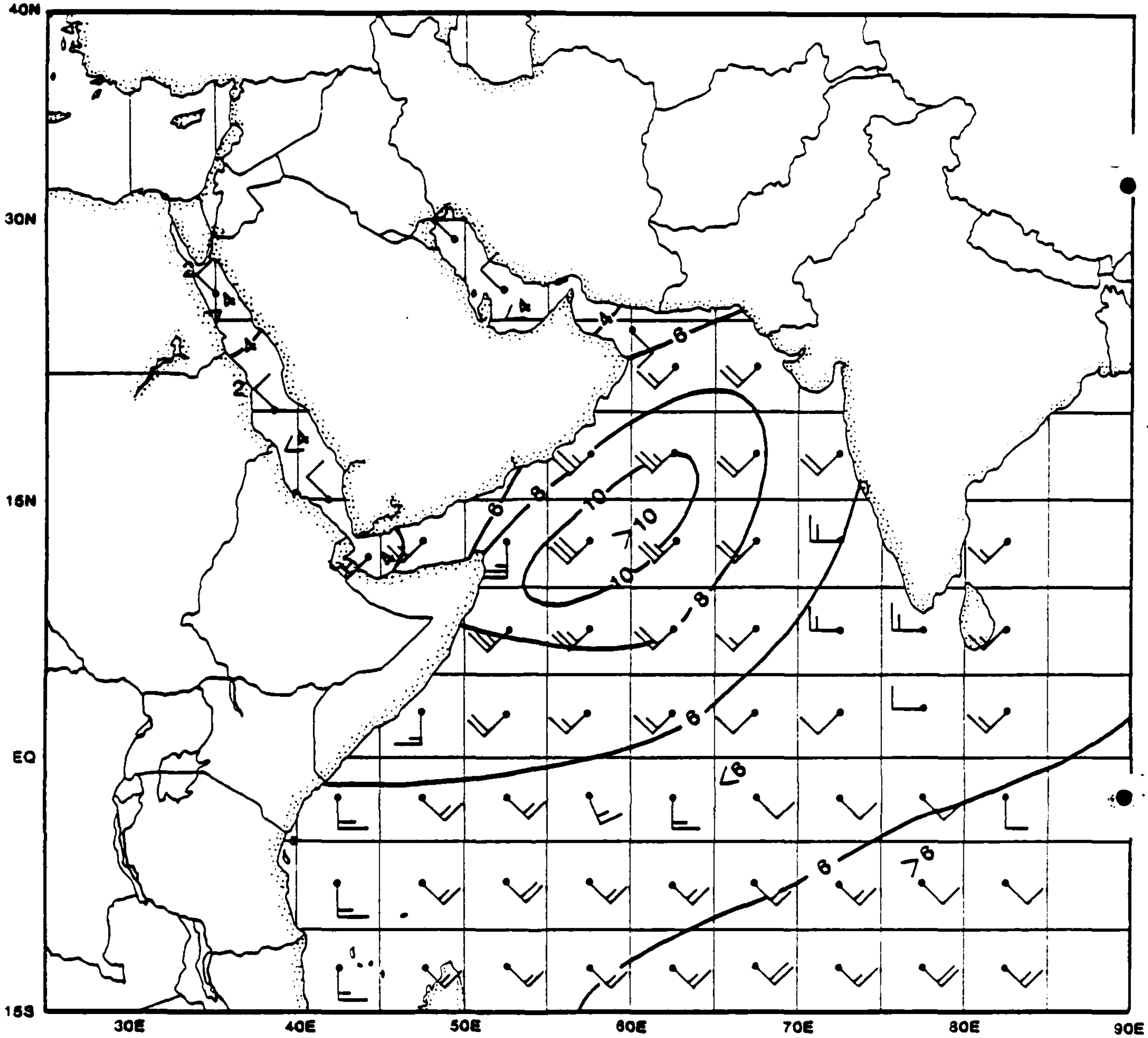

Figure 3-2a. Mean July surface winds (wind barbs) and seasonal mean significant wave heights in feet (contours) (adapted from Naval Weather Service Detachment, Asheville, 1974). The winds represent the average over a 5° rectangle of latitude and longitude. Wind barbs representing the restricted waters of the Red Sea, Persian Gulf and the Gulfs of Aden and Oman are plotted over the water area that they represent. The height contours underspecify wave conditions for mid-June to mid-August for two reasons: (1) the months June through September are averaged, and (2) the data upon which the means are based considered only the higher of the wave and swell components reported.

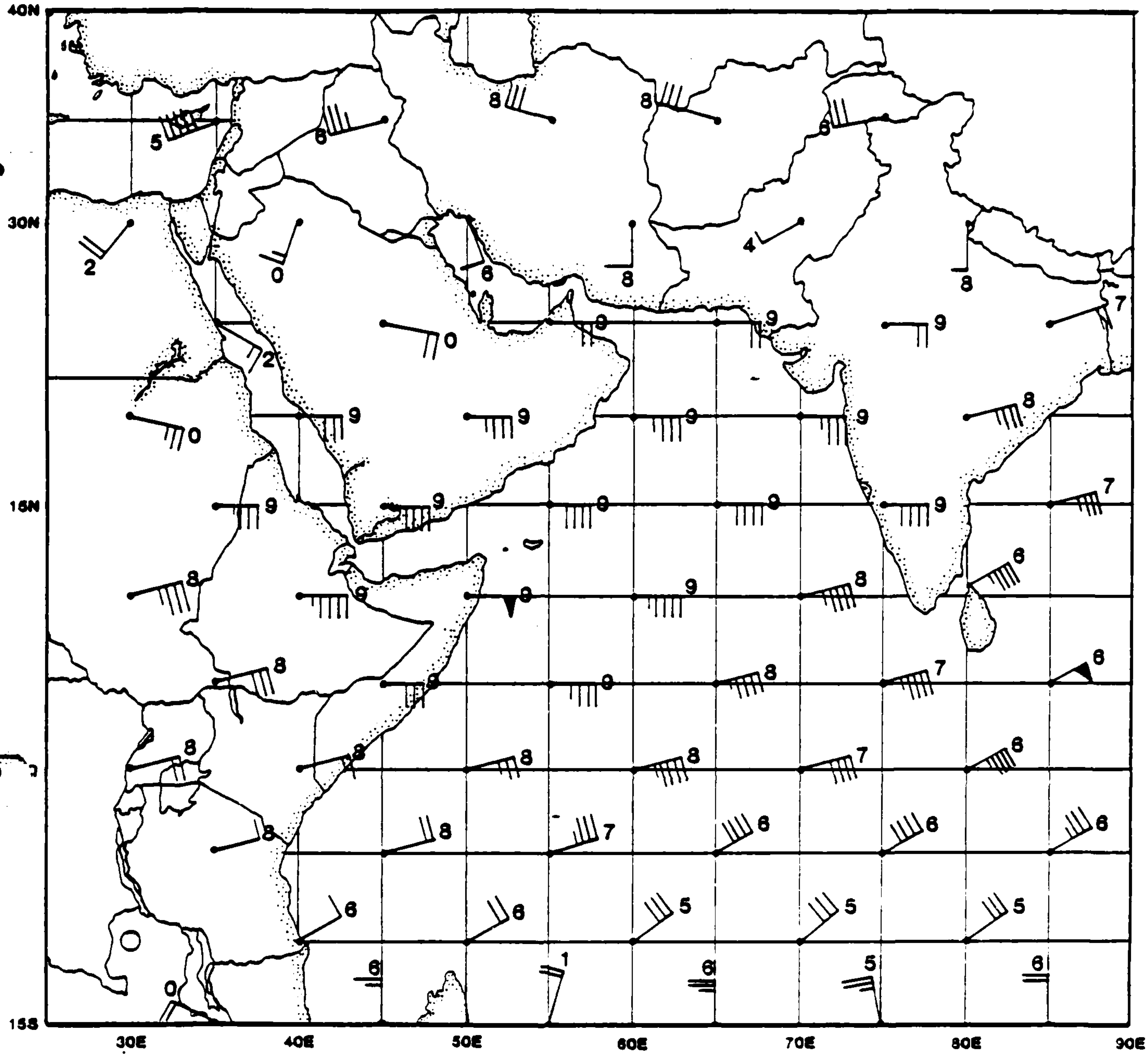

Figure 3-2b. Mean July 200 mb winds (adapted from Sadler, 1975). The numeral by each wind barb is the tens digit of direction. Note the speed maximum in the easterly winds along 10°N and the strong cross-equatorial flow south of India. The Easterly Jet "core" speeds are often stronger than shown because: (1) time averaging was used here, and (2) the jet "core" is usually found above 200 mb.

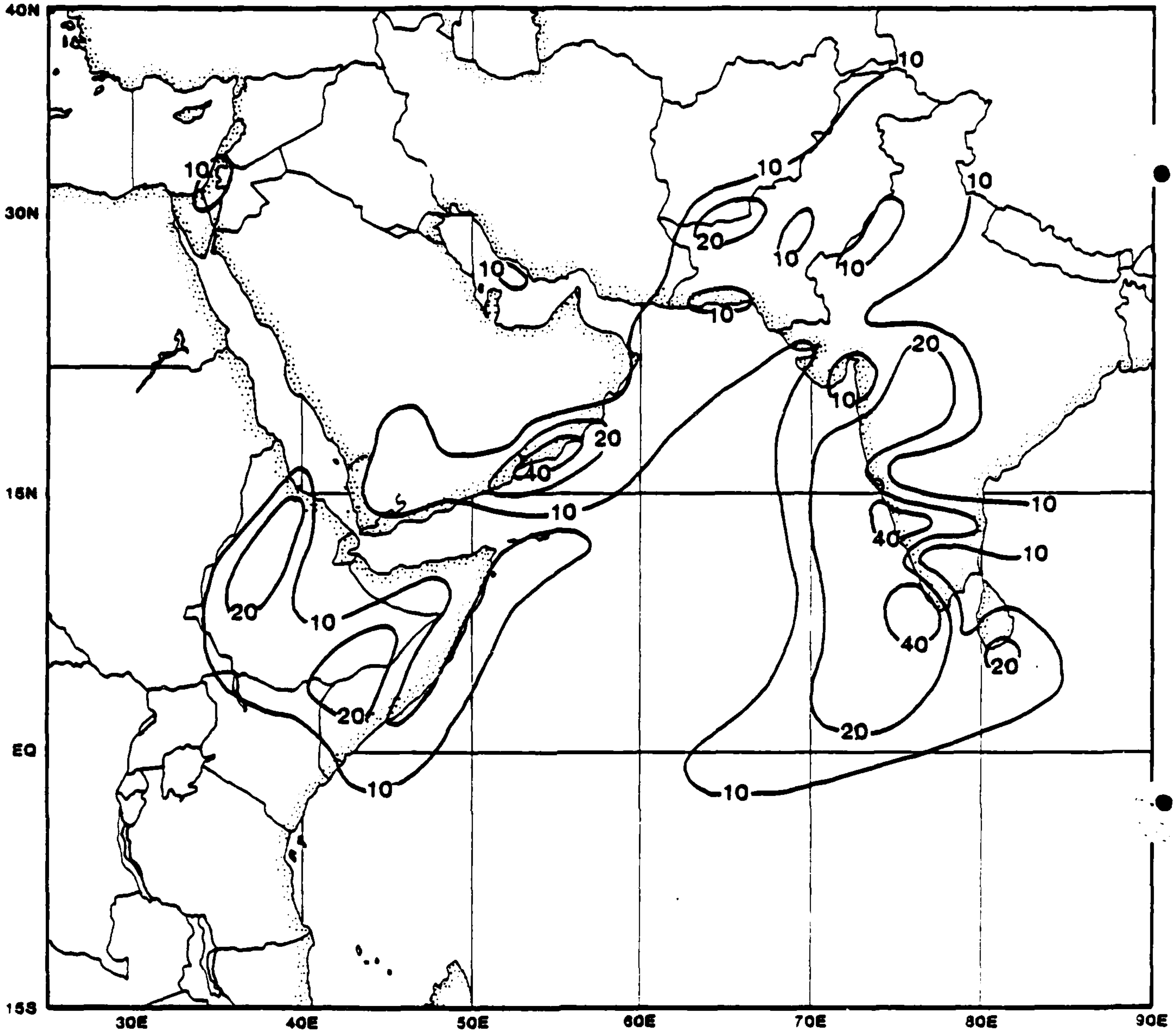

Figure 3-2c. Percent frequency of ceiling less than 1500 ft or visibility less than 3 n mi. Note that ceiling and visibility are infrequently restricted during the Southwest Monsoon except near shore over the central Arabian Coast and along the Indian Coast. Fog is rare; restrictions to visiblity are due to suspended dust (near Africa and Arabian Peninsula) or precipitation (Indian Coast). Low ceilings are primarily responsible for the contour maximum over the Arabian Coast and contribute to the maxima over the Indian Coast.

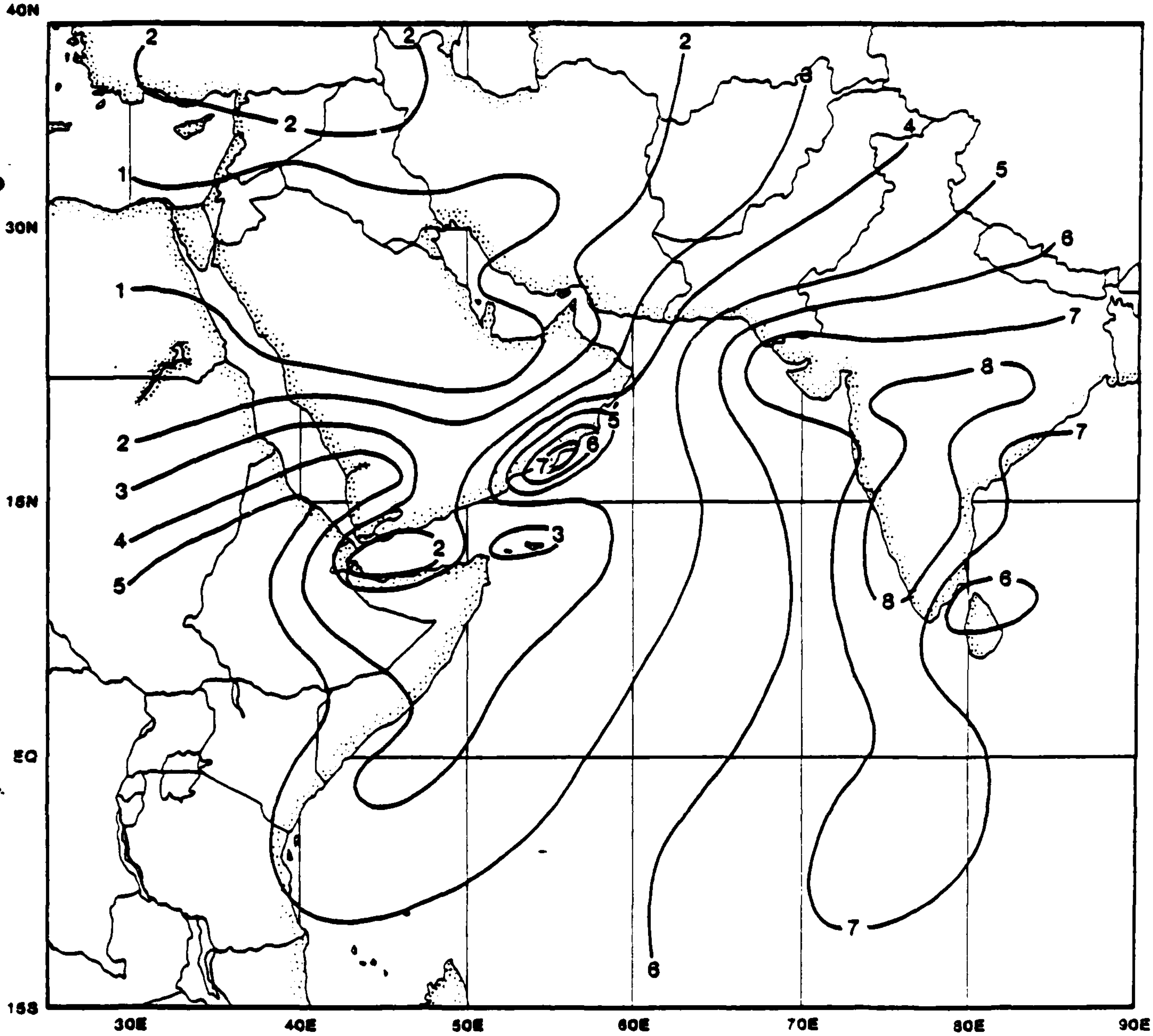

Figure 3-2d. Mean total cloud cover in tenths. The contour maximum over the Arabian Coast is due to persistent low stratus, particularly on the windward side of headlands and islands. The maximum over India is generally convective with considerable cirrus blow-off due to strong vertical wind shear. The relative maximum over the southern Red Sea is generally due to convective activity over neighboring terrain (see Figure 3-2e).

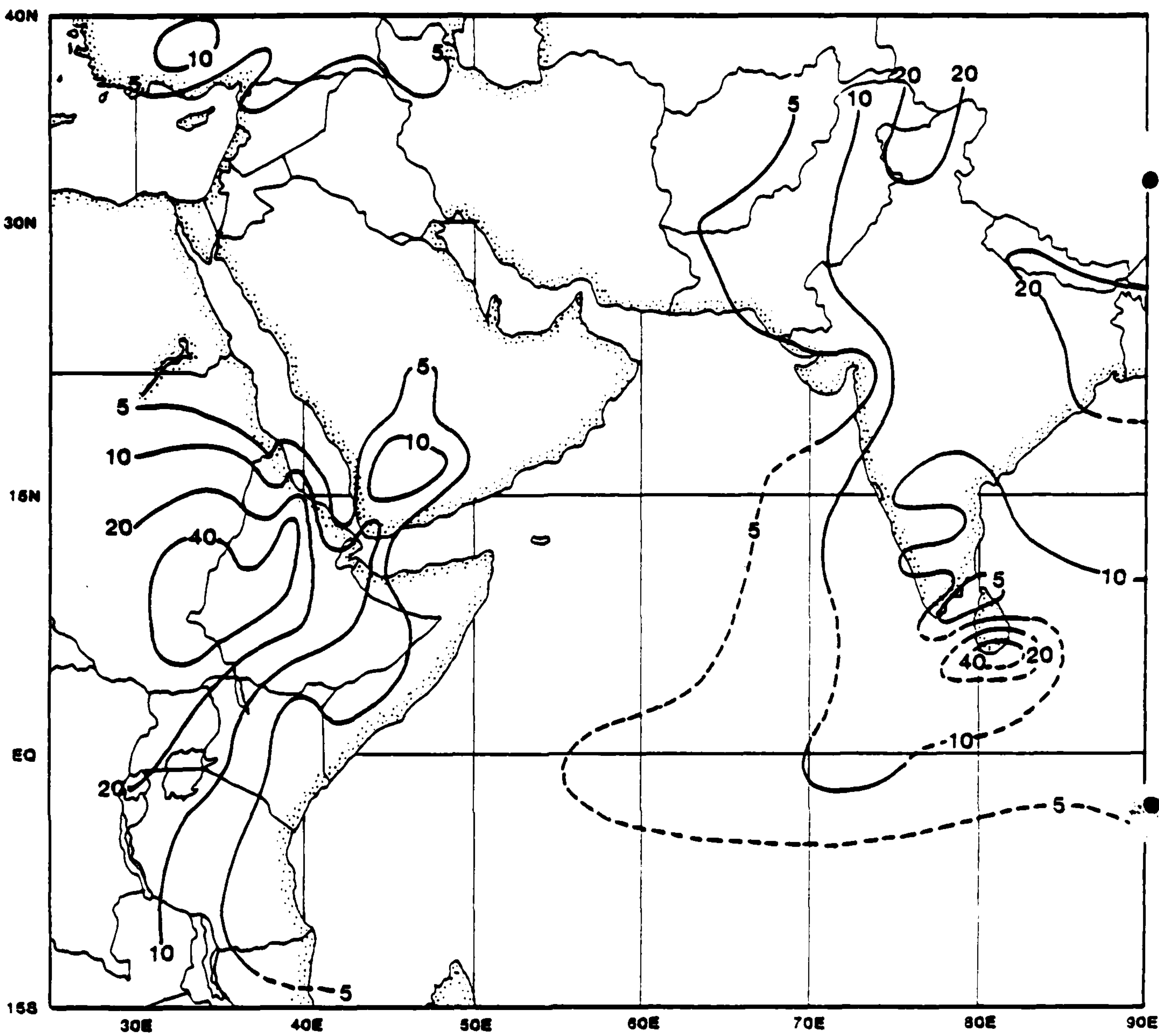

Figure 3-2e. Percent days with thunderstorms. Data for the Central Arabian Sea and the Indian Ocean area shown in the lower portion of the figure are very sparse. Dashed contours are estimates based on satellite imagery; solid contours are based on observations.

b. Monsoon Trough: ". . . the term . . . will be reserved for the intense trough of low pressure which occurs when the primary near-equatorial trough is displaced far to the north (e.g., over northern India and the northern part of the Bay of Bengal) and the Southwest Monsoon becomes well established . . ." (Cuming, 1973)

The preceding definitions tend to explain the characteristics of the sea level pressure pattern associated with each feature, i.e., an area of persistent low pressure. In our area of concern, the Heat Low and the Monsoon Trough are essentially coincident at the surface during the Southwest Monsoon. The differences between the two features occur in the middle and upper troposphere.

The temperature structure of the Heat Low (Thermal Low) over continents is such that the surface Heat Low is overlaid by higher pressure-heights on upper troposphere constant pressure charts used by Navy forecasters. On the other hand, the thermal structure of the Monsoon Trough is not necessarily symmetrical, usually resulting in a horizontal displacement with height of the trough axis. The slope of the trough with height separates (in the vertical) broad wind-flow areas which are nearly of opposite direction. The Monsoon Trough tends to follow the latitudinal migration of the sun's heating but often lags or leads due to terrain influences. Synoptic scale disturbances in the middle troposphere may lead to short-term oscillations of several degrees in the latitudinal position of the Monsoon Trough.

Figure 3-3 is a cross section through western India depicting zonal wind components. It clearly shows the spatial relationships between the low-level Southwest Monsoon, Easterly Jet, Monsoon Trough, Heat Low, Subtropical Ridge and the Extratropical Westerlies aloft.

3.2.3 "Onset" of the Southwest Monsoon

Although weak southwesterly winds may appear during the latter stages of the Spring Transition, the start of the real Southwest Monsoon is usually signalled by a "burst" in the cross-equatorial wind flow (from south to north) near the surface. This increase occurs abruptly, then spreads in an orderly sequence. As the region of strengthening winds expands and progresses northeastward across the Arabian Sea, an area of enhanced convective activity sweeps toward the west coast of India. Cyclonic shear on the northern edge of the "surge" often

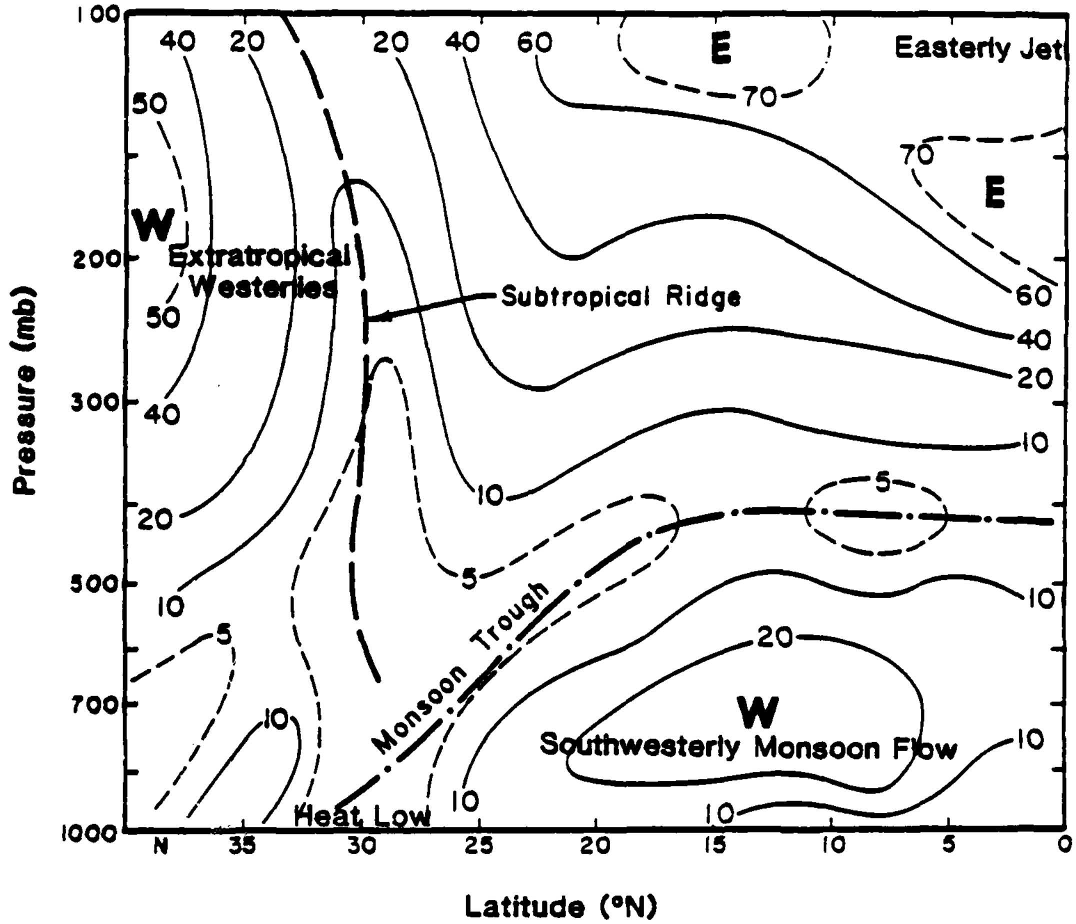

Figure 3-3. Cross section of the July resultant zonal wind speeds (kt) and directions (East or West) along western India showing the relationships among features discussed in the text (adapted from Miller and Keshavamurthy, 1978).

leads to formation of an "Onset Vortex". Satellite imagery of such a vortex is shown in Figure 3-4. The onset may occur at any time between mid-May and mid-June and is nearly always preceded by intensification of the Southeast Trades over the southern Indian Ocean.

"ONSET" FORECAST RULES/AIDS.

a. The sequential steps of the "burst" of the monsoon are:

(1) Increase in the strength of the southern hemisphere tradewinds.
(2) Strengthening of the cross-equatorial flow (see Section 3.3.1 for a description of the Somali Jet).
(3) Speed increase in the southwest flow off the northern African Coast (frequently accompanied by development of an area of enhanced convection).
(4) Formation and development of an "Onset Vortex".
(5) Sharp increase in the precipitation along the southern Indian Coast.
(6) Northward spreading of strong southwesterly flow to eventually cover all of the Arabian Sea.
(7) Establishment and strengthening of upper level easterlies.

b. Satellite imagery "clues":

(1) Low-level cloudiness parallel to the African Coast (off Somalia).
(2) Movement of a convective area or line northeastward across the Arabian Sea.
(3) The development of an "Onset Vortex".
(4) Movement of the "Onset Vortex" northward to about 20°N and then toward the Arabian Coast.
(5) Northward progression of convective clouds along the Indian Coast.

c. The time period from the increase in the Somali Jet to the arrival of the Southwest Monsoon over the southern Indian Coast is 3 to 4 days.

Figure 3-4. This DMSP visual image is typical of the "Onset Vortex" which signals the "burst" at the start of the Southwest Monsoon. These vortices (cyclonic storms) form in the Near-Equatorial Trough as it moves northward toward its mean position over India in this season. Maximum winds in this case reached 55 kt. Similar "Onset Vortices" have been identified in 37 of 68 seasons from 1901-1968. Low-level (cyclonically curved) cloudlines can be seen to the north and east of the center, and upper-level anticyclonic outflow is indicated by the cirrus cloud pattern. Heavy convection is occurring along the coast of India and over the ocean area southeast of the center. Notice that cirrus plumes from cumulonimbus buildups stream westward in response to the upper-level Easterly Jet. It is common for low-level southwesterly flow and upper-level Easterly Jet flow to develop rapidly in the wake of the "Onset Vortex". The approximate local sun time at the center of this image is 1100 (0627Z).

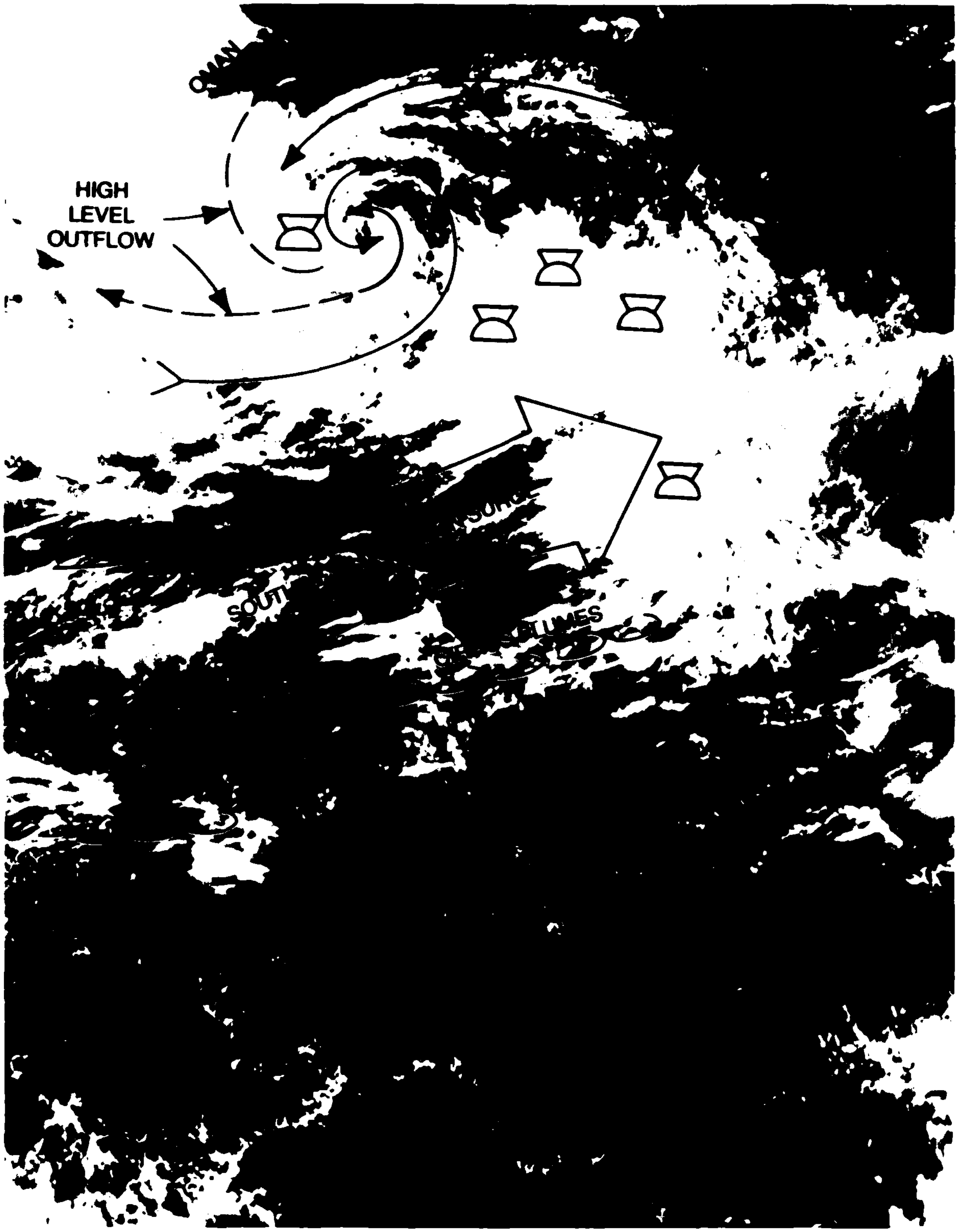

Figure 3-4. DMSP visual image of a mature "Onset Vortex" approaching the coast of the Arabian Peninsula (June 18, 1979).

3.2.4 Basic Southwest Monsoon Flow

The onset of the Southwest Monsoon was described in the previous section. Once the basic flow becomes established, there are two general types based generally on the total amount of cloud cover and the intensity of precipitation over western India. The two major categories are frequently referred to as: (a) "weak" monsoon flow and (b) "strong" monsoon flow. In both cases the total pressure gradient over the Arabian Sea is nearly the same; however, in "weak" situations the maximum gradient is found north of 23°N (mostly over land) and in "strong" situations it is found over water (usually 13°N to 21°N).

Figure 3-5 illustrates moderately "strong" flow during the Southwest Monsoon. This DMSP photo should be compared with the weaker flow depicted during the "Onset Vortex" stage shown in Figure 3-4. Note that the low-level clouds from the Gulf of Oman eastward to the Indian Coast indicate weaker winds here in the "strong" case. However, the clear area east of Socotra Island bounded on the east and north by cloud lines indicates an intense surface wind maximum. Limited data (Brody, 1977) indicate that the northern branch of the monsoon flow is displaced southward and intensified by mid-tropospheric disturbances during "strong" cases. The data also indicate deeper southwesterly flow over the Central Arabian Sea and Indian Coast in "strong" cases. Brody also concluded that the Subtropical Cyclones which influence the northern part of the Arabian Sea and occur in the upper-level Monsoon Trough between 700 and 500 mb are a major producer of clouds and rainfall along the northwest coast of India. These Monsoon Trough depressions frequently originate in the Bay of Bengal but influence monsoon intensity over India and the northern Arabian Sea. These upper circulations sometimes penetrate downward and become detectable at the surface but do not develop into classic tropical storms or hurricanes. Their surface reflections often affect the location of the maximum surface pressure gradient and therefore the strength of the low level winds.

Figure 3-6 is a DMSP visual image of a "strong" Southwest Monsoon situation when virtually all of the Arabian Sea is covered with clouds. This photo should be compared with Figures 3-4 and 3-5 to illustrate possible differences in overall intensity of monsoon flow during this season.

Figure 3-5. This DMSP image shows cloud cover which is typical of a "moderately strong" Southwest Monsoon flow situation. The relatively clear area just east of Socotra Island with diverging cloud lines to the east and north reflects the region of maximum low-level winds. The low level cloud lines clearly show the anticyclonic flow pattern in the Central Arabian Sea. The low-level wind direction is also apparent from heavier cloud formations on the windward slopes of Socotra Island and on headlands along the Arabian Coast. The absence of dense cirrus plumes over the Indian Coast suggests that vertical development is not excessive, and that rainfall may not yet be heavy. A light veil of dust can be seen over the Persian Gulf as greyish plumes; the dust appears to be heaviest near the Qatar Peninsula. The approximate local sun time at the center of this image is 1000 (0610Z).

Figure 3-5. DMSP visual image of the Arabian Sea during a "moderately strong" Southwest Monsoon period (July 10, 1979).

GENERAL SOUTHWEST MONSOON FORECAST RULES/AIDS.

a. When the Somali Jet intensifies, the Southwest Monsoon flow over the Arabian Sea (and clouds/rain over western India) intensifies 1-2 days later.

b. When subtropical cyclones develop between 700 and 500 mb in the Monsoon Trough over the Bay of Bengal or the northern Indian Coast, forecast low-level wind flow to increase by 10-20 kt off the central Indian Coast -- particularly if there is evidence of the cyclonic circulation penetrating downward.

c. If the maximum surface pressure gradient occurs north of 23°N (over land), forecast "weak" monsoon flow over the Arabian Sea with maximum winds near 2000 ft. If the maximum gradient is over water (13°N to 21°N), forecast "strong" monsoon flow conditions with maximum winds above 3500 ft.

d. During "strong" monsoon conditions, the area north of 22°N usually experiences relatively light surface winds.

3.2.5 "Breaks" in the Southwest Monsoon

"Breaks" in the Southwest Monsoon are the result of a breakdown in the entire monsoonal circulation pattern -- including a weakening of the upper-level anticyclone over the Himalayas and the upper-level easterlies over our area of interest. Ramamurthy (1969) found that definite "breaks" in the Southwest Monsoon occurred during 68 out of a total of 80 years studied. The longest breaks last from 17-20 days, but the most frequent duration is 3-4 days. Such breaks are more common in August than in other Southwest Monsoon months. M. Murakami (1976), and Krishnamurti and Bhalme (1976) found a period of alternation between active and inactive monsoon spells of around 2 weeks.

FORECAST RULES/AIDS FOR "BREAKS" IN THE SOUTHWEST MONSOON.

a. "Breaks" do not occur when troughs in the mid-latitude westerlies (40°N-50°N) move unimpeded across the longitude belt 90°E to 120°E.

Figure 3-6. This DMSP image shows cloud cover which is typical of one of the "stronger" Southwest Monsoon situations. Most of the Arabian Sea is cloud-covered and the entire Indian Coast except the northernmost extremity is experiencing heavy convective activity. The low-level inversion (if it exists at all) must be weak because considerable vertical development is evident in several areas of the Arabian Sea. The cirrus plumes over the Central Arabian Sea indicate a diffluent upper-level flow pattern which is favorable for deep convective development. The 200 mb data (from MONEX) for the date support the directional divergence of the plumes although mean wind climatology does not reflect this pattern, indicating that it is transient. Notice that some low-level cloud lines can be seen in the lower-left portion of the image. The approximate local sun time at the center of this image is 1000 (0636Z).

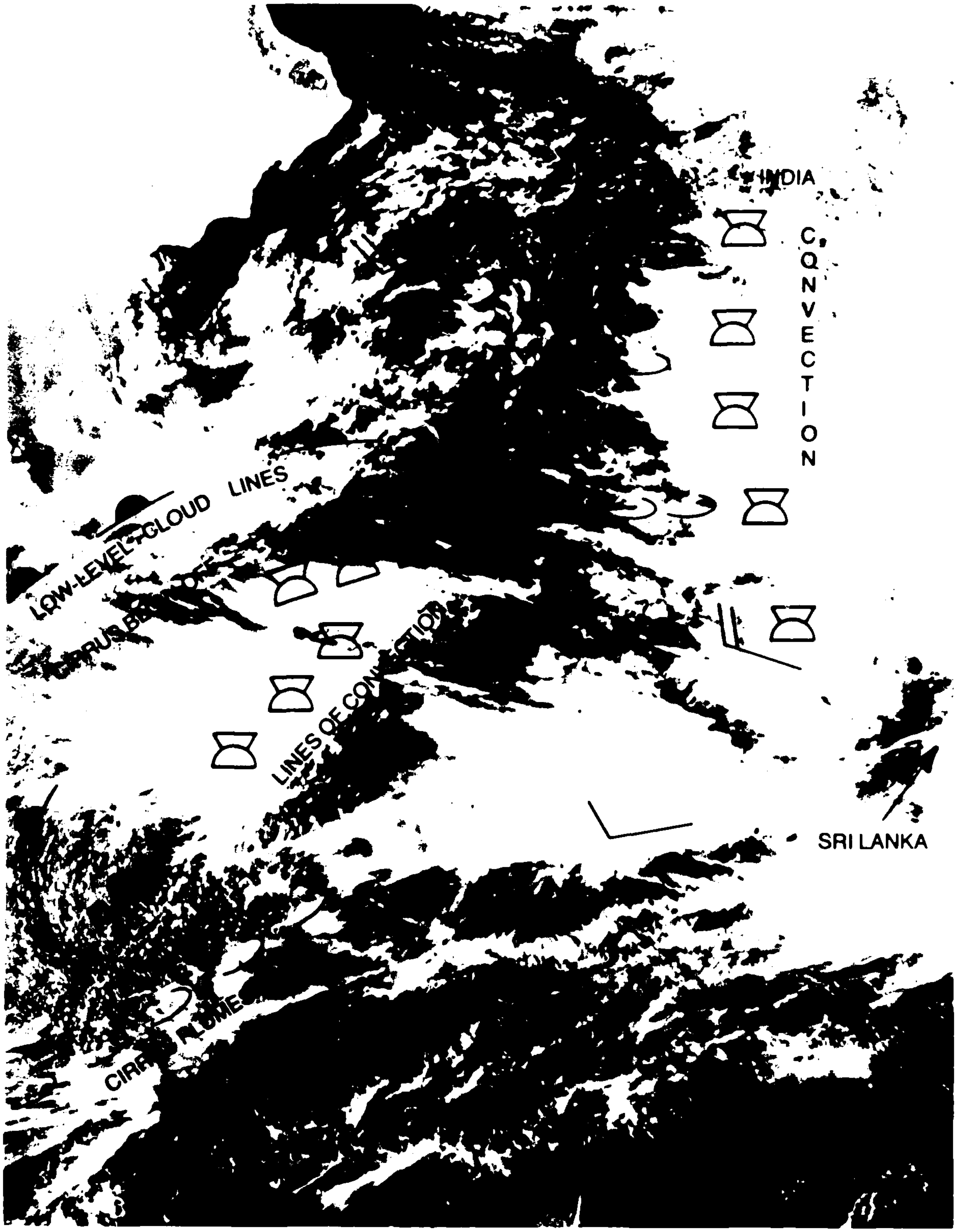

Figure 3-6. DMSP visual image of a "strong" Southwest Monsoon (June 23, 1979).

b. Regular development and movement of mid-troposphere monsoon depressions from the Bay of Bengal across India is not conducive to causing a "break" in the Southwest Monsoon.

c. Development of a blocking high between $35^{\circ}N$ to $70^{\circ}N$ and $90^{\circ}E$ to $115^{\circ}E$ is favorable for causing a "break" in the intensity of the Southwest Monsoon.

d. When a "break" starts to occur, forecast the rainfall belt normally near $20^{\circ}N$ to be replaced by one near $25^{\circ}N$ with a second belt near $7^{\circ}N$. Also forecast the upper-level easterlies to weaken (and shift northward) and the low-level southwesterlies to weaken with the northern branch of the Somali Jet becoming the stronger branch.

3.2.6 The Upper-Level Easterly Jet

The upper level Easterly Jet is an important large-scale aspect of the Southwest Monsoon. As pointed out earlier, its intensity is directly correlated to: (a) the intensity of the upper-level Himalayan anticyclone, (b) the occurrence and intensity of mid-tropospheric monsoon depressions and (c) the intensity of the low-level southwesterly flow over the Arabian Sea. This high tropospheric wind phenomenon is a persistent feature during the Southwest Monsoon. Due to the extremely high air temperatures above the continental heat lows, the pressure minimum decreases rapidly with height and becomes a pressure maximum above 500 mb. This maximum continues to intensify with altitude to the tropical tropopause, forming a strong anticyclone aloft. The strength and persistence of this upper-level feature result in relatively constant easterly winds in the upper troposphere and lower stratosphere over this area throughout the warm season. The mean position of the "Easterly Jet" is above 40,000 ft near $10^{\circ}N$ (see Figure 3-7); however, some climatologies (e.g., Sadler, 1975) show a secondary maximum near the Equator in the Central Arabian Sea. Wind speeds over 100 kt have been observed. Fluctuations appear to be directly related to changes in the strength of the Southwest Monsoon flow, but quantitative (or causal) relationships have not been established. Recent investigations by Verma (1980) and Ramon, et al. (1980), suggest that anomalies in the upper-tropospheric westerly (mid-latitude) flow and the mean temperature in the Subtropical Ridge affect the strength of the monsoonal flow.

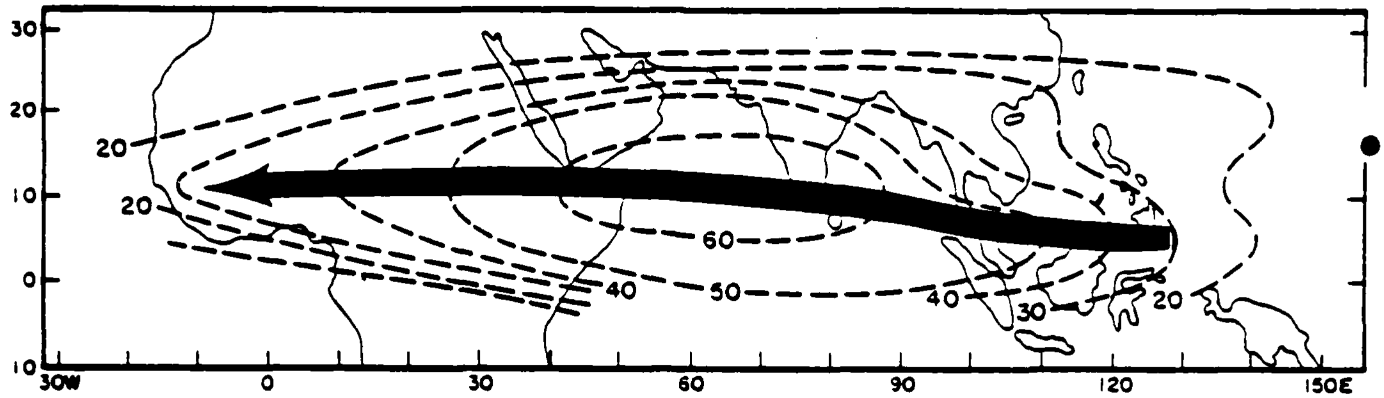

Figure 3-7. The upper-level Easterly Jet over the Asian-African area as illustrated by the resultant wind speeds (kt) at 150 mb during July-August (after Flohn, 1964).

3.3 Regional Features

3.3.1 Arabian Sea

During the Southwest Monsoon regime, weather and oceanographic conditions over the Arabian Sea are dominated by the strong, persistent flow over the area. Both low-level and high-level circulation features are quasi-permanent but exhibit fluctuations which are important. Large-scale aspects of the overall circulation and fluctuations therein were discussed above; this section focuses on wind and cloud conditions on the regional scale.

Low-Level Features

Low-Level Clouds. Two predominant types of low level clouds are found over the Arabian Sea during the Southwest Monsoon: (a) inversion - capped clouds and (b) convective clouds which break through the inversion. Figure 3-8 is typical of "weak" monsoon flow in this season. Note that there is a gradual downward slope of the inversion from east to west across the Arabian Sea. A similar section taken north-south through the Central Arabian Sea would show that the inversion also slopes downward from south to north. Although the inversion heights shown on the overlay are typical, the inversion tends to be higher and weaker during "strong" monsoon flow and lower and stronger during "weak" flow.

Low-Level Winds. During the summer monsoon, intense heat lows form over the desert areas surrounding the Arabian Sea. At the same time, high mountains to the north seal off the area from cold air outbreaks, and mountains over eastern Africa present a barrier to low-level wind flow. As a consequence of these radiational and topographic features, a strong southerly flow occurs along the African Coast and a broad southwesterly flow dominates the Arabian Sea. The southerly flow along the African Coast results in cold upwelling along the northern African Coast (off Somalia). The upwelled water cools the overlying air and produces a local high pressure ridge which intensifies the pressure gradient between the coastal area and the heat low over the inland area. An additional effect of the upwelling is to produce a thermal wind component which increases vertical wind shear in the lower levels. All of these factors contribute to the formation and maintenance of a strong, relatively narrow wind stream (Somali Jet) along the African Coast and a broad, persistent flow (Southwest Monsoon) over the Arabian Sea and its coastal areas.

Somali Low-Level Jetstream. The "Somali Jet", as defined above, occurs from April through October and is one of the strongest and most sustained low-level wind systems on earth. It is normally strongest in July and August when maximum speeds up to 100 kt have been observed. The core is usually centered at an elevation of about 5000 ft. Figure 3-9 shows a monthly mean airflow chart at 3500 ft for July. Notice the local speed maxima north of Madagasgar, off the coast of Kenya and to the northeast of Socotra Island. These are semi-permanent low-level wind features during the Southwest Monsoon. Figure 3-5 showed a satellite view of the Arabian Sea when the Somali Jet and the Southwest Monsoon wind flow were both relatively intense. The low-level wind speed maximum just east of Socotra Island usually appears as a relatively clear area bounded on the north and east by diverging cloud lines. When the Somali Jet is well developed, the Somali coastal area is usually characterized by clear skies; the clear area correlates well with cold upwelling shown by satellite IR data (see Figure 7-2).

Figure 3-8. This DMSP image shows detailed cloud structure over the Arabian Sea during a relatively "weak" Southwest Monsoon situation (see Section 3.2.4 for further discussion). This case was selected to illustrate variations in the strength and height of the low-level inversion during "weak" flow. The inversion is lowest near the African and Arabian coasts and slopes upward toward the east and south. In particular, note the increase in density and brightness of the clouds south and east from the Gulf of Aden. The "wave-like" clouds in the Central Arabian Sea are thought to be the result of gravity waves on the inversion interface. The convective clouds and related cirrus cloud plumes near the central Indian Coast indicate that the inversion is weak or non-existent there. During periods of "weak" Southwest Monsoon flow the low-level winds and cloudiness over the northern Indian Coast usually increase. The cloudiness seen in this image is typical of a "weak" condition. The approximate local sun time at the center of this image is 1030 (0604Z).

Figure 3-8. DMSP visual image for July 5, 1979 showing detailed cloud structure over the Arabian Sea.

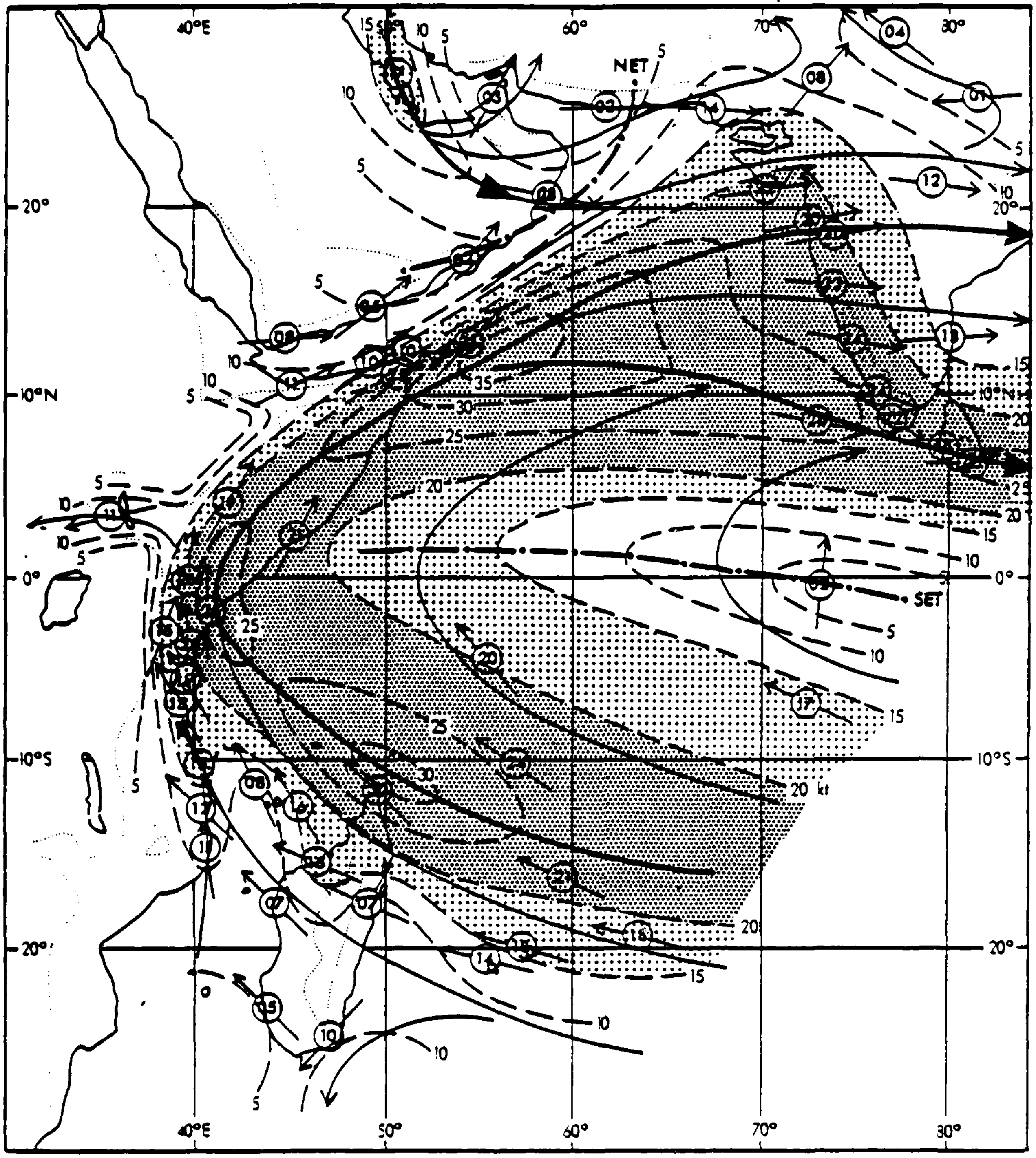

(symbol)	Major streamlines (axes of maximum wind)	NET	Northern Equatorial Trough
(symbol)	Subsidiary streamlines	SET	Southern Equatorial Trough
(symbol)	Isotachs (5-kt intervals)	(12)	Mean resultant wind (kt)
(symbol)	Speeds 15–20kt	(0)	Resultant wind ≤ 1kt
(symbol)	Speeds >20kt	(12)	Interpolated resultant wind (kt)
(symbol)	Axes of maximum wind		

Figure 3-9. Mean July winds near 3,500 ft (adapted from Findlater, 1971).

"SOMALI JET" FORECAST RULES/AIDS.

a. In the absence of observations, forecast core speeds of 50-65 kt at an elevation of 5000 ft along the climatic jet axis shown in Figure 3-9. (Note: Multiple cores (jetlets) are possible.)

b. Fluctuations in core wind speed are associated with southern hemisphere cold-air outbreaks (i.e., strong migratory high pressure cells). Major fluctuations can be expected every 2-3 weeks. Core speeds of 65-80 kt are typical during intensification while speeds of 30-45 kt are most common during lulls.

c. Somali Low-Level Jetstream winds do not significantly impact air operations above 10000-15000 ft. (See other sections for discussion of high-level jetstreams.)

Upper-level Clouds. Much of the Arabian Sea is characterized by subsidence in the middle troposphere. This tends to suppress upper-level cloudiness. An exception to this rule occurs near the Indian Coast where convergence in the low- and mid-level flow causes copious rainfall and considerable convective activity. The High-Level Easterly Jet spreads the moisture which is carried aloft by this convection downstream (westward) over the Arabian Sea. The result is frequently a dense cirrus shield which is dissipating due to subsidence (high-level cloudiness therefore decreases westward). The amount/density of the cirrus deck is generally related to the intensity of the rainfall over western India. Figure 3-6 clearly showed the cirrus shield dissipating as it was being blown westward by the high-level flow.

CLOUD AND WIND FORECAST RULES/AIDS.

a. Density and westward extent of cirrus over the Arabian Sea is directly related to the intensity of monsoon rains over India. In "strong" monsoon flow, cloud cover extends 500-700 n mi to sea off India.

b. The African Coast, particularly in the north where upwelling is strongest, is nearly cloud-free during the Southwest Monsoon.

c. Distinct, closely-spaced cloud lines indicate relatively strong low-level winds.

d. Cloud patterns over the Arabian Sea and coastal areas provide the following information on inversion height:

(1) Cloud free except for stratus -- the inversion is near the surface.

(2) Continuous cloud line or wave pattern -- a strong low to medium level inversion exists (cloud-top temperatures from IR imagery would indicate relative height).

(3) Convective clouds -- the inversion is weak or non-existent.

e. The inversion (where it exists) is generally higher (lower) during "strong" ("weak") monsoon conditions.

Equatorial Cloud and Wind Patterns

The equatorial convergences typical of other tropical areas are not as well developed in the Indian Ocean during summer, hence cloudiness along the equator is somewhat less than in other tropical oceans. Cloudiness is suppressed by subsidence near the African Coast but is enhanced near Sri Lanka due to stronger convective activity; therefore, mean coverage (particularly of high clouds) increases from west to east.

From June through September, surface pressures in the southern hemisphere subtropical ridge are relatively high while those in the Middle East heat trough are at their annual low. The result is a unique wind flow pattern over the tropical Indian Ocean. The Southeast Trades of the Southern Hemisphere veer across the Equator to become the Southwest Monsoon in the Arabian Sea with no doldrum area near the Equator itself. This pattern is relatively steady, but short-period speed fluctuations occur. Climatologically, the southern hemisphere Southeast Trades peak in June while the Southwest Monsoon winds are strongest in July.

Near the African coast, wind speeds increase from south to north as the Somali Jet crosses the Equator. Further eastward, the flow weakens considerably such that a speed minimum is found near the Equator at about 70°E, and winds are generally light and variable along the Equator east of 70°E.

Visibility Restrictions

In general, visibilities over the Arabian Sea and surrounding land areas are lower during the Southwest Monsoon than during the Northeast Monsoon. The following paragraphs discuss the causes for this deterioration.

Dust. The southern portion of the Arabian Peninsula, the coastal areas of the Red Sea and the Persian Gulf and the horn of Africa (Somalia) contain areas from which dust may be carried aloft by the prevailing winds during the Southwest Monsoon. Therefore, coastal areas (African and Arabian Coasts, Gulf of Aden) are frequently affected by dust haze. It is most common from mid-June to mid-August in this area. Occasionally the Gulf of Oman and the Makran Coast will experience dust haze from local sources, but this is usually limited to the period immediately preceding the onset of the Southwest Monsoon in the area.

Salt Haze. The combination of strong surface winds and low-tropospheric stability causes persistent salt haze over most of the Arabian Sea. Surface visibilities generally range 5-8 n mi, depending on wind speed and inversion height. In the northern and western coastal areas where salt haze and dust haze often occur together, lower visibilities are common.

Fog. Although atmospheric conditions are not conducive to the formation of dense fog, the sharp reduction of SST in coastal areas of the northwestern Arabian Sea causes moisture saturation in a shallow layer and contributes to poor visibility. The areas most often affected by lowered visibility or stratus are the windward shores of Socotra and the Arabian Coast between Riyan and Masirah Island. The period of occurrence and intensity is governed by the characteristics of the Southwest Monsoon (which causes the upwelling). The area near Salalah is particularly susceptible to low ceilings and visibilities; July and August observations at Salalah indicate that 60% of the reported visibilities are less than two miles.

Rain. Although salt haze (and occasionally, dust) occurs in the eastern portion of the Arabian Sea, the principal visibility restriction is rainfall occurring during monsoon surges and convective showers. Visibility less than a half-mile is frequently observed for brief periods.

VISIBILITY FORECAST RULES/AIDS.

a. In coastal areas, visibility usually reaches a minimum around 0600 local time and a maximum near mid-day.
b. Horizontal visibility over the Arabian Sea is generally reduced to 5-8 n mi in salt haze. (Dust near the Arabian Peninsula will cause additional restrictions but this varies with time and location.)

Tropical Cyclones

Except during early June, tropical cyclones are rare in the Arabian Sea (and South Indian Ocean) during this period. Past records indicate an average frequency of occurrence of about once every five years for cyclones to reach storm intensity. Of those that occur, most are located in the northeastern portion of the Arabian Sea, have tracks generally paralleling the west coast of India, and dissipate or make landfall east of 60°E. There are no cases on record of a tropical cyclone with maximum wind speeds of 34 kt or greater entering the Gulf of Oman or the Gulf of Aden.

TROPICAL CYCLONE FORECAST RULES/AIDS.

a. Conditions necessary for the formation of a tropical cyclone are:

   (1) Pressure trough over the Arabian Sea north of 5°N
   (2) Weak vertical wind shear
   (3) Existing low-level disturbance
   (4) Upper tropospheric outflow

b. Watch for the formation of a surface circulation near the Indian Coast following the first surge in the low-level cross-equatorial flow and

then watch for development in the enhanced convective area ahead of the surge in the Southwest Monsoon.

c. Normal movement of the "Onset" tropical cyclone is north along the Indian Coast, then curving westward toward the Arabian Coast. The strongest peripheral surface winds are typically found southeast of the surface circulation center.

3.3.2 Red Sea and Gulf of Aden

Large-scale circulation features associated with the Southwest Monsoon were addressed in Section 3.2. Over the Red Sea and Gulf of Aden, fluctuations are less pronounced and much of the variability is due to diurnal and terrain effects.

Low-Level Features

Low Level Clouds. The Red Sea is relatively cloudless during this season, particularly in the northern part (See Figure 3-10). When clouds occur, afternoon cumulus predominate with bases mostly between 2,000 and 5,000 ft MSL. The area south of 15°N and west of 45°E experiences the greatest cloud coverage; however, clouds seldom affect naval operations anywhere in this area. When early morning low cloudiness exists in the Gulf of Aden, it usually dissipates by noon.

CLOUDINESS FORECAST RULES/AIDS.

a. In the Gulf of Aden, morning low cloudiness decreases sharply between 0800 and 1200 local time.

Low-Level Winds. The semi-permanent low pressure systems over land and the terrain bordering the Red Sea cause extremely persistent winds from the northwest quadrant. In the Gulf of Aden, these same influences result in winds from the southwest quadrant. Wind speeds are usually less than 28 kt but occasionally exceed 28 kt near the northern end of the Red Sea and may reach

gale force near the southern shore of the Gulf of Aden. In general, the wind direction is parallel to the long axis of both water areas. Near shore, the direction is usually affected by diurnal (land/sea breeze) forces which add an onshore component during the daytime and an offshore component at night. If the local terrain causes the diurnal influence to oppose/reinforce the gradient wind, significant speed variations can occur; for example, the additive effects can result in local wind maxima in the morning and minima in the afternoon. The southwest coast of the Gulf of Aden (Berbera) provides an example of this phenomenon.

Upper-Level Features

High Clouds. High clouds seldom occur over the northern two-thirds of the Red Sea in summer due to subsidence; however, the southern extremities of the Red Sea and the Gulf of Aden occasionally experience cirrus blow-off from thunderstorms or heavy monsoon storms in the eastern Arabian Sea. The latter effect is most likely to occur in July when the monsoon flow is most intense.

Upper Winds. The slope of the Monsoon Trough from a surface position over the Arabian Peninsula to a middle troposphere position over the horn of Africa (see Figure 3-3) results in a veering of the wind direction with height over the Gulf of Aden. The combination of terrain influences and low-level pressure gradient also produces a veering of wind direction with height over the Red Sea. Above about 20,000 ft, a broad band of easterly winds extends from about 30°N well into the Southern Hemisphere. The mean position of the axis of maximum wind speeds in the upper-level Easterly Jet is directly over the Gulf of Aden at altitudes in excess of 40,000 ft. Maximum jet core speeds over 100 kt have been observed; however, in July over the Gulf of Aden they average about 65 kt. Variations in the wind direction of the Easterly Jet are small throughout the monsoon period but significant speed changes occur. These changes appear to be directly related to the strength of the low-level Southwest Monsoon flow.

Figure 3-10. DMSP photo showing typical cloud cover over the Red Sea and Gulf of Aden during the Southwest Monsoon. This case occurred at the beginning of the season and the "Onset Vortex" can be seen at the right edge of the picture. A meso-scale dust storm is occurring just south of Port Sudan and a thin veil of dust can be seen downwind from the main plume (southwestern portion of the Red Sea). Notice that except for the high-level cirrus blow-off from the "Onset Vortex", the Red Sea, Gulf of Aden (and Persian Gulf) are nearly cloud free. Clouds indicate that precipitation is likely along the Arabian Coast from Salalah to Masirah. The approximate local sun time at the center of this image is 1100 (0750Z).

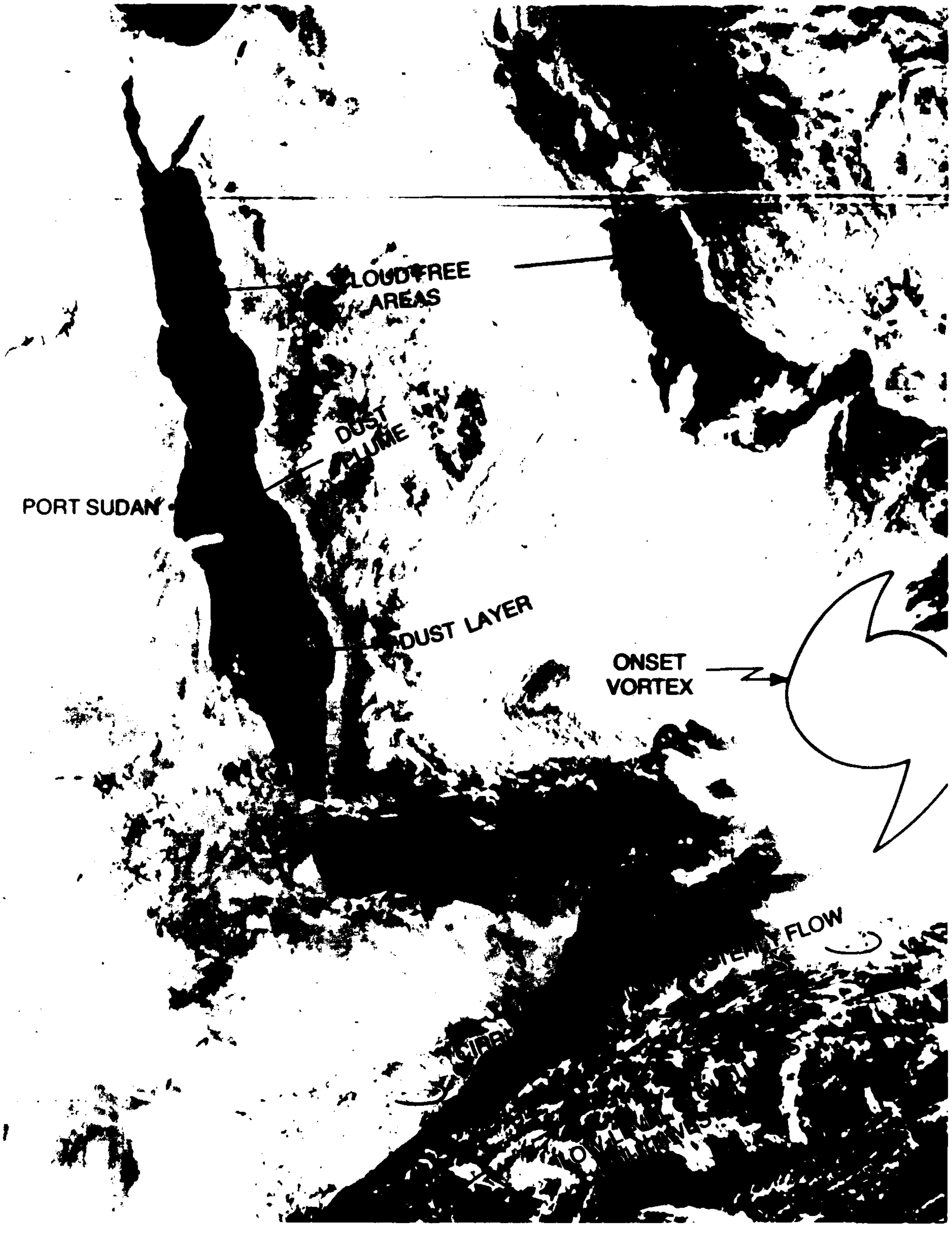

Figure 3-10. DMSP visual image recorded near local noon on June 19, 1979 showing typical cloud cover over the Red Sea/Gulf of Aden during the Southwest Monsoon.

Visibility Restrictions

Dust and Sand. The northern Red Sea experiences its best visibility during the summer monsoon. Dust storms are relatively infrequent. The only area where the visibility decreases to less than 5 n mi more than occasionally is near the Gulf of Aqaba. In the area, visibility below 2 mi occurs about 5% of the time due to the localized winds caused by funneling.

Poor visibility is more frequent in the central and southern Red Sea; visibility below 5 n mi is experienced 10% to 30% of the time in July. Reductions to 1/2 n mi or less occasionally occur near terrain features which tend to funnel local winds (see the area near Port Sudan in Figure 3-10). In most cases, the lowest visibility occurs in the early morning hours; however, poor visibility may also coincide with the most unstable period (usually in the afternoon) if terrain influences predominate.

The summer season is bad for visibility in the Gulf of Aden. Seaward of the effects of local terrain, visibilities below 5 n mi reach a maximum frequency of about 15% percent in July. In general, low visibilities are more frequent near shore. For example, less than 5 n mi visibility is recorded at Aden and Bender Cassim about 30% of the time. Figure 3-11 is a visual image of a large-scale dust storm. The milky appearance of the Red Sea, Gulf of Aden and Arabian Coast results from dust carried to considerable altitude by vertical mixing in the strong wind flow over the Arabian Peninsula. Normally, low-level restrictions to visibility are due to a dust haze which results from these storms. It is not uncommon, however, for mesoscale dust storms and occasionally sand storms to occur along the shores of the Gulf of Aden and the southern Red Sea. These storms generally travel from land toward the water and most often occur in the evening. They are often (but not always) associated with convective cloud cells. During brief periods, the visibility may be reduced to near zero, but rapid improvement in visibility is usually experienced after the wind subsides.

Fog. Fog seldom occurs during this season except in the immediate vicinity of Cape Guardafui.

Figure 3-11. DMSP image of a large-scale dust storm over the southern Red Sea and the Gulf of Oman. This dust cloud originated in the area northwest of the Persian Gulf more than a day earlier. The thickest portion of the dust cloud, which is crossing the coast just west of Aden, extends upward to mid-tropospheric altitudes. (IR image, not shown, indicates brightness equal to that of nearby convective clouds.) Variation in the grey shades along the eastern shore of the Red Sea indicates the effects of local terrain on the dust density. The anomalous dark area just north of the Bab al Mandab is downwind from a small convective cloud mass; it may be caused by downdrafts from showers over the mountains. Low-level cloud lines in the central portion of the figure and the convective activity along the right border indicate a relatively "strong" monsoon condition. Notice that the symbols on the overlay for this image represent the surface winds from actual observations as well as the location of stations reporting dust or haze. The approximate local sun time at the center of this image is 1100 (0722Z).

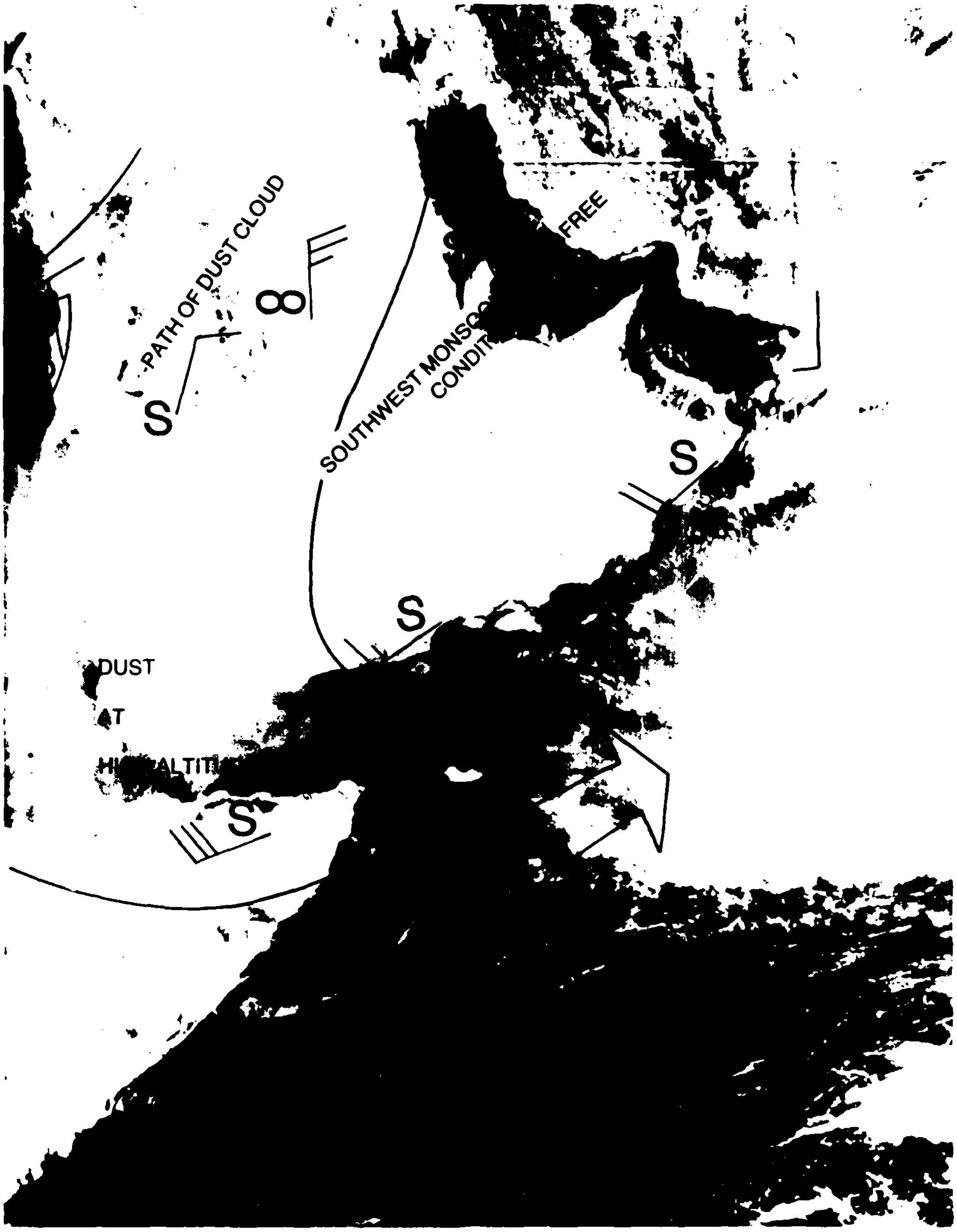

Figure 3-11. DMSP visual image of a large scale dust storm affecting the Gulf of Aden and the southern Red Sea on June 26, 1979.

Precipitation. Visibility restrictions due to precipitation occasionally occur in thunderstorms, but the most serious restriction to visibility is dust rather than rainfall.

VISIBILITY FORECAST RULES/AIDS.

a. Normally, the critical wind speed for raising dust is about 15 kt and for raising sand, about 20 kt. Recent rainfall raises these thresholds and vehicular traffic (e.g., military exercises) lowers them. Regardless of moisture content, greater than normal quantities of particulate material will become airborne at a given wind speed if the surface has been disturbed by heavy traffic.

b. Dust storms are most common in the late afternoon or evening when the atmosphere is most unstable. Exceptions to this general rule occur where the land breeze component opposes/reinforces a strong pressure gradient, (e.g., an early morning maximum at Berbera), or as a result of noctural thunderstorms.

c. Mesoscale dust storms which result from convective activity tend to occur more often on days during which general wind flow is lighter than normal.

d. The first indication of a dust storm is an apparent low cloud on the horizon which appears to be approaching. Often it will consist solely of a low, brown dust cloud. Usually the surface dust/sand cloud will not reach a given point until after the leading edge of the cloud aloft has passed over the point.

e. Air to ground visibility is much less than horizontal visibility in the presence of dust, due to the scattering effect on sunlight.

f. Suspended dust is depicted on satellite visual imagery as a hazy veil. IR brightness is an indicator of the altitude (temperature) of the dust cloud, but is rather inaccurate due to the effect of the warm surface radiation which partially penetrates the dust cloud.

g. When strong dust storms are being reported around the northern end of the Persian Gulf, forecast dust haze one to two days later over the Gulf of Aden and southern Red Sea.

h. The development of large convective cells over coastal ranges increases the probability of local dust/sand storms that evening.

Oceanographic Features

Thermal Structure. The geography of the Red Sea results in an unusual thermal structure. Strong insolation throughout the year keeps the Sea Surface Temperature (SST) above 25°C except in the extreme northern part where it occasionally drops below 22°C during the winter. Since this water is highly saline, it sinks to form the bottom water of the entire basin. The temperature of this deep water is confined to a range between 21.5°C and 22.0°C. The maximum surface temperature occurs in the southern Red Sea where SST reaches about 32.0°C. The vertical temperature variation thus ranges from zero in the north during winter to about 10°C in the south during the summer. The mixed layer ranges from about 300 ft in the winter to less than 100 ft at the beginning of the summer monsoon. Since the sill depth at Bab al Mandab is about 300 ft, the deep water is unusually homogeneous.

The thermal structure of the Gulf of Aden is similar to that of the Arabian Sea except very near Bab al Mandab where high-density water flows out of the Red Sea at sill depth and descends the slope to a depth of nearly 5000 ft. This water is very warm and causes the 15°C isotherm to be depressed to a depth of more than 3000 ft creating near isothermal conditions between depths of about 600 ft and 4000 ft. Considerable cold water upwelling occurs near the entrance to the Gulf of Aden and to a lesser degree, along its northern shore during the Southwest Monsoon. Figures 7-1c and 7-1d show mean vertical temperature profiles from the Gulf of Aden and the southern Red Sea respectively.

Salinity. Since there is no significant inflow of fresh water and very little rainfall, the Red Sea has a negative water budget; therefore, the salinity is extremely high. The water deficit is made up by a net inflow through the Strait of Bab al Mandab, causing salinity to be lowest near the surface. Below the sill depth, salinity exceeds 40 o/oo everywhere and generally increases toward the north at all depths. A small amount of outflow occurs over the sill resulting in highly saline water on the shelf in the Gulf of Aden. Except for this localized phenomenon, Gulf of Aden salinity is typical of the Arabian Sea where excess

evaporation causes salinity to be highest at the surface. Forecasters should expect anomalous underwater sound propagation due to the unusual thermal/salinity structure here.

3.3.3 Persian Gulf and Gulf of Oman

The strong, semi-permanent low-pressure system which persists northeast of this area is the controlling factor of the weather pattern during the summer monsoon period. Local diurnal effects are of secondary importance. Occasionally, subtropical cyclones, which are most intense in the middle troposphere, migrate westward from India and affect the Gulf of Oman during dissipation stages. Figure 3-10 presented an excellent, early-season satellite view of the area.

Low-Level Features

Low-Level Clouds. The Persian Gulf is virtually cloudless during the summer. From the Straits of Hormuz the mean cloudiness increases toward the southeast and also with the season from June to August. In the vicinity of Jiwani, Pakistan, broken to overcast clouds occur nearly half the time in August. Ceilings are below 1500 ft about 15% of the time, but the clouds tend to dissipate during the day, so that afternoon amounts are usually less than half those observed in the morning.

Low-Level Winds. The surface wind flow over the Persian Gulf and Gulf of Oman is controlled by two basic air currents. One flows from the northwest parallel to the long axis of the Persian Gulf; the other is an extension of the broader Southwest Monsoon flow of the Arabian Sea. Both currents are persistent -- particularly in direction. The Gulf of Oman up to the Strait of Hormuz is normally the transition zone between these two currents. The results are northwesterly winds over the Persian Gulf, south to southwesterly winds near the entrance to the Gulf of Oman and variable winds in between. The western approach to the Strait of Hormuz is usually characterized by southwesterly winds due to funneling. Local areas are susceptible to diurnal and terrain effects.

The Summer Shamal. From early June to mid-July, the Persian Gulf experiences what is known as the "Summer Shamal" or the "40-day Shamal". Winds blow steadily from the northwest with few, if any, breaks. The heat low over Pakistan, a trough to the lee of the Zagros Mountains, a semi-permanent high cell over northern Saudi Arabia and local terrain combine to create an enhancement of the low-level flow along the southwest shore of the Persian Gulf — particularly below 5000 ft.

At the surface, this "Summer Shamal" is often strong enough during the day time to cause numerous dust storms over southern Iraq and northwestern Saudi Arabia. The wind speeds decrease at night at the surface but do not decrease aloft. During the night under clear desert skies, radiational cooling causes a strong low-level inversion. The result is a very dangerous, "nocturnal jet stream" with its core located only 1000-2000 ft above the ground. Wind speeds in excess of 50 kt have repeatedly been observed at 1000 ft over Bahrain with the most probable time of occurrence being between midnight and dawn (surface winds at the time are usually less than 20 kt). Because of the potential threat of this phenomenon to Navy aircraft attempting to land at Persian Gulf airfields, a forecasting nomogram developed by Membery (1983) is reproduced in Section 7.4 dealing with Carrier Air Operations.

WIND FORECASTING RULES/AIDS.

a. Wind speeds in the Persian Gulf vary with the strength of the low pressure center and generally change gradually from day to day.

b. When gradient-level winds are 25 kt or more from the north or northwest, expect blowing dust to occur about mid-day if the surface inversion is destroyed by heating.

c. During the "Summer Shamal" expect a strong, low-level, "nocturnal jet" (midnight to dawn) to occur on clear, stable nights along the southern shore of the Persian Gulf. Winds at 1000 ft exceed 50 kt while surface winds are less than 20 kt (see Section 7.4 for forecast nomogram.)

Upper Level Features

The Monsoon Trough slopes sharply southeastward with height from a surface position near the Strait of Hormuz to a position over Bombay at the 500 mb level. The upper-level subtropical ridge extends eastward and west south-westward from a position near the northern end of the Persian Gulf.

High Clouds. Except over the northern Persian Gulf where summer clouds are rare, high clouds reach a secondary maximum during July and August. Generally these clouds consist of cirrus blow-off from monsoon disturbances occurring near the northwestern Indian Coast.

Upper Winds. North of the Monsoon Trough, winds generally veer from northwesterly to easterly with height. Near the northern end of the Persian Gulf, winds generally persist from the northwesterly quadrant below the 500 mb level. These winds are related to the Shamal and are strongest (up to 40 kt) at the lower levels (about 3,000 ft), then decrease with height.

Visibility Restrictions

Dust and Sand. In the northern two-thirds of the Persian Gulf, visibility reaches a minimum with the onset of the "40-day Shamal" in June. For example, Bahrain drops from well over 50% of visibility observations of 5 n mi or more in May to about 35% in June. Gradual improvement occurs in July and August. In the southern third of the Persian Gulf and in the Gulf of Oman, July is the worst month for visibility. Observations taken in the shipping lanes of the Gulf of Oman indicate that visibilities of less than 5 n mi occur 10% to 15% of the time in July, but drop to less than 10% in August.

Coles (1938) found that over land areas surrounding the Persian Gulf the times of start of dust storms are largely influenced by diurnal changes of wind speed. During the "Summer Shamal" wind speeds are generally light at night and free from convectional eddies due to the strong low-level inversion. As the inversion disappears one to two hours after sunrise, turbulence increases rapidly, and surface winds exceed the critical dust-raising speed of about 16 kt. The

winds then slack off again about 1800L with a marked decrease in dust being carried aloft. Forecasters should be aware, however, that layers of dust raised during the day usually form a thin lens under the inversion, and the resulting layer of poor visibility at this level can persist for long periods of time. On the day after a major dust storm, visibility at the surface may still be less than one (1) n mi due to settling of suspended dust.

VISIBILITY FORECAST RULE.

a. If the night sounding (or aircraft reports) indicates 1000-ft winds exceed 30 kt in "Summer Shamal" cases with strong low-level inversions at night, radiational heating will cause surface winds strong enough to raise dust the next day.

Fog. Fog is extremely rare during the summer.

Precipitation. Rainfall is rare during the summer season. Occasionally subtropical cyclones will cause weak thunderstorm activity near the northern shores of the Gulf of Oman.

Oceanographic Features

Temperature. Since the Persian Gulf is very shallow, its thermal characteristics are much like a lake. The surface temperature reaches a winter minimum of about 18°C in the northwest corner. This relatively cold, dense water sinks to form the bottom water of the Gulf which stabilizes at about 20°C during the summer, while the surface temperature increases to a maximum of about 33°C. The characteristics of the water in the Gulf of Oman resemble those in the Arabian Sea except on the narrow shelf near the approaches to the Strait of Hormuz where warm, high-density water flows down the shelf slope, depressing the 20°C isotherm to about 1000 ft. Weak upwelling occurs near Ras Al Hadd.

Salinity. Except for the surface layer near the Strait of Hormuz, salinity in the Persian Gulf ranges between 39 o/oo and 40 o/oo. The water which flows back into the Gulf of Oman has a salinity greater than 39 o/oo. Most of the water in the Gulf of Oman is more saline than that found in the Arabian Sea. For example, at about 600 ft, salinities are about 36.5 o/oo versus about 35.3 o/oo at 10°N.

3.3.4 Indian Peninsula

The Southwest Monsoon winds first influence Indian weather during the last week of May or the first week of June. The first effects are often a period of intense convective activity usually associated with an "Onset Vortex". The average date of the onset of the rainy season varies from about May 29 in the south to about June 12 at Bombay. Monthly mean maximum rainfall occurs in June along the southern Indian coast (south of 12°N) but in July farther north. The intensity of the monsoon winds and rain eases in August and decreases sharply in September. Easterly winds accompanied by strong convective activity often signal the end of the Southwest Monsoon near the end of September. A secondary maximum in rainfall occurs in the area south of 10°N in late September and October as the Near Equatorial Trough is re-established.

Monsoon Intensity. The total pressure gradient from south to north in the Arabian Sea is relatively constant from day to day during the summer season. The distribution of this gradient varies significantly, however. Figure 3-12 shows mean pressure differences between "strong" and "weak" monsoon cases. The "anomaly" centered over the Gulf of Canbay causes a weakening of the gradient toward the north and a strengthening of the gradient toward the south. Figure 3-13 depicts typical pressure distributions.

"Strong" Monsoon Patterns (see Figure 3-6). Strong monsoons are characterized by generally weaker winds over the extreme northern Indian Coast and stronger winds along the central Indian Coast. In some cases, a cyclonic eddy exists near the Kathiawar Peninsula causing the southwesterly winds along the coast of Pakistan to veer to the northwest and weaken. Low-tropospheric

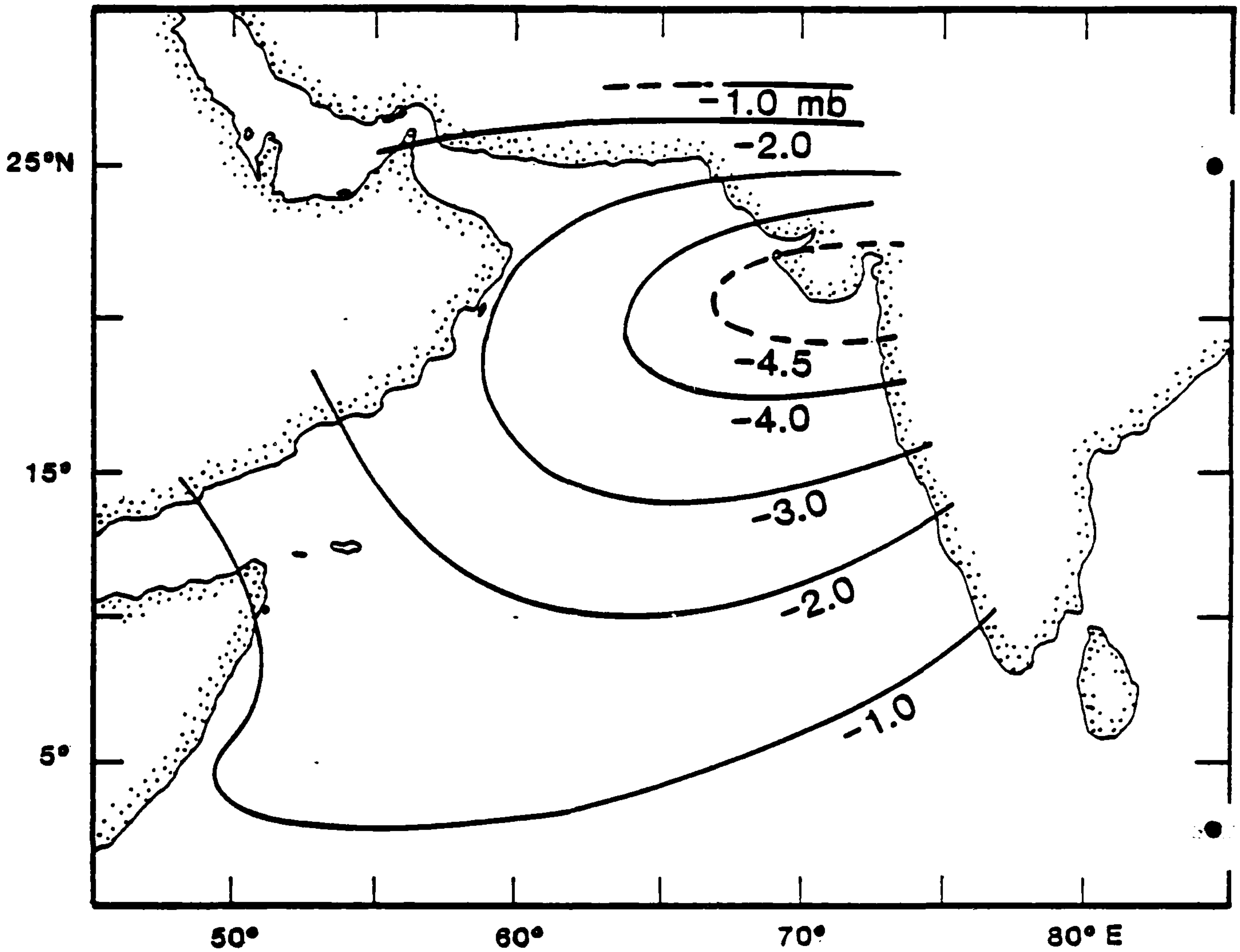

(above)

Figure 3-12. Isopleths of mean pressure differences (mb) between strong and weak Arabian Sea monsoon flow (adapted from Ramamurthy, 1972).

(right)

Figure 3-13. Mean pressure distribution during periods of strong and weak Arabian Sea monsoon flow (adapted from Ramamurthy, 1972).

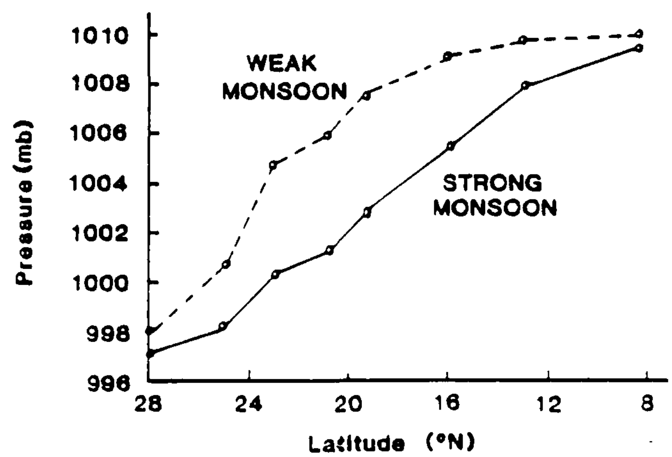

convergence and associated high-level divergence cause extensive heavy precipitation off the Indian Coast. Orographic effects intensify the precipitation inland. Strong westerly winds occur throughout the lower troposphere between 10°N and 15°N with the maximum near 3,500 ft. Multi-level cloudiness extends 500 to 700 n mi westward from the Indian Coast, and cirrus blow-off often covers most of the Arabian Sea.

"Weak" Monsoon Patterns (see Figure 3-8). "Weak" monsoon conditions do not necessarily indicate universally weaker winds. In fact, the pressure distribution which leads to the "weak" case results in stronger winds along the extreme northern Indian and Arabian Coasts. The wind maximum usually found between 10°N and 15°N from 55°E to 60°E is weaker, however, and its extension toward the central Indian Coast disappears and is replaced by a local minimum near Mangalore. This flow pattern tends to suppress vertical motion and convective activity. Terrain induced cloudiness occurs, but coastal areas may be relatively clear and rainfall is more scattered.

INDIAN COASTAL FORECAST RULES/AIDS.

a. When a Mid-Tropospheric Cyclone occurs over the northern Indian Coast, the most severe weather and greatest vertical cloud development occurs in the southwest quadrant.

b. Westerlies along the Indian Coast south of the Gulf of Canbay extend to a higher altitude (above 500 mb) during strong monsoon cases.

c. Overcast conditions extend 500 to 700 n mi westward from the Indian Coast during strong monsoons.

d. Periods of strong convective activity often mark the beginning and the end of the Southwest Monsoon near the Indian coast.

e. Diurnal effects are minimal during the Southwest Monsoon along the Indian Coast.

f. Wind speeds are lower over the Indian Coast than they are farther to seaward.

g. Thunderstorms are much less frequent during the strongest period (July and August) of the Southwest Monsoon than they are near the beginning and end (June and September).

h. An "Onset Vortex" (see Section 3.2.3) frequently forms near the southern Indian Coast and moves northward just prior to the first "strong" monsoon of the season.

i. Weakening of the upper-level subtropical ridge indicates that a monsoon "break" is likely.

3.3.5 Atlantic Approaches to Arabian Sea

Cloud and Wind Patterns

South of 25°S, conditions similar to those in the North Atlantic in the winter can be expected in both the Atlantic and Indian Oceans. On the Indian Ocean side of Africa, cold surges penetrate northward to at least 15°S, often causing a funneling effect in the Mozambique Channel. Figure 3-14 illustrates an example of a cold front accelerating through the passage. These cold surges strengthen the Southeast Trades, which in turn intensify the Somali Jet and the Arabian Sea Southwest Monsoon. Wind directions tend to parallel the African Coast north of 15°S with an onshore component south of the Equator.

Agulhas Current/Wave Patterns

The Agulhas Current flows in a southwesterly direction parallel to the southeast coast of Africa (see Figure 3-15). It is quite strong (maximum greater than 4 kt) and very narrow (within 100 n mi of the shoreline). The axis of maximum current speed tends to coincide with the 100 fathom depth contour and therefore parallels the edge of the continental shelf. The area shown in Figure 3-15 has been the scene of several supertanker casualties due to current/wave interaction phenomena.

The significance of the Agulhas Current stems from its effect upon ocean wave characteristics. Figure 3-16 shows an idealized wave profile and the profiles resulting from the effects of following and opposing currents on the idealized wave. Two effects are important: changes in wave height and changes in steepness. Significant increases occur in both when the current direction opposes the wave direction. Table 3-1 gives examples of what happens to wave height and length when currents and deep water waves are in opposition.

Southerly waves/swell are common in this area, particularly during the southern hemisphere winter. They tend to approach a "fully developed" state for a given wind speed due to unlimited fetch and duration. When these waves oppose the Agulhas Current, their height and steepness increase spectacularly. The effect is much weaker as the wave encounters lower current speeds closer to shore; therefore, the maximum height and steepness due to this interference phenomenon occur near the core of the current. Analysis of many observations indicates that the waves near shore are usually lower (contain less energy) than those occurring in deep water seaward of the Agulhas Current.

AGULHAS CURRENT FORECAST RULES/AIDS.

a. If strong southerly waves/swell are expected, recommend a track as close to shore as safe navigation will permit (particularly if on a southerly track). If this is not feasible, stay well offshore (outside the 100 fathom line).
b. If the predominant wave/swell is from the northeast, the most comfortable track should be found near the 100 fathom line.
c. If expected waves are slight to moderate from any direction, the effect of the Agulhas Current on speed made good is probably the most important factor in the selection of a track.

3.3.6 Pacific Approaches to Arabian Sea

This section treats routes entering the Indian Ocean via the South China Sea (Strait of Malacca), Java Sea or Australian ports. These routes fall within the "monsoon region" as defined by Ramage (1971). Ships sailing from southern Australian ports do not experience true monsoon weather until they approach the Arabian Sea. Cuming (1973) treats the Bay of Bengal in detail.

Cloud and Wind Patterns

During the Southwest Monsoon, sea level pressure decreases continuously from the subtropical high pressure ridge of the Southern Hemisphere to the heat low over southern Asia. This pressure pattern results in a buffer zone straddling

Figure 3-14. DMSP visual image of the southern African Coast. This photo was selected to illustrate the cloud cover to be expected during an "Atlantic Approach" to the Arabian Sea early in the Southwest Monsoon regime. A weakening cold front is moving northward through the Mozambique Channel and across southern Madagasgar. Clouds over the northern part of Madagasgar indicate onshore flow from the Southeast Trades with a clear area to the lee of the island. Low-level cloud lines over the southern African Coast (see Figure 2-1 for definition) indicate that the southerly flow in that area becomes more southwesterly over the horn of Africa. Over Somalia, the low-level cloud lines are partially obscured by higher-level cloud lines which are nearly perpendicular to the low-level wind direction. These transverse cloud lines are often seen when strong vertical wind shear exists. The difference in altitude of the intersecting cloud lines would be obvious in the IR equivalent of this image. Note that the cirrus plumes near the upper border of the image indicate easterly winds at high altitude. The approximate local sun time at the center of this image is 1130 (0836Z).

Figure 3-14. DMSP visual image of the southern African Coast and the Atlantic Approaches to the Arabian Sea (June 22, 1979).

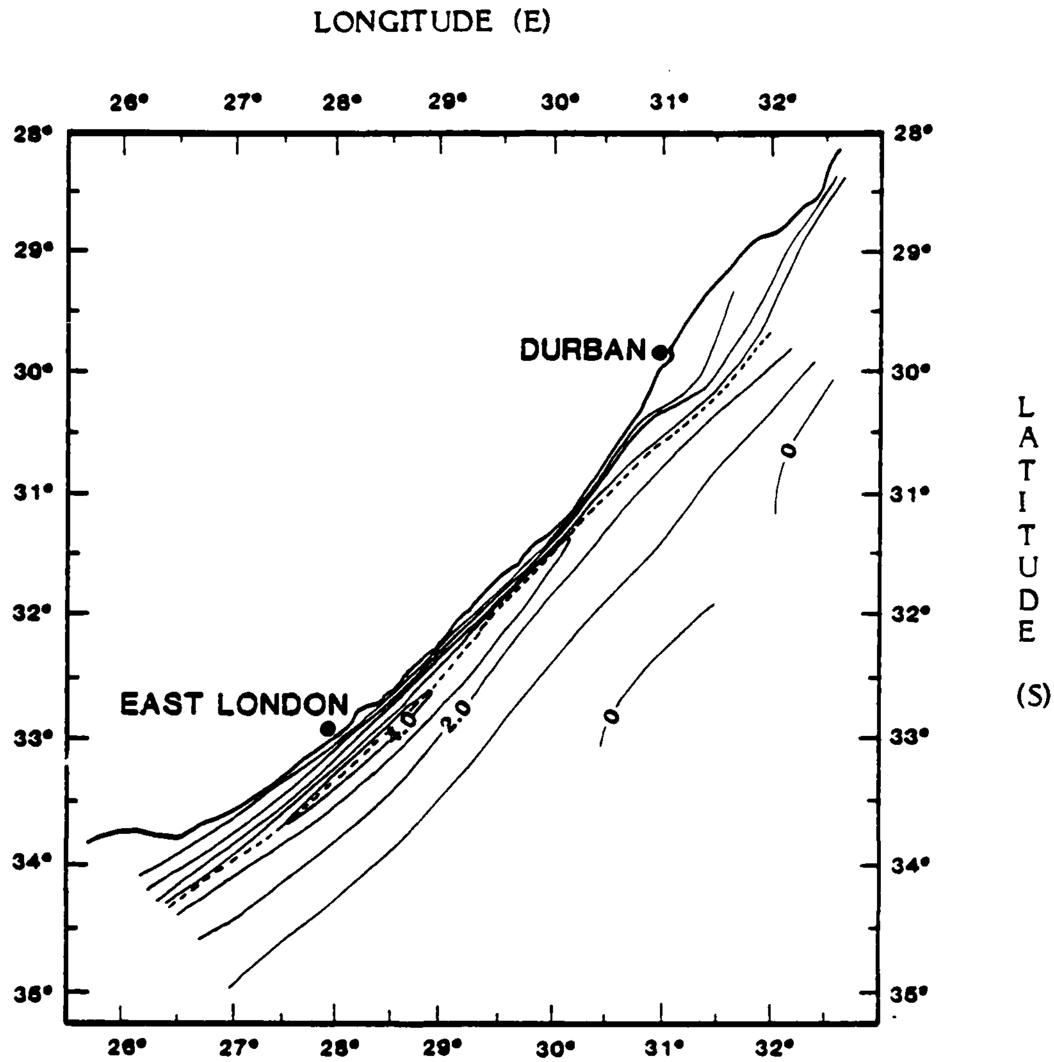

Figure 3-15. Section of southeastern African coast showing Agulhas Current mean speed toward the southwest parallel to the coast. The axis of maximum current speed is shown as a dashed line. The solid lines are current speed in kt (from Schumann and Duncan, 1976).

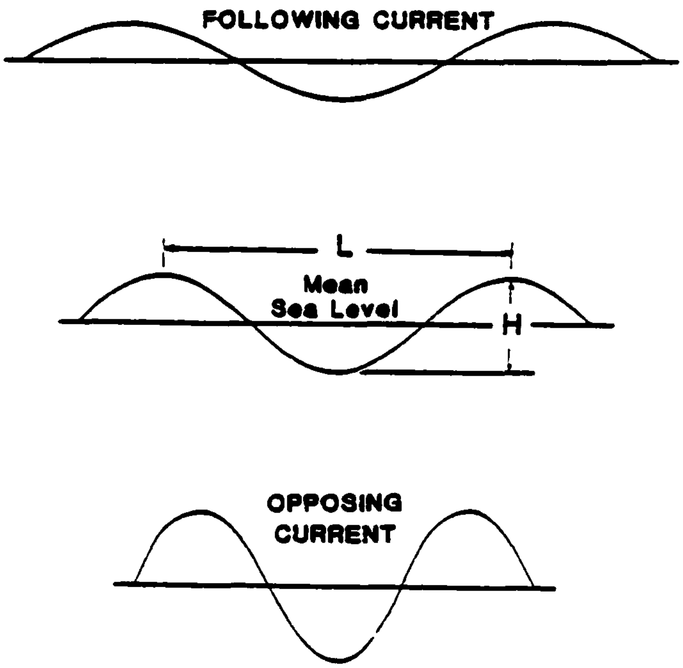

Figure 3-16. An idealized wave profile showing the changes that occur in a following and an opposing current (adapted from Schumann and Duncan, 1976).

Table 3-1. Examples of wave height changes when selected waves with a 10-ft height in deep water meet an opposing current where the current speed is 4 kt.

DEEP WATER WAVE HEIGHT (Ft)	PERIOD (Sec)	DEEP WATER WAVE LENGTH (Ft)	INTERFERENCE WAVE HEIGHT (Ft)	INTERFERENCE WAVE LENGTH (Ft)
10	13	865	13	735
10	10	512	14	384
10	8	328	16	197

the Equator between the Southeast Tradewinds and the Southwest Monsoon. This area is generally characterized by light to moderate southerly winds and scattered to broken cumulus clouds. Scattered light to moderate showers can be expected, particularly near the Equator. Ships on routes from Australia cross the main Southeast Tradewind band ($10^{\circ}S$ - $20^{\circ}S$) where winds to 25 kt can be expected. Ships using the Java Sea route are likely to experience considerable thunderstorm activity, particularly near Selat Sunda. The most direct route through the Strait of Malacca is characterized by broken cumulus, showers and only occasional thunderstorms. Winds and seas on this route may present a problem, particularly on westerly headings. Southwest winds of 10 to 20 kt are most common, but they frequently exceed 20 kt and occasionally reach gale force. Since most winds are steady, they lead to "fully developed" wave heights.

Tropical Cyclones

Tropical cyclones are rare south of $10^{\circ}N$ in the Indian Ocean during the Southwest Monsoon regime.

4.0 FALL TRANSITION (OCT - NOV)

4.1 General Description

In this season, the amount of insolation received over the Northern Hemisphere decreases rapidly causing the heat lows over the land masses to weaken and finally disappear. The Monsoon Trough retreats southward into the Arabian Sea and should more properly be called the "Near Equatorial Trough". In October, the surface winds over the Arabian Sea are mostly light and variable, but by November, light to moderate northeasterlies predominate -- especially over the northern portion. In the upper troposphere the anticyclone which was located over the Himalayan Massif moves southeastward to the vicinity of the coast of Burma.

As a result of these circulation changes, large-scale cloud cover reaches a minimum over the area. However conditions become favorable for the development of tropical cyclones in the Near Equatorial Trough (see Tropical Cyclone Forecast Rules/Aids, Section 3.3.1). Occasional cold fronts influence the northern Arabian Sea during the Fall Transition period, but their effects are relatively weak and of short duration. Visibilities are generally good except around the tropical storms and in moderate dust storms associated with Arabian Peninsula cold frontal passages. Wave heights are generally minimal (except around tropical storms), but weak surface winds may adversely affect carrier aircraft launch/recovery operations.

Figure 4-1 illustrates the major features of the Fall Transition period. A tropical cyclone is affecting the Central Arabian Sea; a weak surge of cold air is moving over the northern Persian Gulf; considerable convective activity is apparent in the Pacific Approaches and in the vicinity of the southern Red Sea; other water areas in the Northern Hemisphere are relatively cloud free. With the exception of tropical cyclones, weather during the Fall Transition period is generally benign.

4.2 Large Scale Circulation Features

The Southwest Monsoon and the Northeast Monsoon are typified by persistent wind flow patterns with variations generally limited to changes in the

Figure 4-1. Visual mosaic showing typical cloud conditions for the Fall Transition period. Weakening of the thermal troughs and a southward shift of the Near-Equatorial Trough bring light northerly flow to the northern regions. A tropical cyclone is shown over the Central Arabian Sea. The cloud band over the Persian Gulf reflects an extratropical disturbance. These disturbances are usually weak and short-lived at this time of year and only rarely penetrate to the Arabian Coast. Wide-spread convective activity is seen over the southern Bay of Bengal, Southeast Asia and equatorial eastern Africa. In areas clear of tropical cyclones and convective activity, light winds and fair weather prevail. This is reflected in the satellite image by a general lack of clouds. In the Southern Hemisphere the storm track is moving poleward, improving weather and sea conditions in the Atlantic Approaches, but significant frontal weather can still be expected off South Africa.

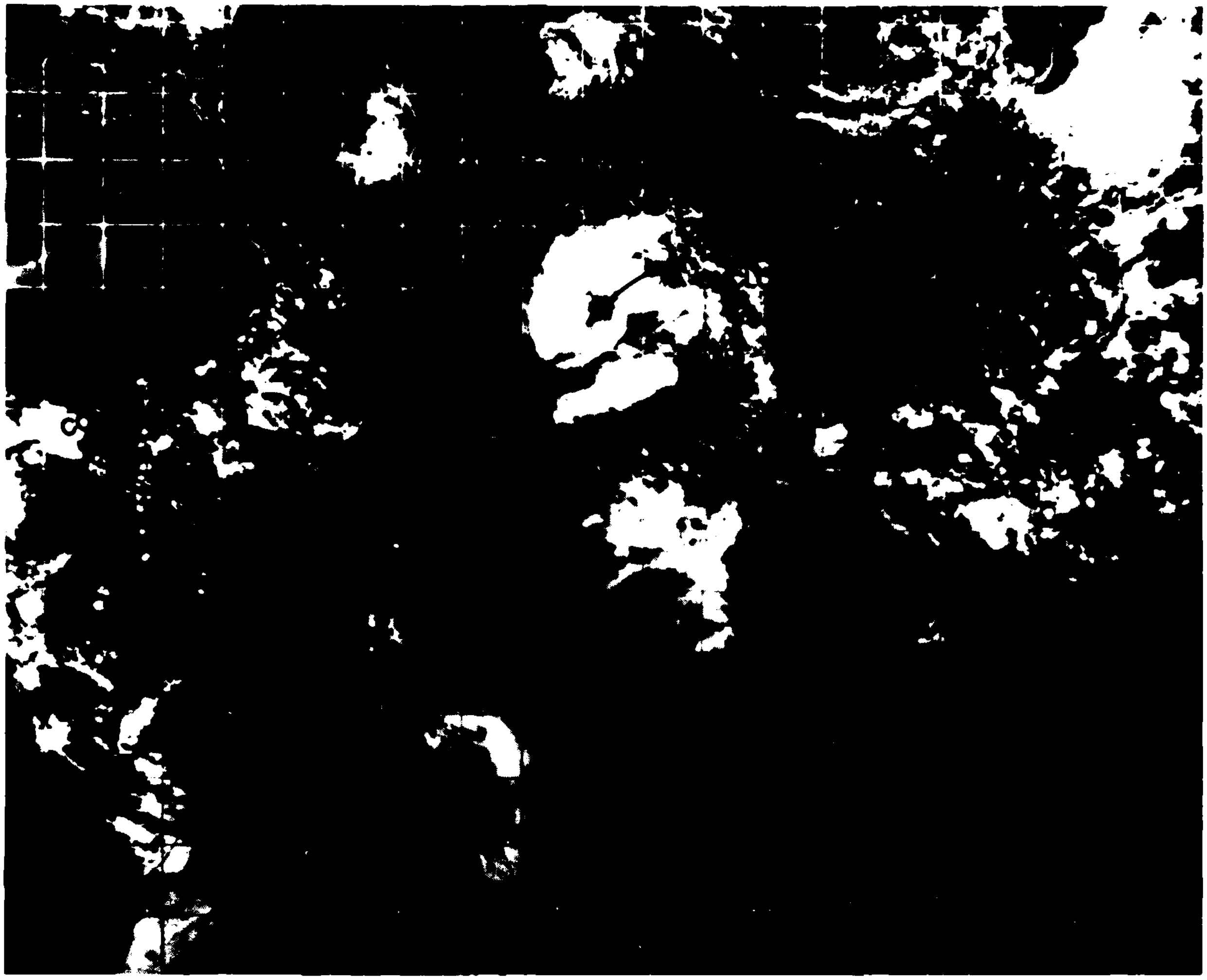

Figure 4-1. Visual mosaic produced from data recorded on November 6, 1982 showing cloud conditions typical of the Fall Transition.

wind speed. The transition seasons are periods of pattern reversal; directional and temporal changes are therefore maximized. This leads to somewhat meaningless mean values for parameters such as winds, clouds, ocean waves, etc.

The flow reversals result from the rapid decrease in solar radiation which cools the lower troposphere causing the heat trough to be replaced by a cool ridge. As one pressure gradient regime disappears and the opposite is being established, relatively calm conditions with considerable short-period variability predominate. In general, this is the most pleasant and benign season of the year. An exception to this rule is an increase in tropical cyclone activity.

4.2.1 Climatology

Naval Oceanography Command climatological publications (see Appendix A) contain monthly and seasonal data on several operationally significant parameters and the data used in Figure 4-2a were extracted from them. It is not the purpose of this Handbook to duplicate existing publications; however, for ready reference and to illustrate the discussion which follows, Figures 4-2a through e provide pertinent climatological data which are representative of the Fall Transition season.

The data on which these figures are based are not uniformly distributed over the region; they are biased by coastal and island station observations. In spite of some loss of reliability and detail over ocean areas, the figures provide a useful summary of parameters used in routine forecasting. It must be remembered, however, that mean values are less likely to be representative of daily conditions during this season — especially if they are derived from vector quantities of opposite sense (e.g., winds).

4.2.2 Troughs and Frontal Systems

During late September or early October, the heat lows disappear and are replaced by a weak high pressure regime. Th Near-Equatorial Trough reforms with an eastnortheast - westsouthwest orientation between 10°N and 15°N but migrates southward as the continental high pressure strengthens. A quasi-permanent, low-pressure area over Sudan usually has a trough extending northeastward across the Red Sea.

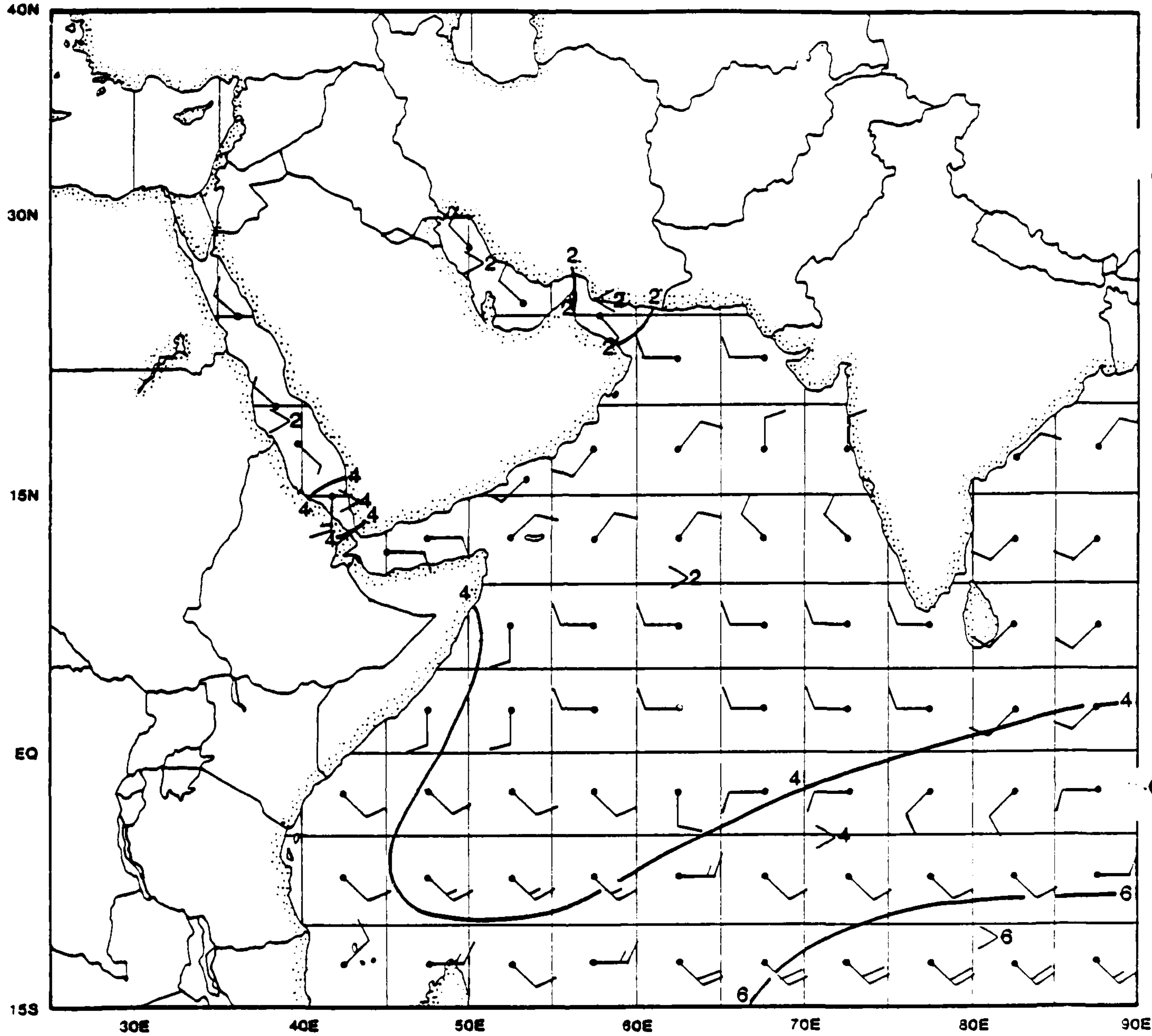

Figure 4-2a. Mean October surface winds (wind barbs) and seasonal mean significant wave heights in feet (contours). The wind barbs represent the average over a 5^{o} rectangle of latitude and longitude in the Arabian Sea. Wind barbs representing the restricted waters of the Red Sea, Persian Gulf and the Gulfs of Aden and Oman are plotted over the water area that they represent. When two or more wave groups were reported, only the one with the high^st wave was selected for the data set from which the significant wave height contours were produced. Therefore, where separate wind waves and swell are common, the values shown will tend to be low. (Data for this figure were extracted from Naval Weather Service Detachment, Asheville, 1973 and 1974, and Naval Oceanography Command Detachment, Asheville, 1980 and 1982.)

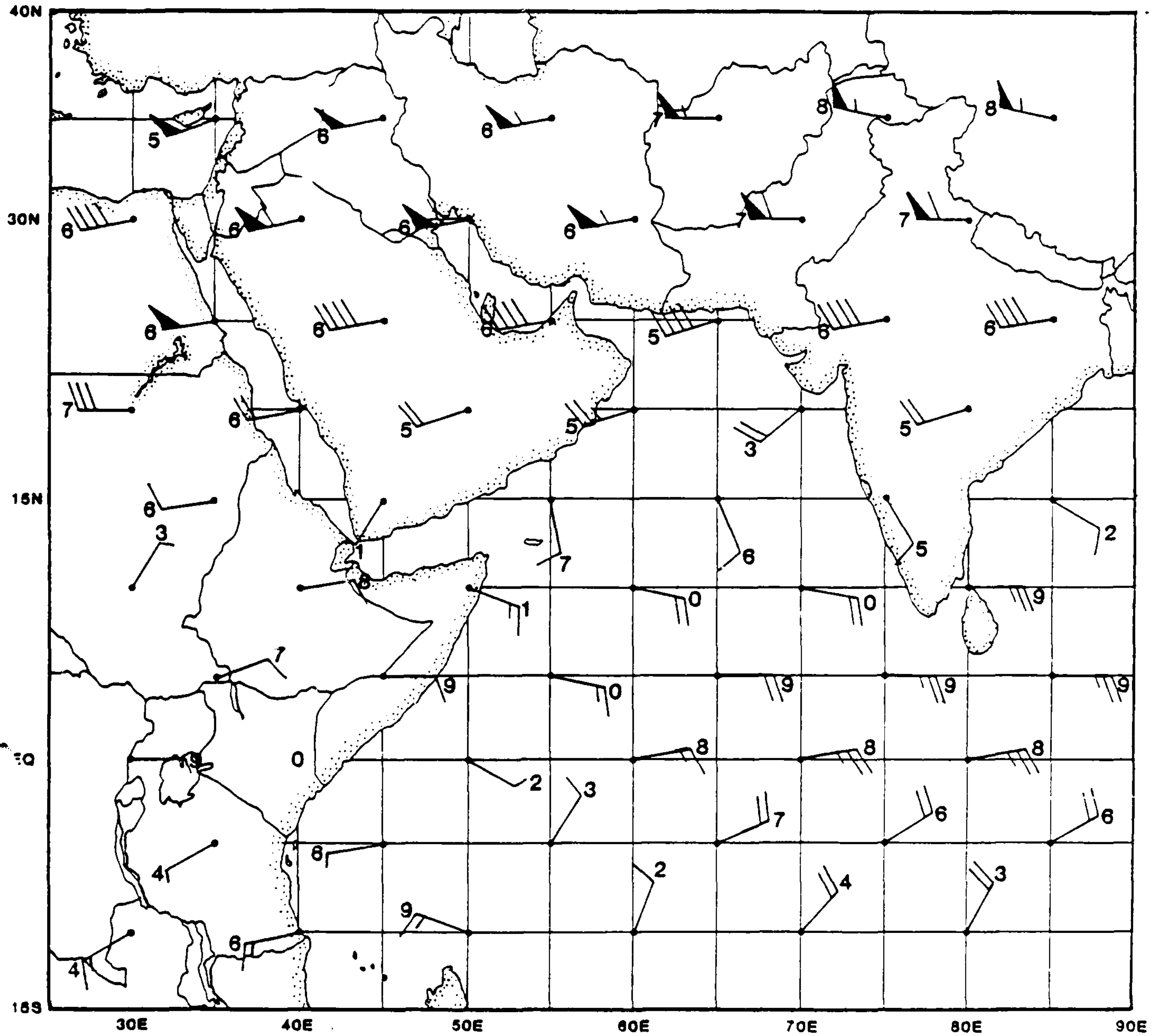

Figure 4-2b. Mean October 200 mb winds (adapted from Sadler, 1975). The numeral by each wind barb is the tens digit of direction. A circle around the latitude-longitude intersection indicates a light, variable wind. Note that the axis of the Subtropical Ridge has shifted southward to about 16°N and that the Subtropical Jet is appearing in the area which was occupied by the ridge during the Southwest Monsoon.

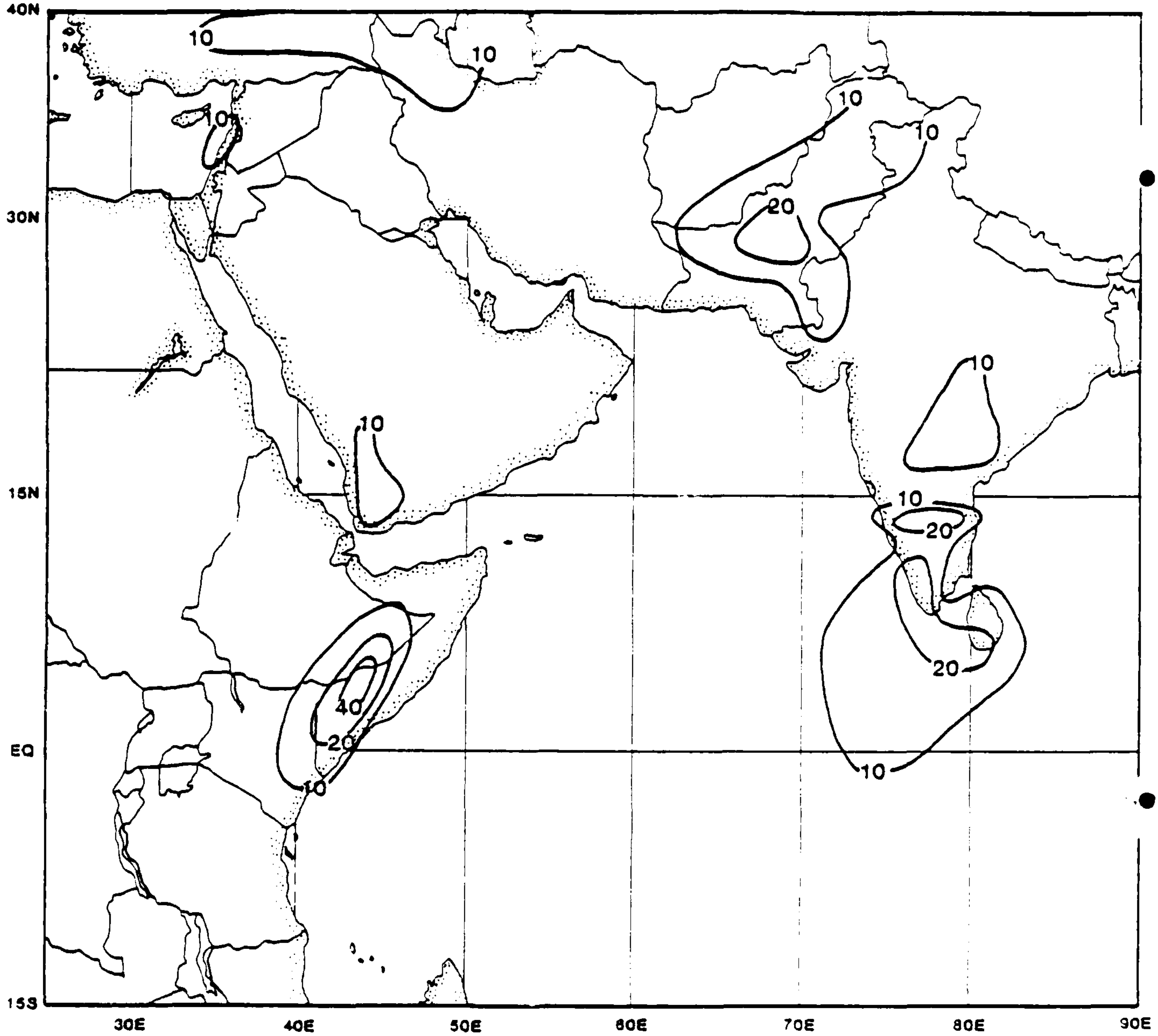

Figure 4-2c. Percent frequency of ceiling less than 1500 ft or visibility less than 3 n mi. Nearly all of the water areas of this region experience the least low cloudiness and the best visibility during the Fall Transition period. Most of the areas showing higher than 10% frequencies are due to persistent convective activity (see Figure 4-2e).

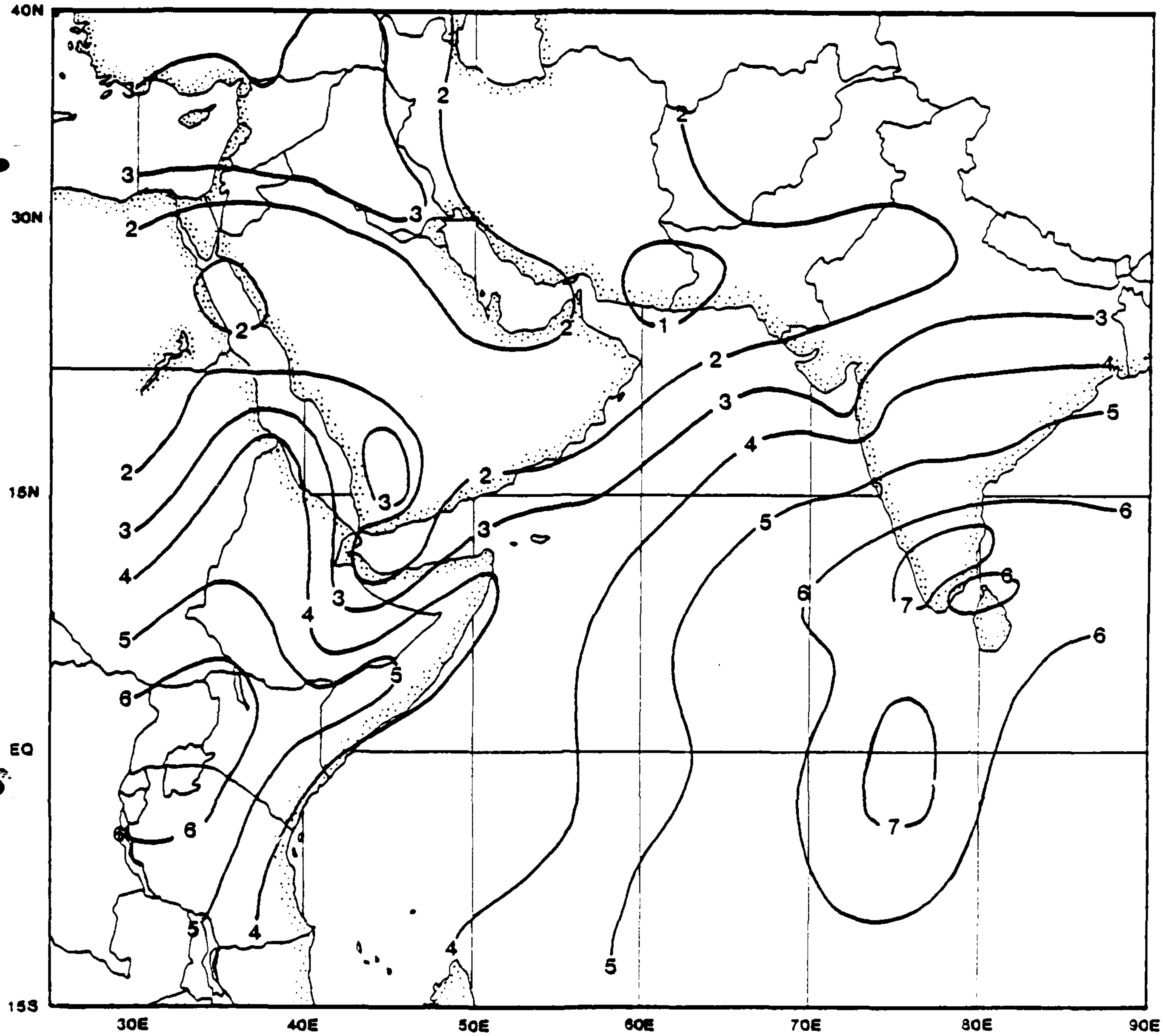

Figure 4-2d. Mean total cloud cover in tenths. The cloudiness maxima are highly correlated with thunderstorm frequency (see Figure 4-2e) and consist mostly of cumiliform clouds and cirrus blow-off.

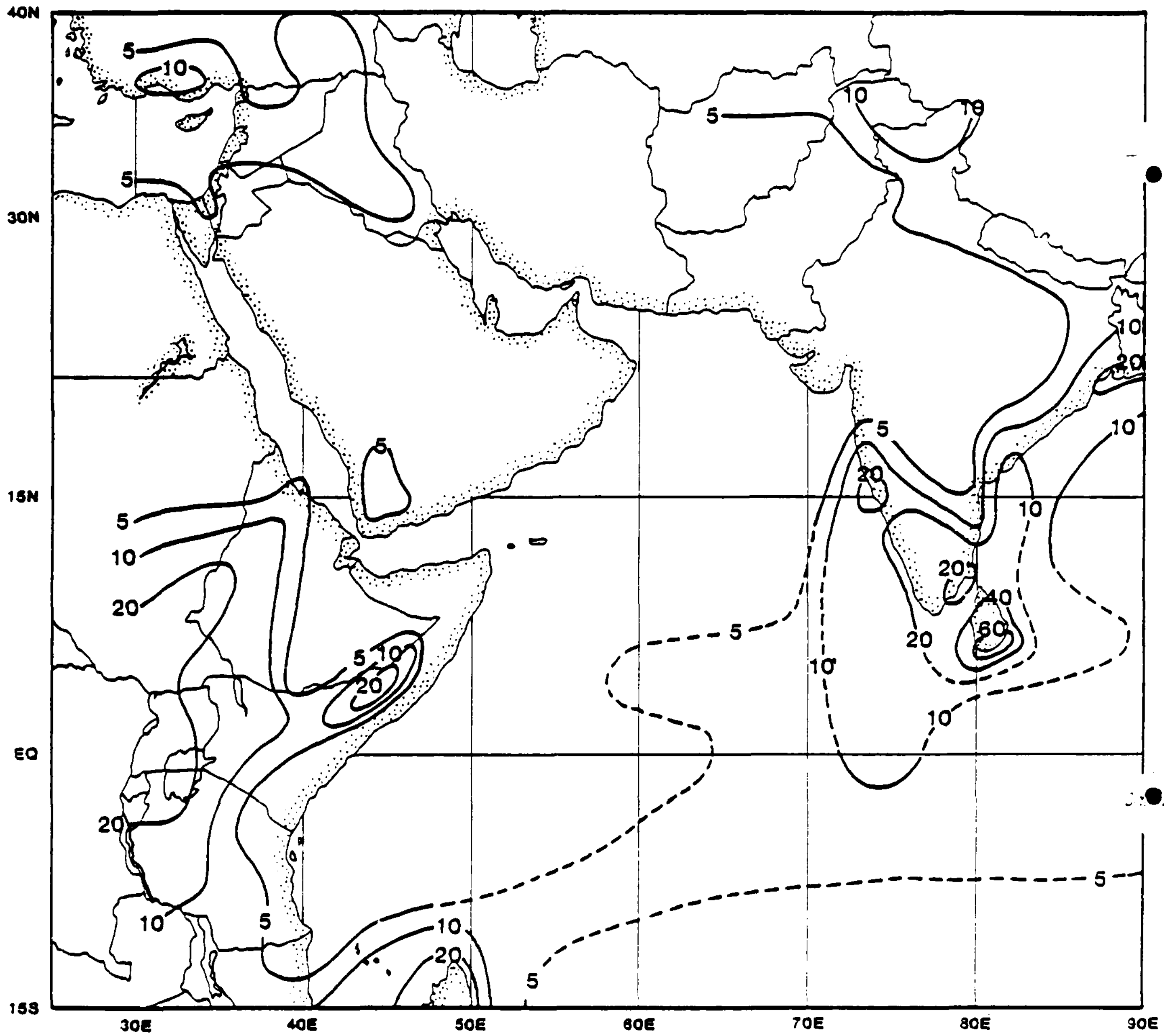

Figure 4-2e. Percent of days with thunderstorms. Data on thunderstorms near the Equator in the Central Arabian Sea are very sparse. Dashed contours are estimates based on satellite imagery; solid contours are based on observations. The south coast of Sri Lanka experiences thunderstorms on more than 75% of the days in October and November!

As the transition to the Northeast Monsoon progresses, the Near-Equatorial Trough is forced southward to a position near the Equator by late November, and most of the Arabian Sea is influenced by weak to moderate northeast flow. The the quasi-permanent East African low-pressure area extends southward to straddle the Equator. A trough continues to extend northeastward over the Red Sea. Frontal passages start to influence the northwest portion of the area covered by this Handbook.

The Red Sea Convergence Zone. As the Southwest Monsoon weakens and is replaced by the Northeast Monsoon, the wind flow in the Gulf of Aden and the southern Red Sea is reversed to become easterly and southeasterly, respectively. The continued northwest flow over the remainder of the Red Sea forms a sharp Convergence Zone in the southern part of the sea. As the monsoon progresses, this zone drifts northward to a mean winter position near 20°N. This zone of convergence migrates with the season and with synoptic changes but seldom retreats to the southern end and rarely advances all the way to the northern end of the Red Sea. It is usually marked by a distinct cloud band which is unmistakable on satellite photos.

Figure 4-3 illustrates a typical Convergence Zone Cloud Band (CZCB). South of the cloud band, surface winds are southerly; to the north they are northwesterly. The Convergence Zone itself is usually characterized by light, variable winds. Development of an anticyclone over the Arabian Peninsula will strengthen the southerly winds, forcing the CZCB northward. The movement of a surface low pressure center from Sudan across the Red Sea results first in a northward migration of the CZCB due to enhanced southerly flow and then a rapid southerly movement as the cold surge penetrates southward behind the low center. The CZCB persists until the latter part of the Spring Transition period when southerly winds cease in the Red Sea.

Frontal Disturbances. The southerly drift of the Subtropical Ridge permits intrusion of disturbances of extratropical origin. Although typical frontal passages are rare until late in the transition period, disturbance bands with time and space continuity occur in the Arabian Peninsula area (particularly over the Persian Gulf) with increasing frequency. They are often delineated by moderate to severe squalls with accompanying sand, dust and thunderstorms. These disturbances seldom reach the Arabian Coast but occasionally affect the Gulf of Oman.

Figure 4-3. DMSP visual image of the Red Sea and Gulf of Aden. This photo was selected to illustrate a well-developed Convergence Zone Cloud Band (CZCB) which forms during the Fall Transition and continues through the winter. The northern Red Sea is experiencing north-westerly surface winds while the southern portion has southerly flow. The CZCB is seen as low stratiform clouds with an embedded CB near 18°N. A cold front is approaching the CZCB from the northwest. Low-level winds behind the front are channeled by the steep terrain bordering the Red Sea. Since the water is warmer than the air, it rapidly absorbs moisture and heat and forms scattered to broken cumuliform cloudiness along the central axis of the sea. Heating of the surface air by the water and the downslope flow of the cold air along the shore creates a land-breeze effect which constrains the cloudiness to the open water. (Note the relatively clear areas near shore in the northern Red Sea.) Faint bands of cirrus oriented west-southwest to east-northeast are noted across the Red Sea near 15°N and 20°N. Cirrus bands of this nature are usually aligned with jet streams, although the individual cirrus filaments often form an angle with the axis of the jet stream core. The approximate local sun time at the center of this image is 0900 (0612Z).

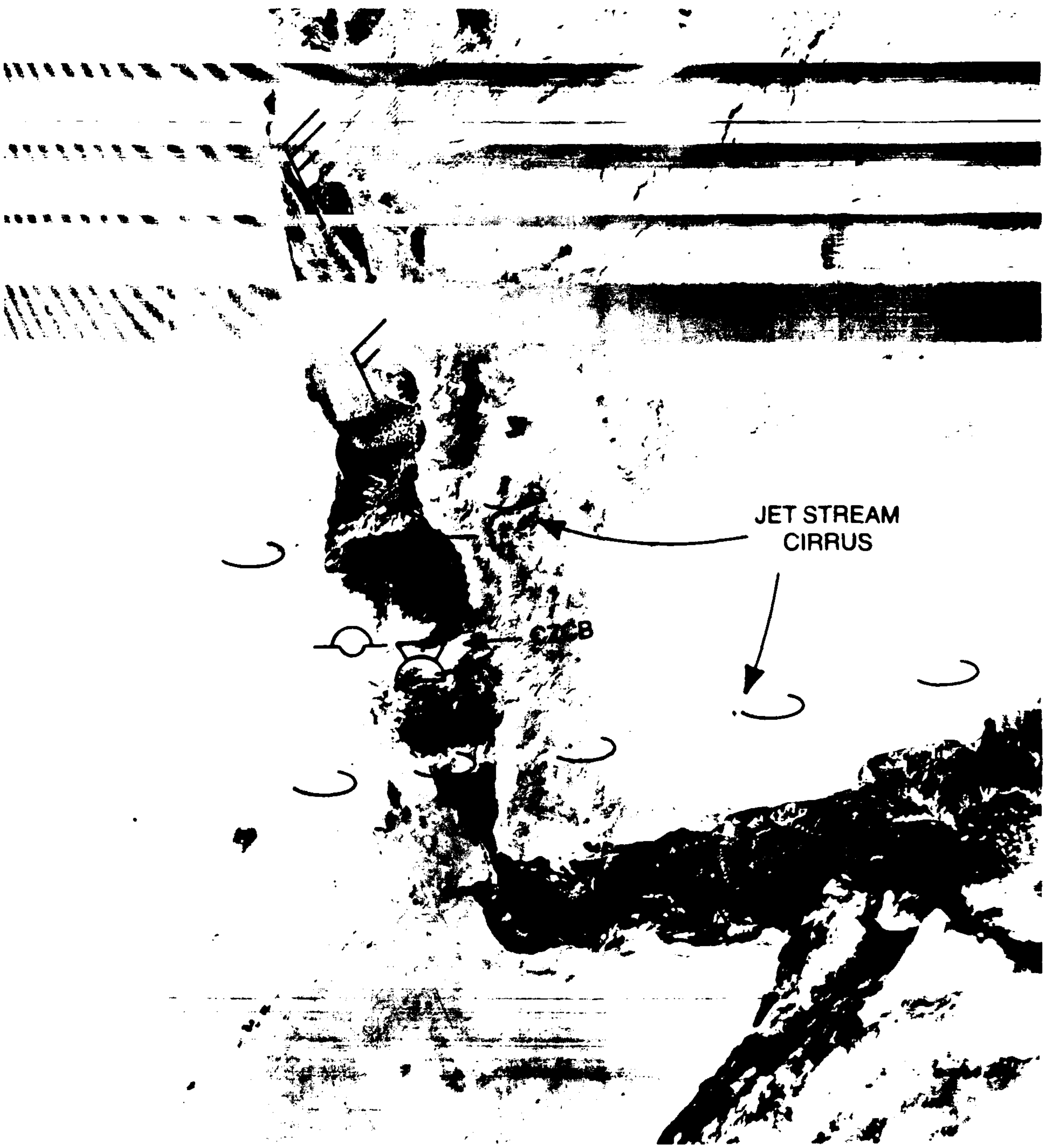

Figure 4-3. DMSP visual image of the Red Sea and Gulf of Aden on December 15, 1979 showing a well-developed Convergence Zone Cloud Band (CZCB).

TROUGH, FRONT AND SQUALL FORECASTING RULES/AIDS.

a. At least one severe squall line (locally called "Uhaimir") should be expected to move across the Persian Gulf during the October-November transition period. Generally cooler and drier weather follows.

b. "Winter Shamals" start to occur in October or November (see Section 5.3.3).

c. The wind direction of the Winter Shamal is generally parallel to the shorelines of the Gulfs.

d. A frequent forewarning of an approaching Shamal is the arrival of longer period swell.

e. The occurrence of Shamals is not dependent on the time of day.

f. The Convergence Zone in the Red Sea is usually formed by early October when winds near Bab al Mandab shift from northwest to southeast. It migrates rapidly to its mean position near 20°N.

g. The Convergence Zone is usually marked by a cloud band (CZCB) which is easily recognizable on satellite imagery.

4.2.3 Large Scale Cloud and Wind Patterns

The Arabian Sea

The shift from the southwesterly to northeasterly surface flow usually becomes apparent first along the Arabian Coast. Light variable winds appear in the Gulf of Aden in September and along most of the Arabian Coast in October. As the pressure gradient over the northern Arabian Sea reverses direction (usually in October), and the Near Equatorial Trough forms further south, winds become light northeasterly over the western portions of the Arabian Sea and north to northwest near the northern Indian Coast. By late November, north to northeast winds spread over the entire Arabian Sea north of a line from the intersection of the Equator and the African Coast to the southern tip of India. Throughout the transition season, land and sea breezes strongly influence coastal areas, particularly where the terrain height increases rapidly near the coastline.

The most extensive changes in cloud patterns occur along and seaward of the Arabian and Indian Coasts. As the Southwest Monsoon weakens, general low-stratiform cloudiness near the Arabian Coast is gradually replaced by scattered cumuliform clouds, and the time of occurrence of maximum coverage shifts from early morning to afternoon. Near the Indian Coast, a temporary burst of enhanced convective activity usually accompanies the cessation of the persistent Southwest Monsoon flow, but thereafter the mean coverage is significantly less. Once the Northeast Monsoon has become established, overall cloudiness reaches a minimum, and convective activity subsides.

The Red Sea

As the Southwest Monsoon weakens in September, the winds near Bab al Mandab become light and variable. Usually by the end of the month they have shifted to southeast to form the Convergence Zone in the southern Red Sea. This zone then migrates northward during October to a mean position near 20°N (see Section 4.2.2). North of the Convergence Zone the winds remain northwesterly. The semi-permanent, low-pressure trough associated with this flow provides a channel for the passage of extratropical disturbances from the Sudan Low across the Red Sea. As the disturbances transit the Red Sea, the Convergence Zone moves northward, then southward with the gradient changes. The Convergence Zone is usually marked by a recognizable cloud band.

Strong, gusty winds can occur in the Bab al Mandab in November. All coastal areas are strongly affected by diurnal effects; however, these effects are less noticable in the areas of stronger flow. Strong convective activity is uncommon except when frontal zones penetrate the northern Red Sea.

The Persian Gulf

The Persian Gulf does not have a monsoon climate; the prevailing winds are northwesterly throughout the year. Therefore, the transition season resembles other subtropical areas in that there is a gradual cooling and an increasing frequency of extratropical disturbances. The prevailing northwest wind becomes weaker and somewhat less persistent as the continental heat low dissipates. Extratropical disturbances crossing the Arabian Peninsula cause winds to shift to a southerly direction for periods of increasing length and frequency as the season

progresses. These disturbances often bring cloudiness and occasionally rain to the area. They are principally responsible for the steady increase in mean cloud coverage from its September minimum to a winter maximum. The "Winter" Shamal first makes its appearance during this season (occasionally in late September) and is usually accompanied by strong convective activity or dust or both.

CLOUD AND WIND FORECAST RULES/AIDS.

a. Land/sea breezes are usually important during the transition seasons, particularly near coastlines with steep terrain gradients.
b. Land/sea breezes are strongest during periods of settled weather (i.e., maximum day-night temperature range).
c. Land/sea breeze effects will modify the direction and speed of weak to moderate gradient winds by adding an onshore component during the day and an offshore component at night.
d. Winds are weak and extremely variable with a high percentage of calms during October and November in the Gulf of Oman.
e. Severe squall lines (locally called "Uhaimir") can occur in tne Persian Gulf between mid-October and late November. Wind speeds of storm force (>47 kt) have been recorded.
f. Morning fog often occurs near the northwestern Indian Coast during calm conditions.

4.2.4 Tropical Cyclones

The tropical cyclone season is bimodal in the northern Indian Ocean, because the prerequisites for formation (Ramage, 1971) occur most often during the periods between the monsoons. The Autumn season extends from mid-September to early-January but reaches a peak in October or November. The southern Indian Ocean tropical storm season is in its early stages during this period.

The intensity (maximum wind speed) definitions of tropical cyclones have not been standardized world-wide. Table 4-1 shows the relationships between definitions most commonly used in the Indian Ocean. Other locally-used terminology is likely. This Handbook will use the U.S. definitions.

Table 4-1. Tropical Cyclone Intensity Definitions Used in the Indian Ocean (after Atkinson, 1971).

Country	Approximate Wind Speed Range (kt)*			
	> 63	48-63	34-47	< 34
USA	Typhoon	Tropical Storm	Tropical Storm	Tropical Depression
India	Severe Cyclonic Storm (core of hurricane winds)	Severe Cyclonic Storm	Moderate Cyclonic Storm	Tropical Depression
France	Intense Tropical Cyclone	Tropical Cyclone (strong depression)	Weak Tropical Cyclone (moderate depression)	Weak Tropical Perturbation
Mauritius	Intense Cyclone [>65]	Severe Depression [43-65]	Moderate Depression [32-42]	Weak Disturbance [< 32]
Australia	Class 1: Major Tropical Cyclone [winds > 33 kt with radius > 100 n mi]	Class 2: Tropical Cyclone [winds > 33 kt with radius < 100 n mi]		Class 3: Minor Tropical Disturbance

* Wind thresholds in brackets deviate from values used by the U.S. but define similar speed ranges.

Arabian Sea Area

Preferred Tracks. One of the prerequisites for tropical cyclone formation is the existence of a convective disturbance. During the Autumn season, this criterion is met by the reappearance of the Near-Equatorial Trough in the Arabian Sea. A similar development is found in the southern Bay of Bengal. These troughs may also lead to the satisfaction of the other prerequisites and are the source region for most of the tropical cyclone activity in the Arabian Sea. Figure 4-4 shows the tracks of significant tropical cyclones recorded during the 80-year period, 1891-1970. September and December cyclones are seen to be rare and have rather erratic tracks. Cyclones forming in October and November tend to follow one of two tracks: westnorthwest toward the Arabian Coast or a recurving track making landfall on the northern Indian Coast. Note that in the 80 years of record, only one cyclone entered the Gulf of Oman and none made landfall on the Makran Coast. Note also that a significant percentage of the Arabian Sea cyclones originated in the Bay of Bengal and moved across the Indian Peninsula or passed just south of it.

Tropical Cyclone Frequency. The 80-year record indicates that tropical cyclones are relatively uncommon in the Arabian Sea. Table 4-2 shows the mean monthly frequency of occurrence. Since winds less that 34 kt seldom disrupt operations at sea, a threat to operations during the Autumn season occurs (on the average) only once every two years. Figure 4-5 shows the frequency of occurrence (and movement probability) of significant tropical cyclones in each 5° latitude-longitude rectangle. It indicates a maximum frequency of 0.25 (September and December included) occurring in the rectangle bounded by latitudes 15°N and 20°N and longitudes 65°E and 70°E, showing that the threat in any given location exists (on the average) not more often than one year in four. Since the speed of movement of Arabian Sea tropical cyclones is much less than that of most warships, the probability of hazard to an underway vessel is minimal.(*) However, due to restricted mobility and susceptibility to wind speeds less than storm force, amphibious operations on Arabian Sea coastal areas north of 5°N (excluding the Gulf of Oman and the western Gulf of Aden) could be jeopardized by winds or seas from tropical cyclones.

(*) Assumes operable detection systems and prudent seamanship.

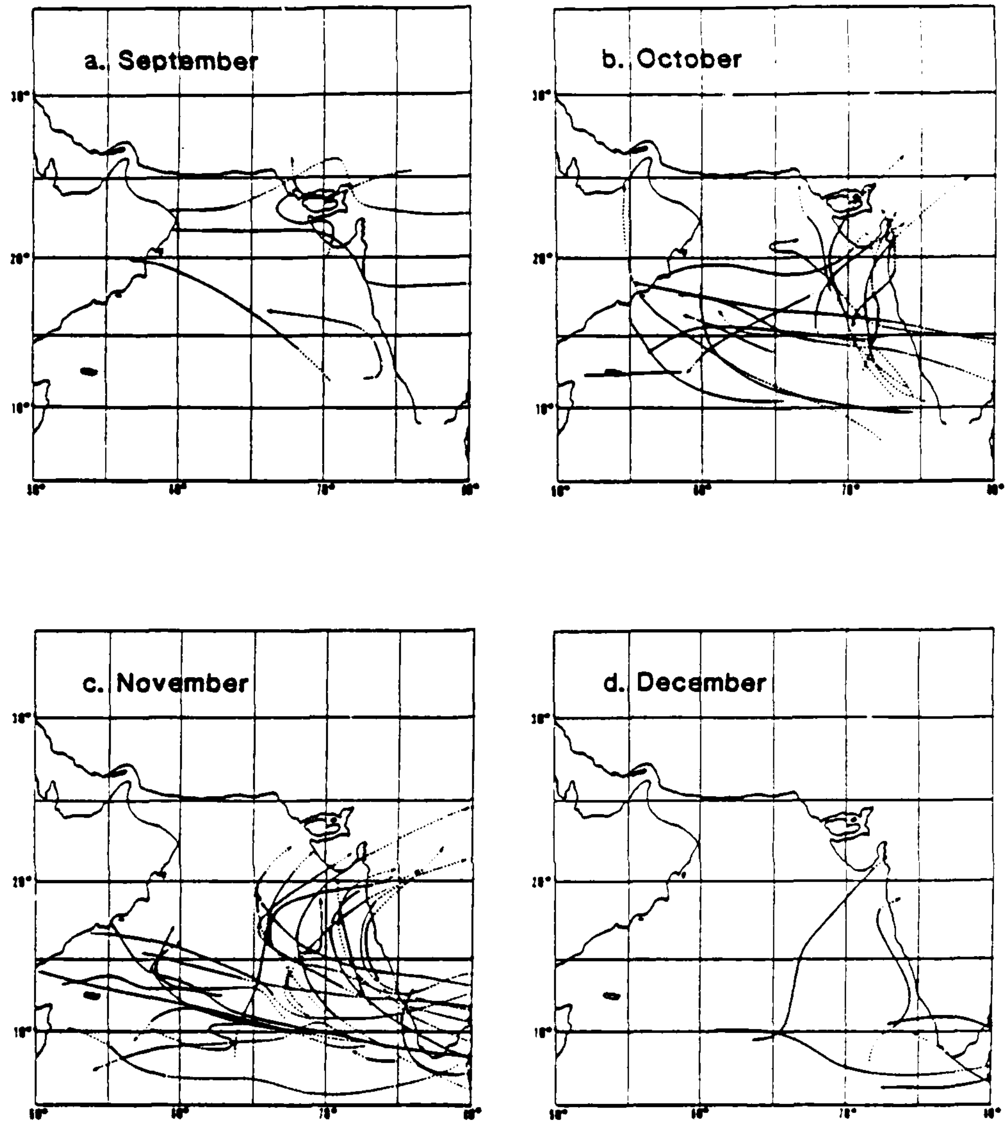

Figure 4-4. Tracks of significant tropical cyclones occurring in the months straddling the Fall Transition (a. September, b. October, c. November, d. December) during the 80-year period 1891-1970. Solid lines indicate that portion of the track during which maximum winds exceeded 33 kt (adapted from Brody, 1977).

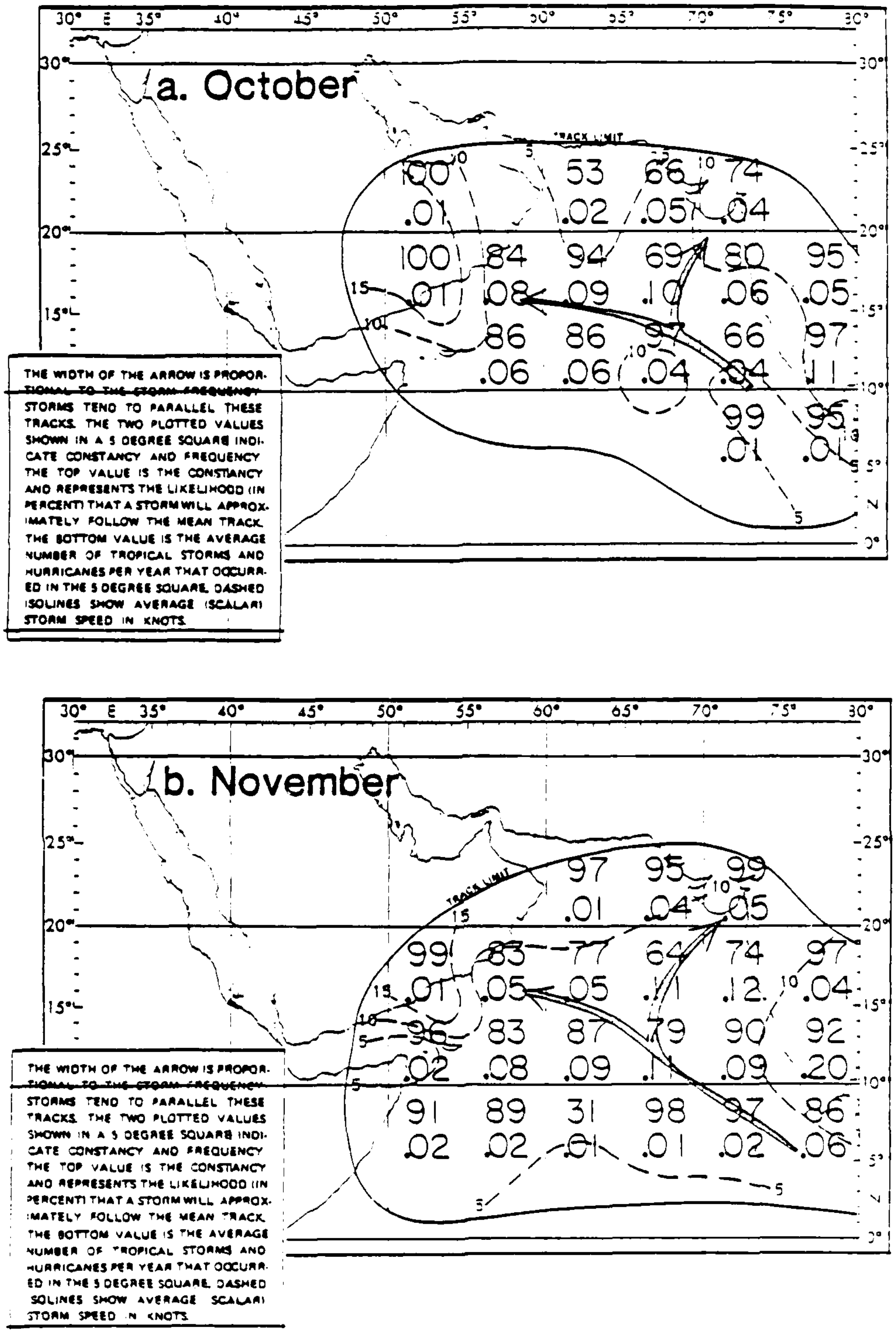

Figure 4-5. Frequency of occurrence (lower number), probability of movement nearly parallel to the mean track (upper number), and average speed of movement in kt (dashed contours) of tropical cyclones with maximum winds greater than 33 kt (from Naval Weather Service Detachment, Asheville, 1974).

Table 4-2. Mean Monthly Frequency of Tropical Cyclones in the Arabian Sea 1890-1967 (after Atkinson, 1971)

CYCLONE CLASSIFICATION	SEP	OCT	NOV	DEC	TOTAL
TROPICAL DEPRESSION	0.1	0.3	0.2	0.1	0.7
STORM OR TYPHOON	0.1	0.2	0.2	0.1	0.6

Atlantic Approaches

Although the tropical cyclone season begins in the Southern Hemisphere during this period, the probability of occurrence of a significant storm (maximum winds greater than 33 kt) in any 5° latitude-longitude rectangle during either of the Transition Period months does not exceed 15% (Naval Weather Service Detachment, Asheville, 1974). Movement is usually toward the west, except near Madagasgar; therefore, any encounter is likely to be a crossing situation which further minimizes the threat. If a tropical cyclone is approaching Madagasgar, the Mozambique Channel should be avoided.

Pacific Approaches

One of the requirements for tropical cyclone formation is a Coriolis force of sufficient magnitude; generally it is too small within seven degrees of the Equator. In the northern Indian Ocean, 80 years of records show that only one tropical cyclone formed south of 5°N and only a few between 5°N and 7°N. Therefore, ships on direct routes from the Strait of Malacca or Selat Sunda to a point south of Sri Lanka are not likely to encounter damaging winds due to a tropical cyclone, though thunderstorm squalls are common. However, if a tropical storm or typhoon exists in the Bay of Bengal south of 15°N, a northerly swell train of significant height is likely — particularly if the cyclone is on a westerly track.

Figure 4-6 shows the frequency, mean track and average speed of tropical cyclones affecting the Pacific approaches during the Fall Transition period. It

AD-A134 312 FORECASTERS HANDBOOK FOR THE MIDDLE EAST/ARABIAN SEA (U) OCEAN DATA SYSTEMS INC MONTEREY CALIF W E HUBERT ET AL. JUN 83 NEPRF-CR-83-06

UNCLASSIFIED N00228-82-C-6433 F/G 4/2 NL

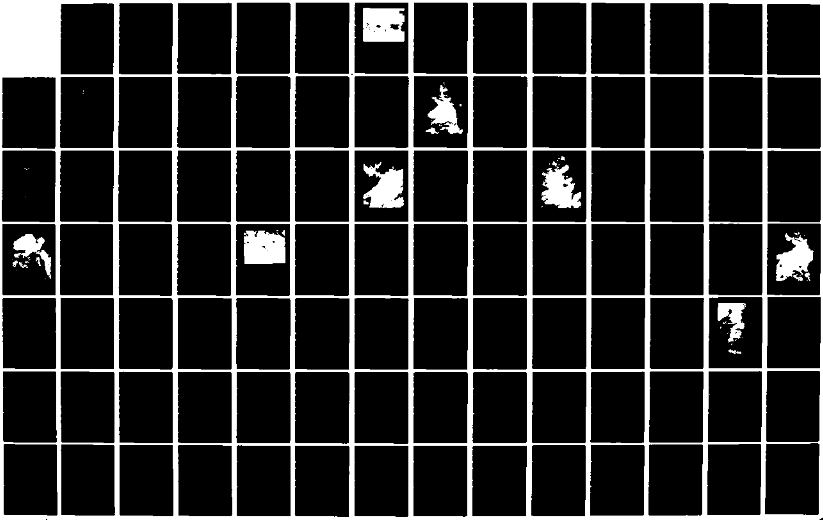

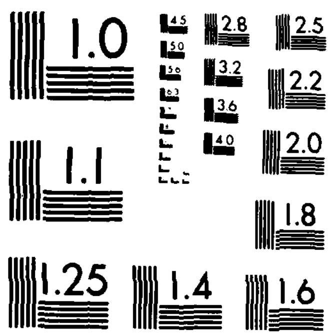

MICROCOPY RESOLUTION TEST CHART
NATIONAL BUREAU OF STANDARDS-1963-A

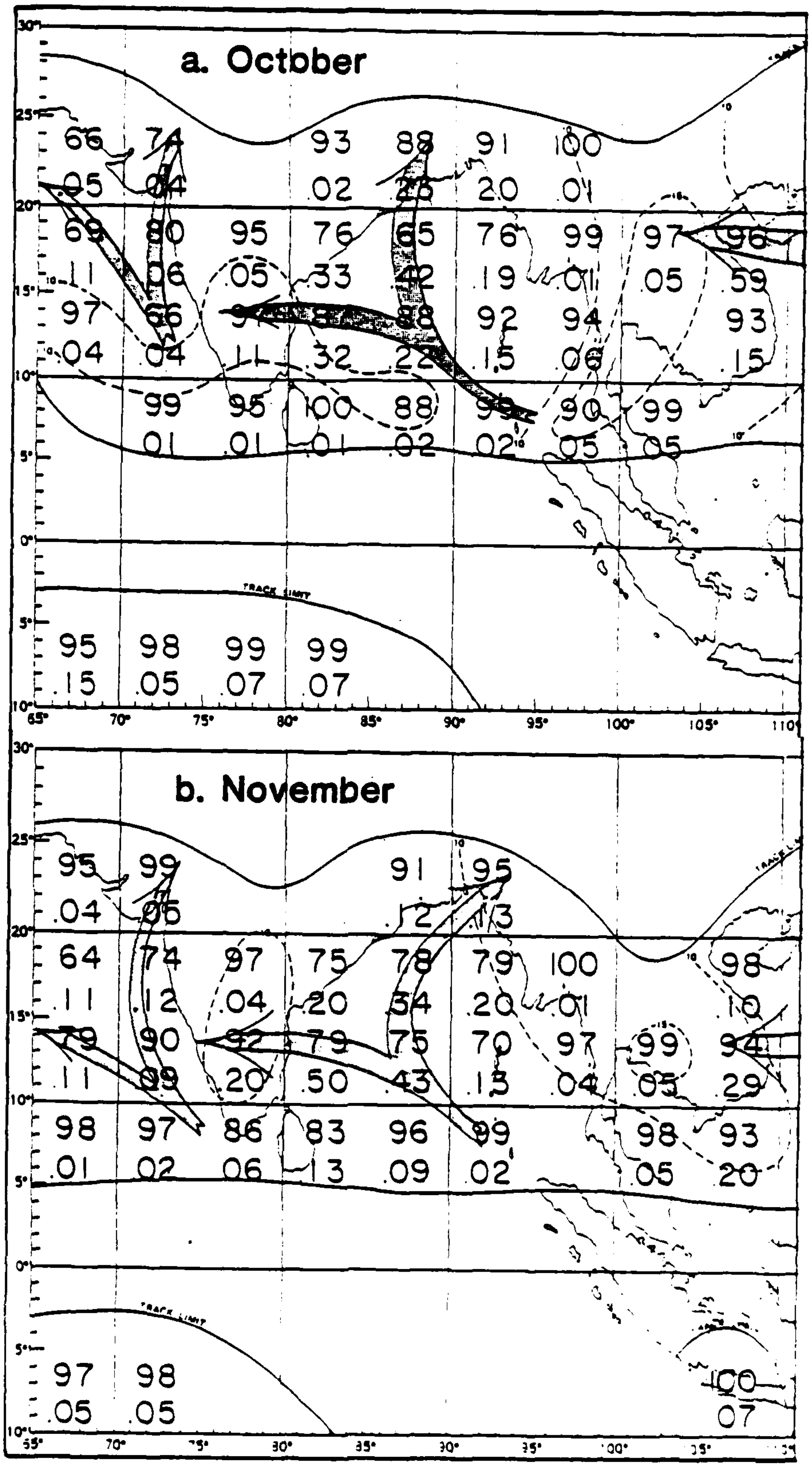

Figure 4-6. Frequency of occurrence (lower number), probability of movement nearly parallel to the mean track (upper number) and average speed of movement in kt (dashed contours) of tropical cyclones with maximum winds greater than 33 kt (from Naval Weather Service Detachment, Asheville, 1973).

can be seen that Bay of Bengal tropical cyclones are rare south of $10^{\circ}N$ except for the area east of Sri Lanka during November when the Near-Equatorial Trough migrates to a mean position near $10^{\circ}N$. This leads to a significant peak in tropical cyclone activity near Sri Lanka. Speed of movement of these cyclones (average < 10 kt) is generally much less than ship evasion speeds, and small course adjustments toward the south will clear the danger area. Although the probability of encounter is small, vessels transiting between Australian ports and Diego Garcia should remain alert for signs of tropical cyclone formation so that timely avoidance action may be taken.

FALL TRANSITION TROPICAL CYCLONE FORECAST RULES/AIDS.

a. The average speed of movement of Arabian Sea tropical cyclones is about 8.5 knots.

b. Nearly all of the tropical cyclones which take the westnorthwest track in the Arabian Sea originate south of $13^{\circ}N$.

c. Sea Surface Temperature (SST) is not a limiting factor for tropical cyclone development in the Arabian Sea. (SST values always exceed the critical limit.)

d. Tropical cyclones moving across India from the Bay of Bengal may re-intensify as they move offshore into the Arabian Sea.

e. Swell from tropical cyclones usually precedes arrival of damaging winds and affects a much larger area.

f. The ports of Colombo and Karachi are considered to be havens from tropical cyclones with maximum winds less than typhoon force (<64 kt).

5.0 NORTHEAST MONSOON REGIME (DEC-MAR)

5.1 General Description

During the winter season, the surface air over southern Asia is much colder than that over the sea. The resulting pressure gradient causes surface air to flow southward over the Arabian Sea. There are cold outbreaks into the Middle East/Arabian Sea throughout this season; however, the Himalayan and Caucasus Mountains block many of the cold surges from the Siberian anticyclone so that the Northeast Monsoon flow over the Arabian Sea is not nearly so intense as over the South China Sea.

During the Northeast Monsoon season, the principal trough in the tropics is the Near-Equatorial Trough of the Southern Hemisphere, but there is a weaker Near-Equatorial Trough east-west near 5°N. North of the latter trough, surface winds are from the northeast, are generally less than 21 kt and are frequently light and variable in the lee trough in the extreme northern Arabian Sea and Gulf of Oman. Fluctuations in surface wind flow are typically associated with cold air outbreaks from the north and west; these outbreaks are also the cause of the Winter Shamals over the Persian Gulf area (Perrone, 1979). Wave heights over the Arabian Sea are generally less than 4 ft except off the African Coast or in areas affected by a Shamal. Cloud amounts are generally low and visibilities are good over most of the Arabian Sea. Cloud amounts typically increase southward, however, with a maximum in the northern Near-Equatorial Trough at about 5°N. Clouds, rain and dust are frequently associated with the stronger cold frontal passages in the northern part of the area. Tropical cyclones are practically non-existent in the Arabian Sea during the Northeast Monsoon.

Figure 5-1 is a mosaic of satellite visual images showing much of the Indian Ocean during the Northeast Monsoon regime. The situation is somewhat abnormal in that it is unusually cloud-free north of 25°N, and tropical cyclone activity is unusually high in the Southern Hemisphere. The primary areas of interest to this Handbook are quite typical, however.

5.2 Large-Scale Circulation Features

The upper tropospheric anticylone which resides over the Himalayas in summer continues to retreat southward forming one anticylonic center over

Figure 5-1. NOAA visual mosaic selected to illustrate the fair weather and light wind conditions typical of the Northeast Monsoon Regime in the area covered by this Handbook. The Near-Equatorial Trough in the Southern Hemisphere shows considerable convective activity and vortex development. Clouds seen over the northern Arabian Sea are caused by the penetration of an extra-tropical disturbance. During the period December through March, 4 to 7 frontal passages per month can be expected over the Arabian Peninsula. Strong north-westerly flow usually occurs over the Persian Gulf following frontal passages. This wind condition is known as a "Shamal" and is addressed in Section 5.3.3. During a Shamal, cold air flows over the warmer Persian Gulf water and produces the cumulus cloud lines seen (faintly) in the image. The low-level Northeast Monsoon flow is constrained by the steep terrain surrounding the Gulf of Aden and is channeled into the southern Red Sea where it converges with northerly flow producing a persistent cloud band. The band is evident in the image near 18°N (see Section 4.2.2 for a detailed discussion of the Convergence Zone Cloud Band). Dust storms during this season are primarily caused by winds in the strong pressure gradients behind cold fronts. The primary sources of dust are the Arabian Peninsula and the coastal areas of Iran and Pakistan.

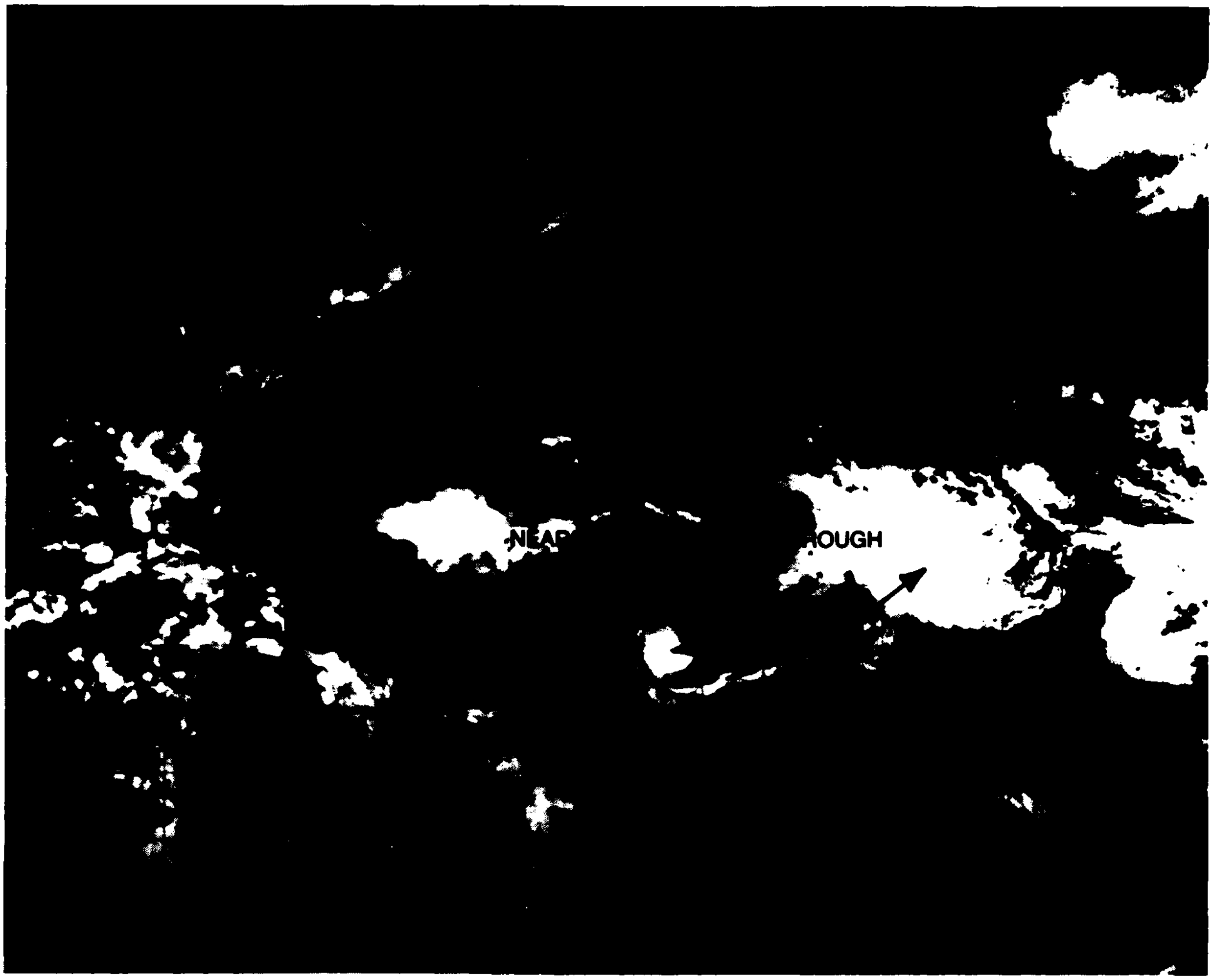

Figure 5-1. NOAA visual mosaic produced from data recorded on January 13, 1982 during the heart of the Northeast Monsoon.

Africa and another in the western North Pacific (both between 10^{o}N and 15^{o}N). The upper tropospheric flow over all parts of the area north of 15^{o}N is westerly and quite strong at the tropopause level. The mean position of the Polar Front Jet is located south of the Himalayas and the higher Subtropical Jet is well developed over northern Africa and the Arabian Peninsula (see Figure 5-2b). During periods of normal upper air flow, cold air outbreaks from continental Europe and Asia are inhibited by the mountain barriers which border the region on the north. However, when large-amplitude perturbations occur in the Polar Jet, sufficient cold air is advected over the barriers to cause frontal surges to penetrate into the northern Arabian Sea. The most vigorous of these cold air outbreaks occurs with a blocking high over eastern Europe and a downstream trough over western Iran.

5.2.1 Climatology

Naval Oceanography Command climatological publications (see Appendix A) contain monthly and seasonal data on several operationally significant parameters. It is not the purpose of this Handbook to duplicate existing publications; however, for ready reference and to illustrate the discussion which follows, Figures 5-2a through e provide pertinent climatological data which are representative of the Northeast Monsoon Regime.

The data on which these figures are based are not uniformly distributed over the region; they are biased by coastal and island station observations. In areas where the position of the isopleths are in doubt due to scarcity of data, dashes have been used to show probable features.

5.2.2 Troughs and Fronts

Although frontal systems pass over the Arabian Peninsula several times each year, the most common synoptic pattern during this season consists of high pressure centered over southern Asia with ridges over the Arabian Peninsula and North Africa. Inverted troughs commonly exist over the Persian Gulf/Gulf of Oman and across the central Red Sea.

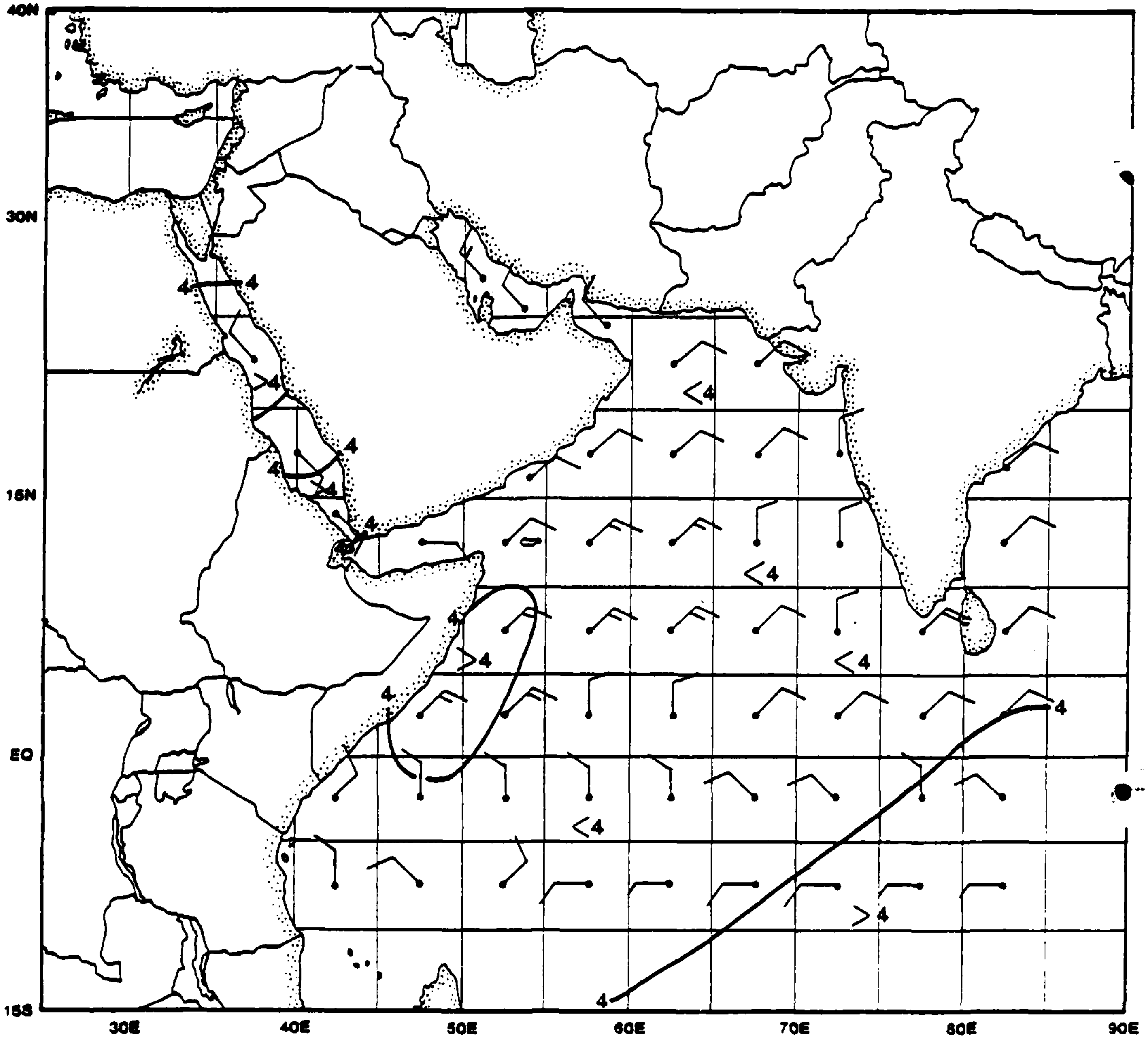

Figure 5-2a. Mean January surface winds (wind barbs) and seasonal mean significant wave heights in feet (contours). The wind barbs represent the average over a 5° rectangle of latitude and longitude in the Arabian Sea. Wind barbs representing the restricted waters of the Red Sea, Persian Gulf and the Gulfs of Aden and Oman are plotted over the water area that they represent. When two or more wave groups were reported, only the one with the highest wave was selected for the data set from which the significant wave height contours were produced. Therefore, where separate wind waves and swell are common, the values will tend to be too low. (Data for this figure were extracted from Naval Weather Service Detachment, Asheville, 1973 and 1974, and Naval Oceanography Command Detachment, Asheville, 1980 and 1982.)

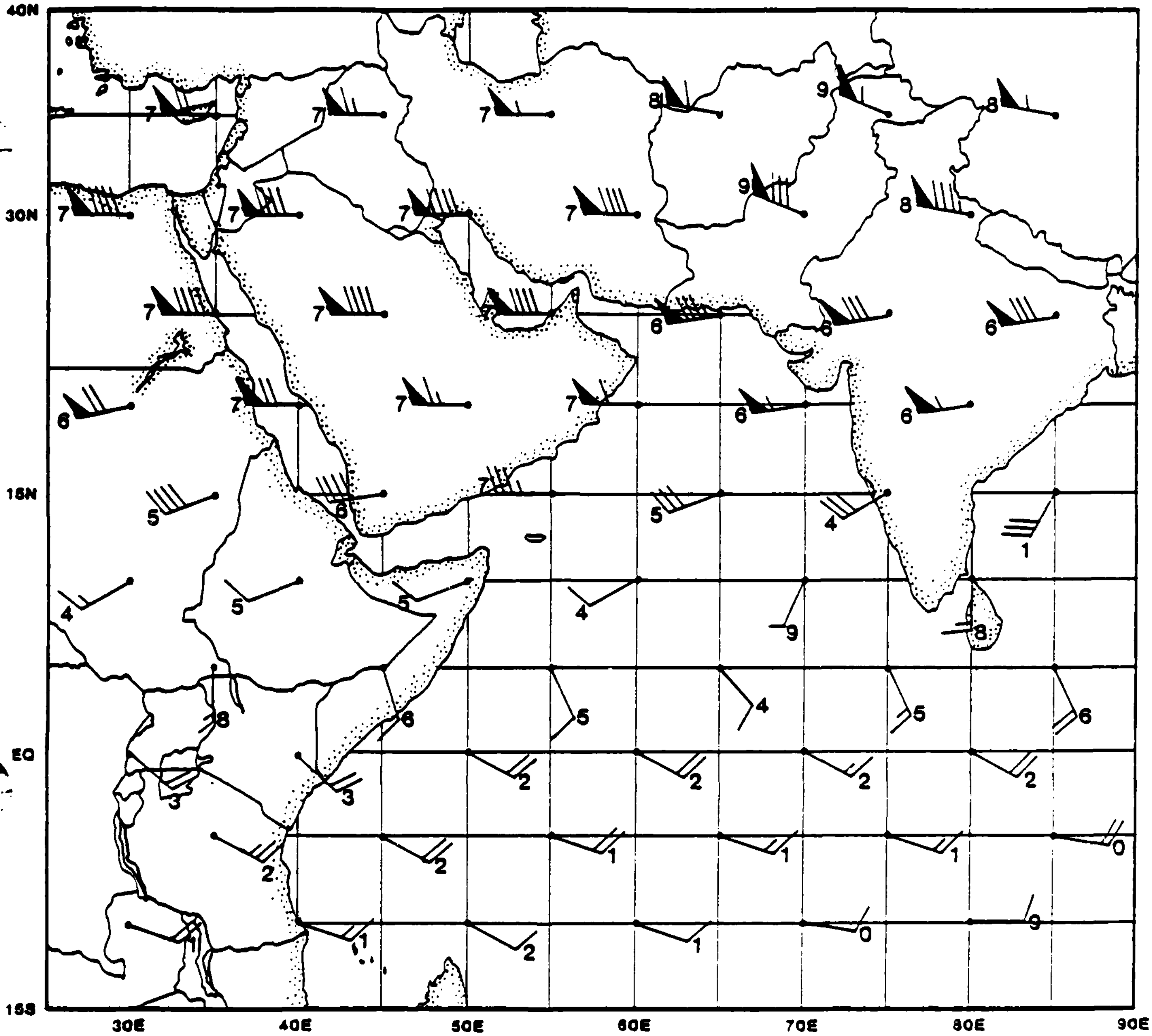

Figure 5-2b. Mean January 200 mb winds (adapted from Sadler, 1975). The numeral by each wind barb is the tens digit of direction. The westerly winds extend southward to about 10°N during this season and the Subtropical Ridge in the Northern Hemisphere becomes quite weak. The mean position of the Subtropical Jet over the northern portion of the Arabian Peninsula (near 30°N) accounts for the speed maximum shown. Wind speed and direction will show considerable variability from day to day in the tropics due to migratory cyclonic and anticyclonic circulations.

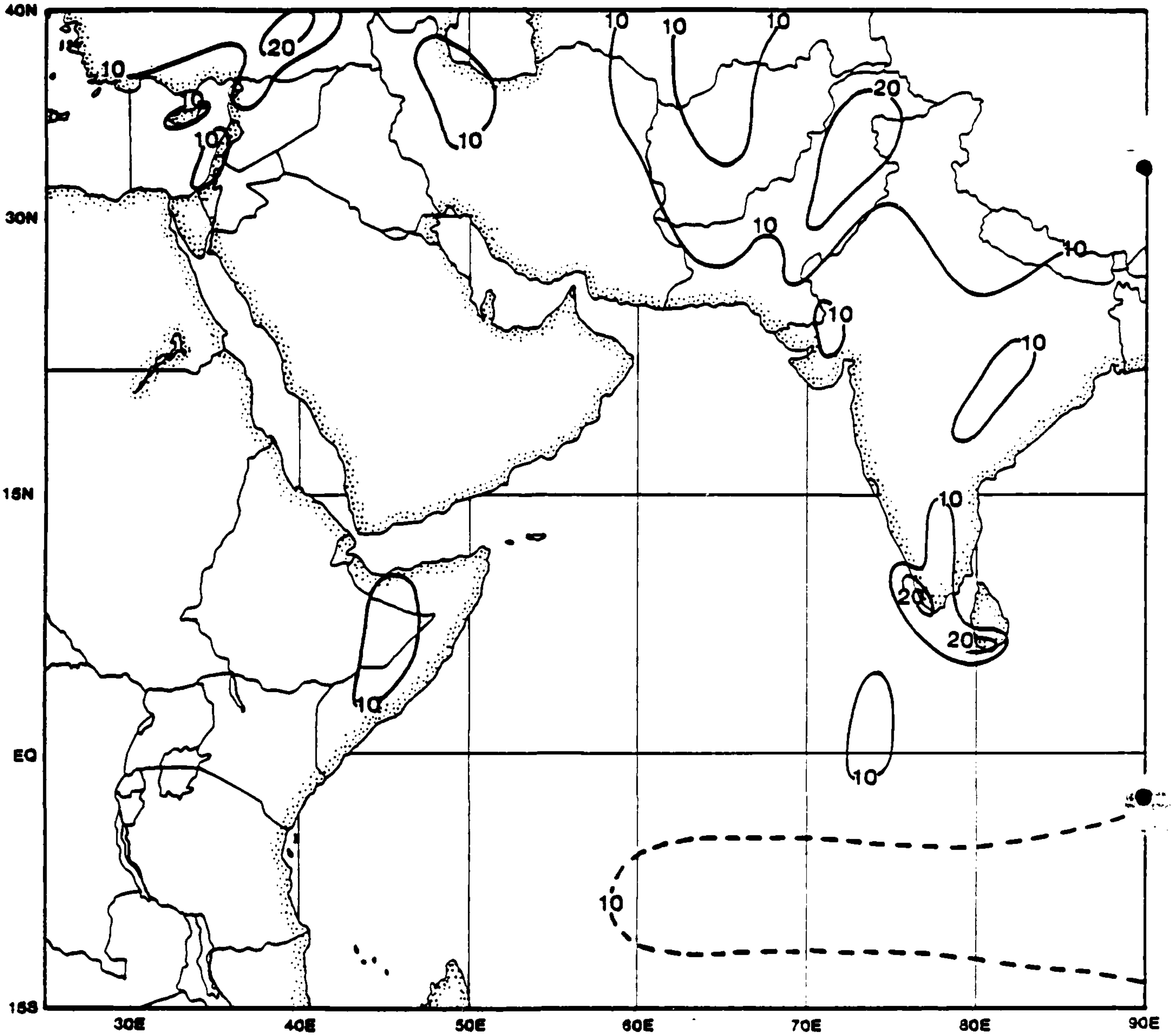

Figure 5-2c. Percent frequency of ceiling less than 1500 ft or visibility less than 3 n mi. Low ceilings and visibility are uncommon during this season; however, percentages are questionable in the tropics due to lack of data. Since the Near-Equatorial Trough is convectively active during this period, the area near $10^{\circ}S$ probably should show a 10% contour from about $60^{\circ}E$ to the right margin of the figure (shown as a dashed contour).

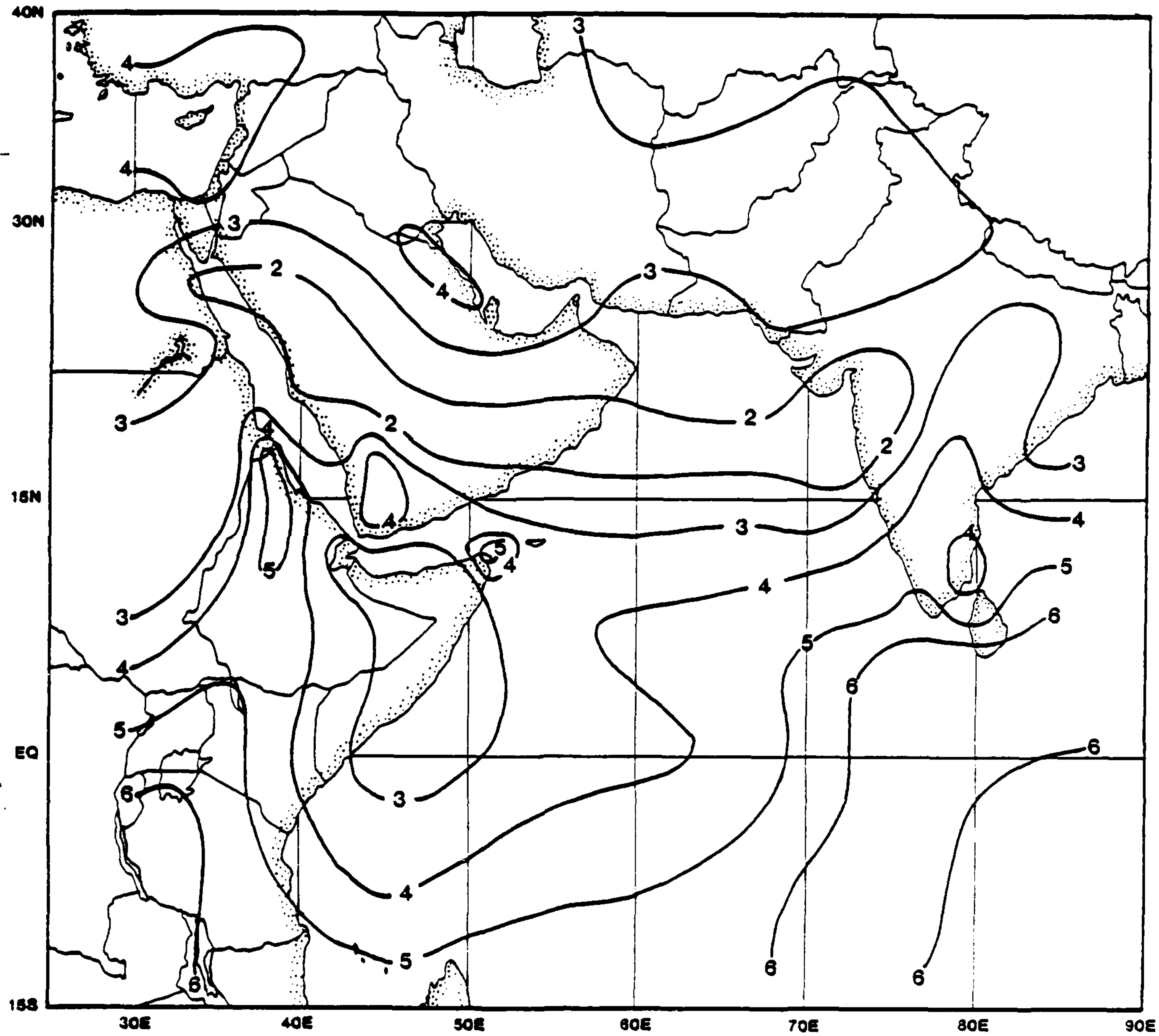

Figure 5-2d. Mean total cloud cover in tenths. The accuracy of the contours south of the Equator and east of about 60°E is questionable due to sparsity of data. Since satellite images frequently show rather dense convective activity in the Near-Equatorial Trough near 10°S, a cloudiness maximum oriented east-west near 10°S is possible. The relative maximum along the western shore of the Persian Gulf is due to middle and high cloudiness associated with extratropical disturbances. The southwestern shore of the Red Sea is noted for stratus and stratocumulus, particularly in the mornings. Onshore flow and terrain effects probably account for the maximum over Cape Guardafui.

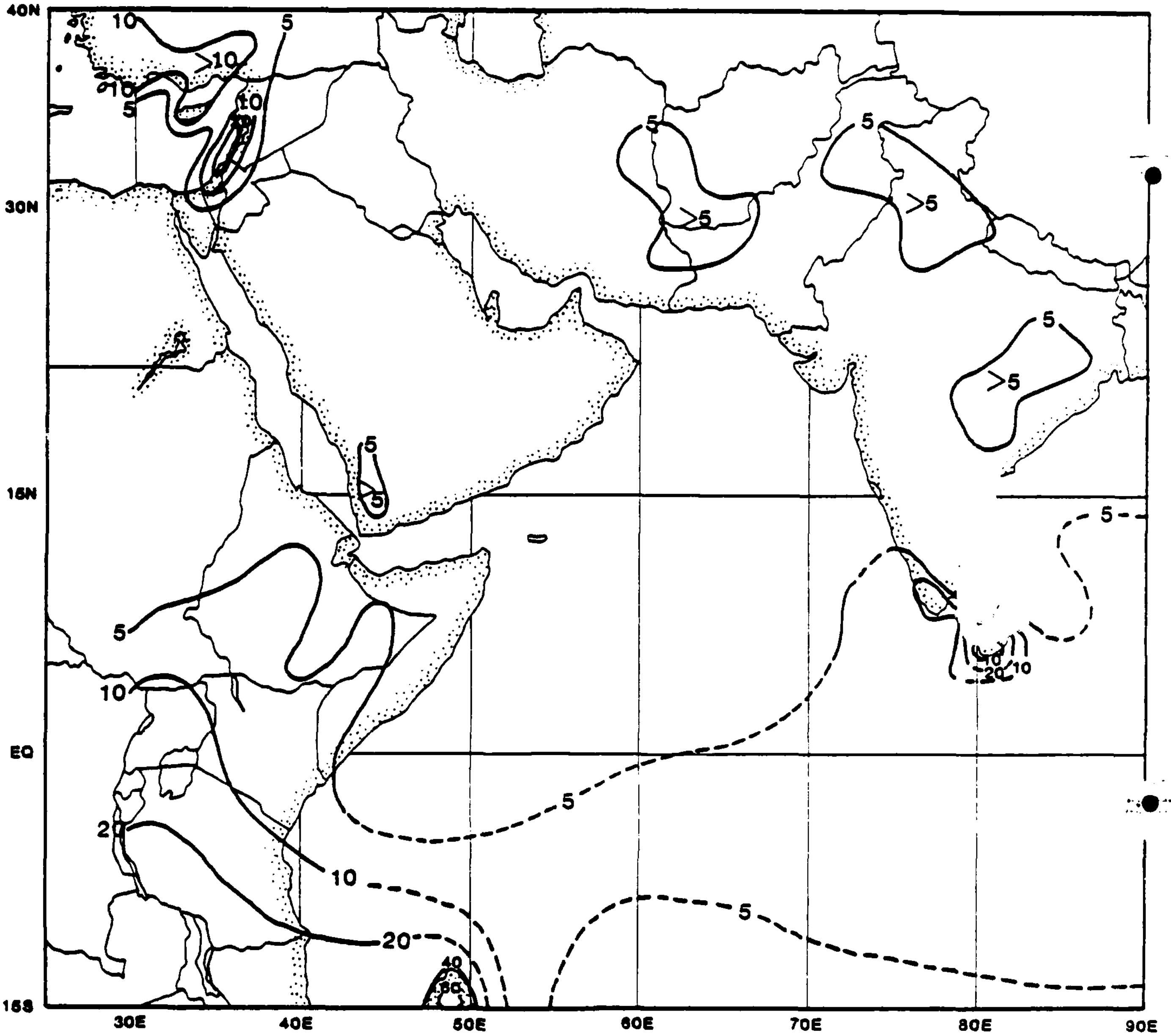

Figure 5-2e. Percent of days with thunderstorms. The only area of significant convective activity during this season is the tropical zone. During December, strong convective activity persists in the vicinity of Sri Lanka, then decreases gradually through March. Early season activity is likely to be greater than shown and late season activity is likely to be less. Contours over the ocean in the southeastern portion of the figure are dashed because of poor data coverage.

Figure 5-3a shows a typical surface analysis during the Northeast Monsoon. This pressure pattern accounts for the northeast flow over the Arabian Sea, the weak and variable winds in the Gulf of Oman, the strong southerly winds in the southern entrance to the Red Sea and the convergence zone in the central Red Sea. The storm track extends northeastward from the Mediterranean, and cold outbreaks are inhibited by the mountain ranges bordering the area to the north. Figure 5-3a also shows that the Near-Equatorial Trough is south of 5°N except near the southern tip of India.

When low-latitude, upper-level troughs move over the area, a rather different pattern develops. The storm track extends more eastward (sometimes southeastward) from the southeast Mediterranean or Egypt. As low centers track to the vicinity of the northern Persian Gulf, pre-frontal (warm) weather usually occurs in the Persian Gulf and sometimes over the Gulf of Oman and the Makran Coast. As the trailing cold front is swept southward over the Arabian Peninsula, strong cold air advection west of the upper-level trough causes rapidly rising pressure. The resulting strong pressure gradient causes the Winter Shamal (see Section 5.3.3) and often pushes the cold front well off the Arabian coast into the northern Arabian Sea. Figure 5-3b shows a synoptic situation typical of the Winter Shamal. If the cold advection is very strong, the cold front will be forced southeastward into the Central Arabian Sea before surface warming dissipates the air mass contrast. Weaker outbreaks often stall just off the Arabian Coast and result in a line of showery weather.

TROUGH/FRONT FORECAST RULES/AIDS. The following rules/aids were adapted from Fett et al. (1983):

a. When a blocking high is located north of the Arabian Sea and the band of westerlies in the southern branch of the split flow is well organized, upper-level short waves and surface fronts move across the Arabian Peninsula.
b. Surface winds over water areas are usually stronger than those reported by shore stations following frontal passages.
c. Weak surface frontal zones, which are not well-identified by cloud patterns over land, usually show increased cloudiness and relative intensity when they move over water areas.

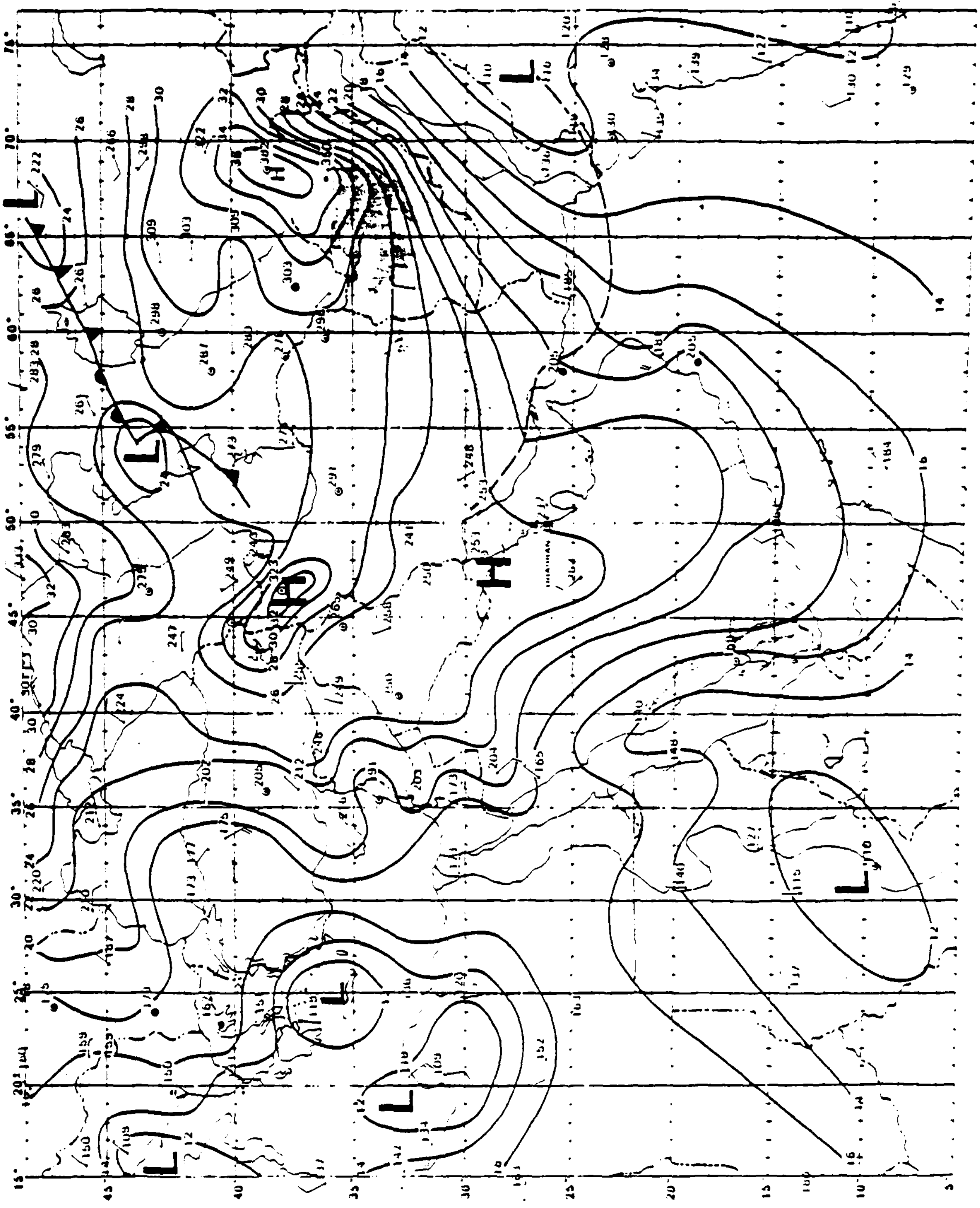

Figure 5-3a. Surface analysis 0000Z January 20, 1973. This pattern is typical of the Northeast Monsoon (from Perrone, 1979).

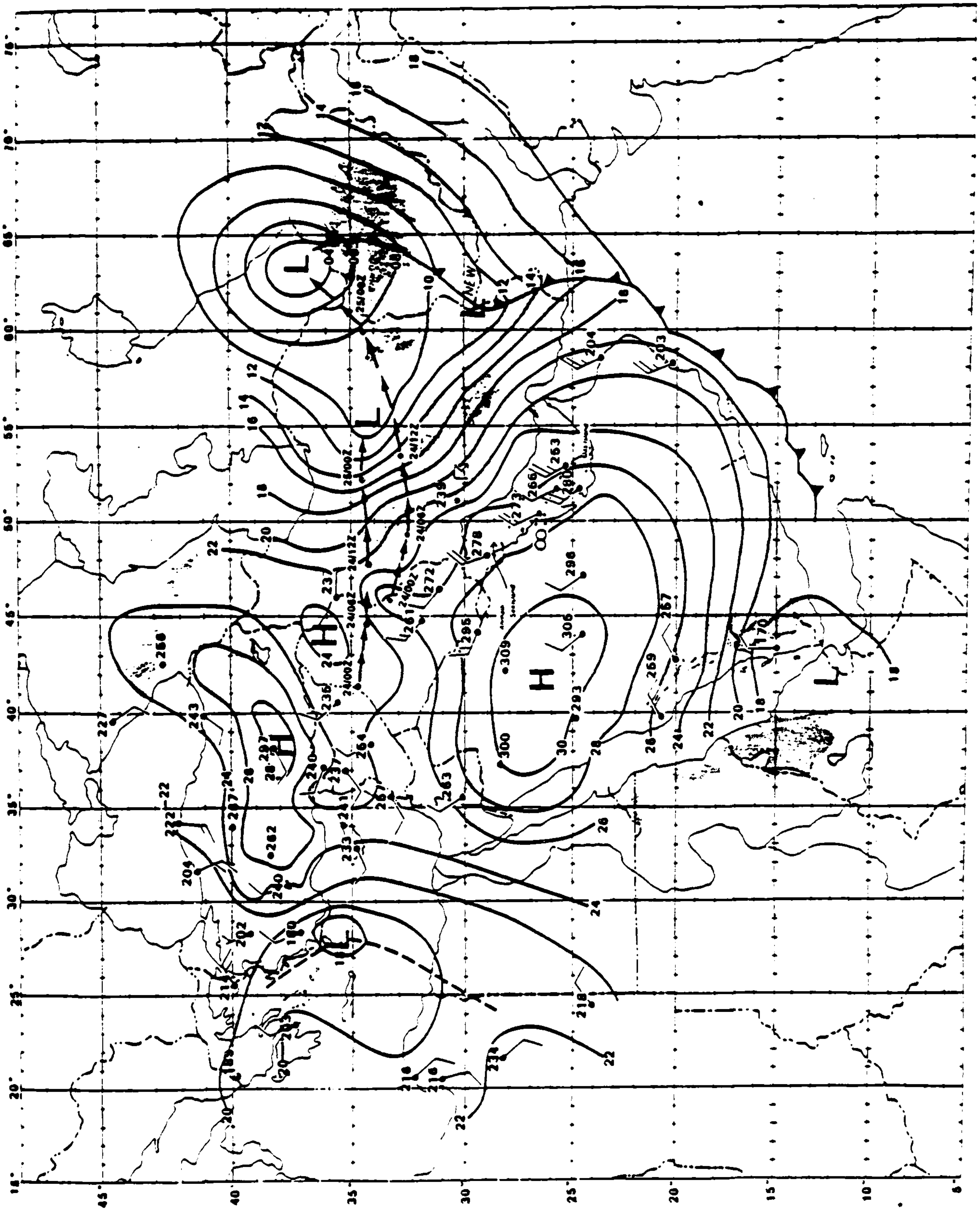

Figure 5-3b. Surface analysis 0600Z January 25, 1974. This pattern is typical of a Winter Shamal situation (from Perrone, 1979).

d. The surface region below the Subtropical Jet (STJ) is normally a fair weather region; however, when a polar trough "undercuts" the STJ, a frontogenetic zone is created.

5.3 Regional Features

Although the Northeast Monsoon is the dominant feature during the winter season, considerably more variability occurs in the flow pattern than during the Southwest Monsoon. Most of this variability is due to cold air intrusions resulting from the penetration of Polar Jet troughs south of the mountain barrier. This phenomenon affects the Red Sea, Gulf of Aden, Persian Gulf, Gulf of Oman and the northern Arabian Sea. Each sub-region exhibits typically distinct features largely related to geography and often having dimensions in the mesoscale range.

5.3.1 Arabian Sea

Typical Frontal Systems

The very persistent anticyclonic flow centered on the Arabian Peninsula tends to perpetuate a frontogenetical zone extending northeastward from the East African low pressure area (Sudan Low). Extratropical disturbances cause perturbations in this zone to migrate across the Red Sea, Arabian Peninsula and northern Persian Gulf. Normally these perturbations are not sufficiently intense to cause a significant cold air outbreak over the Arabian Peninsula. Lacking strong cold air advection, the frontal zone fails to penetrate to the Arabian Coast.

When an upper-level long wave trough is positioned over the area, however, the northwesterly flow aloft advects cold air from the eastern European continental areas over the natural terrain barriers toward the Persian Gulf. As perturbations move into western Iran, subsidence raises surface pressure over the northern Arabian Peninsula. The resulting pressure gradient forces the frontal zone rapidly southeastward, and occasionally into the Arabian Sea. Once over the warm Arabian Sea waters, the cold air mass is rapidly modified and seldom penetrates more than 100-200 n mi beyond the coastline. Particularly strong outbreaks may, however, penetrate as far as a line from the Somali coast near

Ras Hafun to the vicinity of Bombay. These stronger outbreaks usually carry a considerable amount of dust and cause extended periods of reduced visibility and particulate fall-out.

Arabian Sea Anticyclone

Climatologically, the Northeast Monsoon results from a persistent high pressure ridge which protrudes from the Asian anticyclone over the Arabian Peninsula and extends more or less continuously into the Arabian Sea. However, extratropical disturbances migrate across the northern part of the area in this season, and the normal high-pressure ridge over the Arabian Peninsula is temporarily replaced by pressure much lower than that found over the northern Arabian Sea. This pressure pattern shifts the center of anticyclonic circulation to the Central Arabian Sea and results in southerly winds along the Arabian Coast and in the southern Persian Gulf (locally called "Kaus"). As these disturbances move into Iran, a high pressure ridge is reestablished over the Arabian Peninsula behind the front/trough. Naval units operating along the Arabian Coast (as defined in Figure 2-1) report that these fronts/troughs often stall near the coastline (either slightly inland or slightly offshore), and this is verified by satellite imagery.

Cloud and Wind Patterns

Clouds. Figure 5-4 shows cloudiness typical of the Arabian Sea during the Northeast Monsoon. Overall cloud cover is relatively light and generally consists of scattered cumulus or stratocumulus except in the fronts/troughs which occasionally influence the Arabian Peninsula and Makran coasts (vertical development here can be sufficient to cause showers). Based on satellite cloud imagery, Gurunadham (1971) has determined that there is a semi-permanent area of clouds which spreads southwestward from a point near 20^{O}N and 65^{O}E. This pattern can persist for days at a time. The density of the cloud cover in this feature appears to be correlated with low-level wind speeds in the Northeast Monsoon flow.

Winds. Winds from the northeast quadrant prevail over most of the Arabian Sea in this season. Exceptions are: (a) ahead of fronts/troughs which

move off the Arabian Coast where south to southwest winds up to gale force occur for short periods of time and (b) along the coast of India where they are often from the north or northwest -- particularly late in the season. The winds are not as strong as they are during the Southwest Monsoon or in the Northeast Monsoon which Navy forecasters are accustomed to in the South China Sea. Typical wind speeds are 10 to 20 kt. Stronger winds are usually associated with troughs/fronts (see Section 5.3.3 for a description of the Shamal). Near coastlines, both direction and speed are influenced by land/sea breeze effects; for example, afternoon wind speeds near Mombasa are much stronger than indicated by the pressure gradient due to the additive effects of the Northeast Monsoon and the sea breeze. Also, deviations from the predominant northeasterly flow often occur along the Makran Coast and in the Gulf of Oman. Under typical northeasterly flow a lee trough forms south of the coastal mountains of Iran and Pakistan, resulting in a zone of light and variable winds. Each month several trough/front passages occur preceded by southerly winds and followed by northwesterlies.

Equatorial Cloud and Wind Patterns

Cloudiness increases toward the south with the maximum occurring in the vicinity of the southern hemisphere Near-Equatorial Trough at about 10°S. A secondary maximum is often found in a weak Near-Equatorial Trough at about 5°N. Most of this cloudiness is typical of tropical convergent areas and may contain locally intense convective activity. Mean cloud coverage increases from west to east. Winds are light except for the tradewind band south of 10°S and in an area off the southeast Somali coast where the Northeast Monsoon penetrates to the Equator and beyond. Hazardous winds may be associated with local thunderstorms.

ARABIAN SEA NORTHEAST MONSOON FORECAST RULES/AIDS.

a. (*) The density of stratocumulus is directly related to near-surface wind speed (i.e., more and thicker clouds correlate with higher speeds).
b. (*) Cloud amount increases tend to precede surface wind increases by 6 to 12 hours.

(*) Along Arabian Coast

c. (*) Wind maxima tend to occur about 0300 and 1300 (local time). Minima are common near 0830 and 1500. The diurnal extremes usually occur at 0830 (minimum) and 1300 (maximum).

d. (*) If the surface wind has not started to freshen by 1000, expect relatively low wind speeds that day.

e. An upper-level trough over western Iran and upper-level winds with a northerly component over the Arabian Peninsula are necessary conditions for movement of a cold surge into the Arabian Sea.

f. Land breezes are intensified in the vicinity of large river valleys or steep coastal terrain.

g. Cloud lines which form offshore during a cold surge are usually parallel to the near-surface wind direction.

h. The afternoon sea breeze strongly enhances the Northeast Monsoon near Mombasa, Kenya. Northeasterlies of 18-25 kt are common.

i. In the approaches to the Gulf of Oman, rain is most common with slow-moving cold fronts. Fast-moving fronts tend to be dry.

j. Both large scale and local scale dust storms occur around the Arabian Sea. Large scale dust storms are caused by turbulent synoptic scale flow patterns where dust is carried upward several thousand feet into the atmosphere and advected thousands of miles from the source region. Local scale dust storms (and sand storms) occur where sand dunes or dry lake beds provide point sources for small scale dust/sand plumes to be raised by local winds.

k. In the coastal zones (see Figure 2-1) of the northern Arabian Sea, strong cold frontal passages, particularly when dry, can be expected to be followed by moderate to heavy dust in 3 to 6 hours.

l. Unless obscured by other clouds, approaching dust resembles dirty fog and usually passes overhead before arrival at the surface.

m. Local scale duststorms seldom affect ocean areas more than 60 n mi from land.

n. Large scale dust storms seldom restrict horizontal visibility over the ocean areas to less than 2 n mi. However, reductions to less than 7 n mi may persist for several days. The boundaries of large scale dust storms tend to be quite diffuse.

(*) Along Arabian Coast

Figure 5-4. DMSP image showing typical winds and cloud cover over the Arabian Sea during the Northeast Monsoon. The large-scale, weak, northeast flow advects dry air over the northern Arabian Sea. Over the southern Persian Gulf, cloud lines near the center of the gulf indicate converging flows (land breezes) from the opposing coasts. Westerly flow out of the Gulf of Oman blocks cloud advection into the gulf by the weaker flow from the northeast. This blocking creates a sharp demarcation line in the cloud pattern near the mouth of the gulf. The faint cloud pattern and lack of well defined cloud lines indicate that winds are light throughout this area. Typically the winds and clouds increase from the northeast to the southwest across the Arabian Sea during this season. Moderate convective activity is indicated south of about 10^{o}N. The cirrus plumes from these convective clouds indicate that at middle and upper levels westerly winds prevail to at least 5^{o}N. The cool dry air flowing off Pakistan and India forms a low-level temperature inversion. Advection over the warmer ocean results in modification of the lower layer and a gradual weakening of the inversion. At some distance to seaward in the downwind direction, mixing becomes deep enough for a cloud layer to form. Continued advection over progressively warmer water results in a deeper cloud layer and eventually to convective activity that breaks through the inversion. This evolution of cloud forms is seen in the DMSP image, i.e., scattered cloud conditions over the northeastern Arabian Sea, inversion capped clouds in the central region and convective cells to the south and west. The approximate local sun time at the center of this image is 0900 (0448Z).

Figure 5-4. DMSP visual image recorded on December 14, 1979 showing Arabian Sea cloud cover typical of the Northeast Monsoon.

o. Local scale dust storms may reduce visibility to near zero close to shore and the lateral boundaries are frequently sharply defined. Their occurrence is normally associated with local terrain.

5.3.2 Red Sea and Gulf of Aden

Severe weather is infrequent in these regions during the winter season. In the northern Red Sea, weather is influenced by extratropical systems (frontal passages), but the lack of moisture sources and relatively strong solar heating tend to moderate the effects. The Gulf of Aden and the southern Red Sea are dominated by the Northeast Monsoon, but the direction of flow is easterly in the gulf and southeasterly in the Red Sea due to the channelling effects of the terrain.

The Low-Level Convergence Zone

The formation of the Convergence Zone Cloud Band (CZCB) is discussed in section 4.2.2. It is a semi-permanent feature during this season but may vary in position from the southern end of the Red Sea to near the northern end. The mean position is near 20^{o}N. It moves up and down the Red Sea in response to the passage of extratropical disturbances from the eastern Mediterranean and northern Africa toward northern Saudi Arabia and Iraq. It persists near its mean position during undisturbed Northeast Monsoon flow. It is often well-defined on satellite pictures as a persistent cloud band or area which is usually more dense over the water.

Low-Level Cloud and Wind Patterns

Low level clouds in the northern Red Sea are mostly associated with extratropical disturbances and are seldom heavy or persistent. Occasionally they produce light showers. South of the CZCB, broken to overcast stratocumulus is rather common during night and early morning hours (particularly along the African shore). These clouds usually dissipate by afternoon. Gulf of Aden cloudiness is similar to that of the southern Red Sea, but the amounts are somewhat less.

The winds in the Gulf of Aden and the extreme southern Red Sea are very persistent; the largest variation is diurnal. The direction tends to be parallel to the orientation of the basin but includes strong land breeze components -- particularly near steep terrain. Gulf of Aden wind speeds average about 10 kt and winds over 20 kt are unusual; however, there is strong funnelling through the southern entrance to the Red Sea causing large speed increases in the northern approaches to the strait of Bab al Mandab. Average speeds through the strait in December and January approach 20 kt and are greater than 11 kt more than 80% of the time. Occasionally, winds here reach gale force. In the maximum wind region (vicinity of the Hanish Islands), land/sea breeze effects are less noticeable due to the strength of the gradient and terrain-forcing effects. Wind speeds near the straits are somewhat less in February and March than in December and January.

Winds are increasingly variable northward of 15°N due to the effects of extratropical disturbances moving across the northern Red Sea and southeast Mediterranean. Locations north of 20°N have a high percentage of fresh northwesterly winds but southerly winds ("Khamsin", "Aziab") are not uncommon in advance of transient low pressure systems. Coastal areas along the Gulf of Aqaba are known as one of the most windswept in the world. The CZCB is, of course, an area of light variable winds.

High Level Cloud and Wind Patterns

Middle and high cloudiness is uncommon during this season and is usually associated with the Polar or Subtropical Jet. When a Polar Jet trough passes through the region, the area between the trough line and the downstream ridge lines usually experiences middle and high-level clouds (occasionally of sufficient density to produce rain). These cloudy areas have been typed (Brody, 1977) according to shape and location relative to the polar trough. Occasionally, bands of high clouds with slight anticyclonic curvature will appear. Usually these clouds are associated with the Subtropical Jet. They are easily identified on satellite pictures (very cold, striated, cast shadow on lower surfaces).

The Subtropical Jet is important to flight forecasting in this region. The mean position of the core as shown in Figure 5-5 is north of the area; however, polar troughs transiting the Arabian Peninsula tend to displace it southward

(Perrone, 1979). (See Section 5.3.3 for a discussion of CAT potential.) The cloud banding mentioned earlier is useful in locating the horizontal position of the Subtropical Jet on a given day.

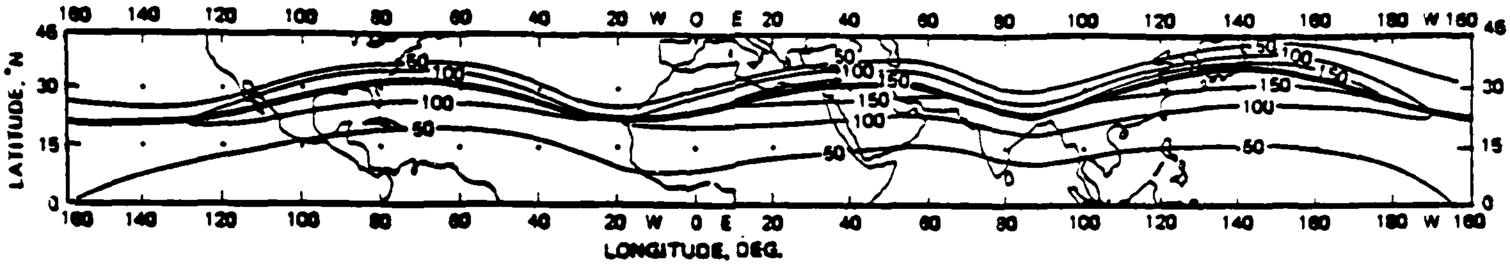

Figure 5-5. Mean Subtropical Jet Stream for winter 1955-1956. Isotach analysis at 200 mb, drawn every 50 kt. Mean latitude of jet axis is 27.5^{o}N (after Reiter, 1969).

Visibility Restrictions.

Particularly vigorous cold fronts or Khamsin winds will raise enough dust to temporarily reduce visibility, particularly late in the season (February and March). These restrictions are usually confined to the northern two-thirds of the Red Sea and are generally of short duration (1 or 2 days). Fog patches may occur in coastal areas in the early morning hours, but are uncommon.

RED SEA/GULF OF ADEN FORECAST RULES/AIDS.

a. A low-level cloudiness maximum occurs in the vicinity of Cape Guardafui during the NE Monsoon. Total coverage averages greater than 5 tenths.

b. Stratocumulus which forms during night and early morning hours in coastal areas usually dissipates by mid-afternoon.

c. Thunderstorms seldom occur in the Gulf of Aden during the NE Monsoon.

d. One or more "moisture fronts", which mark the limits of maritime air surges, may exist south of the Convergence Zone Cloud Band (CZCB). During a vigorous surge, these bands resemble cold fronts as they move southeastward into the Gulf of Aden.

e. Depressions transiting the Mediterranean frequently induce a northerly, then southerly displacement of the CZCB.

f. As perturbations from the Sudan Low move northeastward across the Arabian Peninsula, winds in the central and/or southern Red Sea can increase temporarily to gale force.

g. The entrance to the Gulf of Aqaba is known for gusty winds. Strong northerly winds result in momentary gusts with large speed and direction variations.

h. In the southern Red Sea (south of the CZCB) stratocumulus coverage is greatest near 0900 and least near 2100 local time. It is most common along the western shore.

i. There is a semi-permanent area of low clouds which extends from the vicinity of 20N, 65E into the Gulf of Aden during much of the Northeast Monsoon.

j. Dust storms are infrequent during the NE Monsoon season except in the northern Red Sea where vigorous extratropical disturbances cause temporary strong, gusty winds.

k. The Subtropical Jet core is located over the poleward (northern) edge of the cirrus cloud band, and speeds in excess of 100 kt at 200 mb should be expected when:

   (1) A high-level cloud band extends WSW-ENE from tropical toward temperate latitudes, and

   (2) The cloud band has a "streaky" appearance with a well-defined northern edge and a relatively cloud-free band just north of the edge, and

   (3) A trough in the westerlies extends southward into low latitudes west of the cloud band.

5.3.3 Persian Gulf and Gulf of Oman

In sharp contrast to the Red Sea, which is a narrow passage separating two prominent mountain ranges, the Persian Gulf and surrounding terrain form a broad basin with no significant barriers to air flow except along the Iranian coast. It is protected in the north from extratropical disturbances and cold air-mass invasions by the mountain ranges of Iran and Turkey. Vigorous upper-air disturbances which penetrate to low latitudes are required to surmount these barriers. When these conditions are met, the potentially destructive Winter Shamal occurs; however, most of the time the weather conditions in this season are mild, sunny and generally uneventful.

The Winter Shamal

Perrone (1979) in NEPRF Technical Report TR 79-06, prepared a comprehensive description of the Winter Shamal and compiled a number of forecasting rules/aids. His publication should be held by every embarked meteorological unit and thoroughly studied by all forecasters operating in the Arabian Sea during the Northeast Monsoon season. A highly condensed summary of the contents of TR 79-06 follows:

Synoptic Sequence of Events. An upper level trough and its associated surface low center and frontal system move eastward or northeastward from the eastern Mediterranean into Syria. Simultaneously, a second transient low center moves eastward from the Sudan Low across the Red Sea and the Arabian Peninsula. The resulting pressure gradient over the Persian Gulf causes moderate to strong southerly winds ("Kaus") over the Persian Gulf. These winds are strengthened by a compaction of the pressure gradient along the Zagros Mountains of western Iran. As the cold front moves across the northern Arabian Peninsula, a new low pressure center typically forms on the front in southern Iraq or over the northern Persian Gulf, and eventually becomes the dominant low pressure center as the original low to the north and secondary low to the south weaken. As the upper air trough moves into Iran, cold air is advected over the mountains of Turkey and Iran where it contributes to strong pressure rises west

of the low. The resulting strong northerly (Shamal) winds force the cold front rapidly southeastward in the Persian Gulf basin. If the cold advection is sufficiently strong and the eastward movement of the upper level trough is slow (usually satisfied by a blocking pattern), the cold front will move off the southeast coast of the Arabian Peninsula and some distance out over the northern Arabian Sea. Weaker, fast-moving disturbances (more zonal pattern) usually result in the cold front becoming stationary near the southeast coast of the Arabian Peninsula. As high pressure rebuilds over Iran, an inverted trough (occasionally a low center) forms over the Gulf of Oman and extends northwestward along the eastern shore of the Persian Gulf. The final stage of the Shamal is a weakening of the high pressure center over the Arabian Peninsula (and a possible westward regression of the inverted trough).

Variations in the Sequence. The majority of the Shamal outbreaks continue for a period from 24 to 36 hours. Occasionally (1-2 times each year), the upper level trough will stall in the vicinity of the Strait of Hormuz. Extended cold advection over the Arabian Peninsula resulting therefrom will perpetuate the Shamal for 3 to 5 days. The strongest winds are normally associated with these occasions. Early and late in the season (October-November, March-April), small amplitude troughs result in similar sequences of events, but the limited cold air advection fails to push the front to the Arabian Coast. On these occasions, Shamal winds occur only in the northern portions of the Persian Gulf. If sufficient Positive Vorticity Advection (PVA) exists aloft, a rather intense low pressure center may develop on the front in the central Persian Gulf, causing strong southerly winds in the southeastern portion.

Clear Air Turbulence (CAT). The same conditions which cause the Shamal may also lead to moderate to severe CAT. Figures 5-6a and b depict typical relationships between the Subtropical and Polar Jets during strong Shamal-producing conditions. The strong wind shear near the jet maxima is likely to produce a complicated CAT pattern in both the vertical and horizontal directions in the shaded area. Additional complexity may be introduced by the generation of mountain wave conditions where jet cores are nearly perpendicular to major mountain ranges. Rough terrain will also produce moderate mechanical turbulence in the lower levels within the Shamal area.

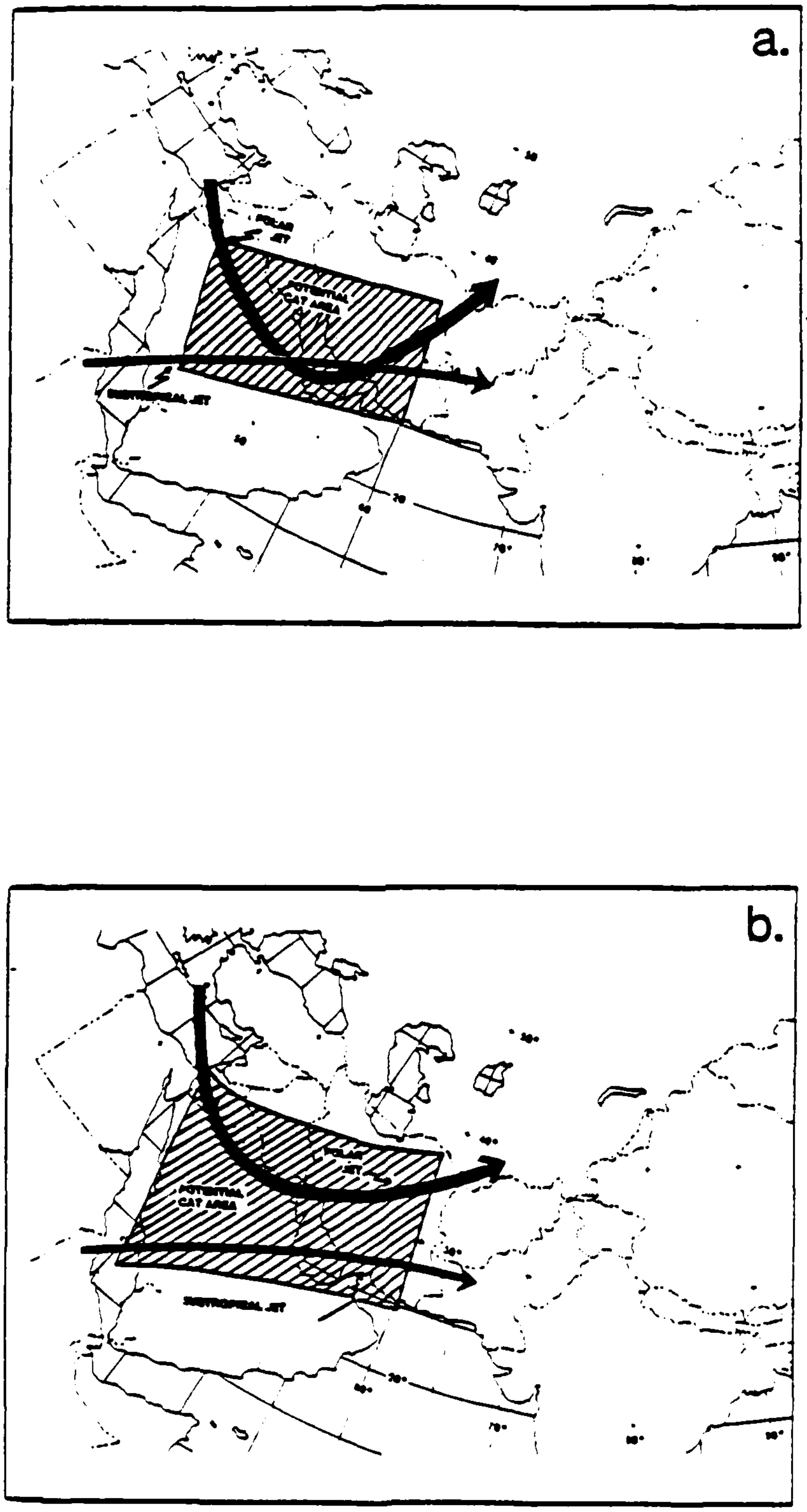

Figure 5-6. Potential CAT areas when, (a) Subtropical Jet overlays Polar Jet, and (b) Polar and Subtropical Jets are horizontally separated but in close proximity (from Perrone, 1979).

SHAMAL FORECAST RULES/AIDS.

a. Favorable pre-conditions are

(1) Cold long-wave trough (at least -25° C at 500 mb) south of the Taurus Mountains of Turkey.

(2) Eastward movement of long-wave troughs toward the longitude of the northern Persian Gulf.

(3) A conditionally unstable atmosphere based on soundings from southeastern Iraq or Kuwait.

(4) Daily mean surface temperatures at least 10°C colder in the upper Euphrates Valley (e.g., station 40045) than around the northern gulf (e.g., Kuwait; station 40372).

(5) A blocking ridge found over central or eastern Europe.

(6) Surface cyclogenesis occurring over the Tigris-Euphrates Valley or the northwestern Persian Gulf.

b. Onset intensity and direction

(1) If ΔT is the average surface temperature difference between the central Persian Gulf and the Tigris-Euphrates Valley (northern Iraq, eastern Syria), the average onset wind speed will be:

30 kt for $\Delta T = 10°C$
35 kt for $\Delta T = 15°C$
40 kt for $\Delta T = 20°C$
45 kt for $\Delta T = 25°C$

(2) Average gusts will be about 10 kt greater and peak gusts about 15-20 kt greater than the average speeds shown above.

(3) The onset is indicated by a shift in wind direction from southerly to northwesterly.

c. Duration

(1) If upper-air prog charts indicate rapid trough movement with no stalling near the Strait of Hormuz, forecast a Shamal duration of 24-36 hours.

(2) If upper-air prog charts indicate slow movement and possible stalling over the Strait of Hormuz, forecast a Shamal duration of 3-5 days. (Wind speeds over the southern Persian Gulf average 35-45 kt in these cases.)

d. Cessation

(1) Forecast a 3-5 day Shamal to break by sunset on the day the upper-air trough moves out to the east of the Gulf of Oman.

(2) If a convergence cloud band can be seen off Oman in morning satellite photos, forecast the Shamal to end that evening.

e. Associated sea conditions

(1) If the onset wind speed is computed from b(1) to be 30-40 kt, forecast the following significant wave heights:

10-12 ft in 12-24 hours after onset
12-14 ft in 24-36 hours after onset
15-18 ft in the southern Persian Gulf (particularly off the Qatar Peninsula) if the Shamal lasts more than 36 hours.

(2) For a 3-5 day Shamal, forecast residual swell heights as follows:

6-8 ft the day after the Shamal breaks
3-5 ft on the second day
1-3 ft on the third day.

f. Associated thunderstorms

(1) Thunderstorms are more frequent over the northern Persian Gulf
(2) Thunderstorms precede the front which initiates Shamal winds by 3-6 hours
(3) The most severe thunderstorms occur north of the Subtropical Jet axis
(4) When the Polar Jet and the Subtropical Jet overlap, they form a favorable high-level environment for the release of instability and the growth of convection.

g. If the surface wind speed during a Kaus (southerly wind) is near gale force or higher, forecast light to moderate turbulence:

(1) from the surface to 5,000 ft over the central gulf
(2) from 3,000 ft to 8,000 ft over the eastern gulf.

h. Forecast light to moderate turbulence below 5,000 ft behind the cold front.

i. Forecast moderate turbulence in the vicinity of cumulus development over water behind the cold front.

j. Moderate mechanical turbulence is likely along the western edge of the Zagros Mountains during extended (3-5 day) Shamals.

k. Mountain waves are common and are often detectable on satellite pictures.

l. Forecast light to moderate turbulence 20,000 ft - 35,000 ft near the position of the Subtropical Jet (Perrone, 1979).

m. When the Polar Jet and the Subtropical Jet overlap (Perrone, 1979):

(1) Enlarge the turbulence area to include the area from the northern edge of either jet to the southern edge of the other
(2) Forecast moderate to severe CAT from 15,000 ft to 30,000 ft near the Polar Jet
(3) Forecast moderate to severe CAT from 20,000 ft to 35,000 ft near the Subtropical Jet.

Low Level Cloud and Wind Patterns

The Shamal and the Kaus (southerly winds which often precede the Shamal) are the only significant disturbances to the winter weather in this region. Winds are generally light and rather variable. Cloudiness is usually limited to scattered, occasionally broken stratocumulus. Middle and high cloudiness is usually associated with the passage of upper level disturbances which may not be accompanied by low-level disturbances (i.e, Shamal, Kaus). Precipitation is limited to the more vigorous extratropical systems and is highly terrain-dependent; the Iranian coasts have much heavier rainfall than the Arabian coasts.

Clouds. Mean cloudiness reaches its annual maximum during the Northeast Monsoon season but still averages less than one-third total coverage. Less than half of the total is due to low clouds. Of the low cloud total, most occurs during the passage of strong extratropical disturbances which produce a Kaus followed by a Shamal. The Kaus produces typical warm front weather with multilayer cloudiness and precipitation. The heaviest cloudiness occurs over the Iranian coast due to terrain effects. The Shamal usually is accompanied by a band of convective clouds. The majority of the precipitation over the Arabian shores occurs during Shamals. As cold air sweeps out over the Persian Gulf and the Gulf of Oman, stratocumulus lines form over the relatively warm water. Figure 5-7 illustrates the cloud patterns which result from a cold front as it traverses the area.

By far the most common situation at this time of year is the weak to moderate Northeast Monsoon flow regime. It is characterized by clear to scattered clouds in a rather random pattern. During this regime, diurnal effects exert a strong influence on the clouds, causing them to be oriented generally parallel to the nearby shorelines. Figure 5-4 shown earlier in this section is representative of the "normal" Northeast Monsoon regime in most regions, except that the cloud coverage in the Persian Gulf is somewhat excessive.

A feature often found in the Gulf of Oman and occasionally along the Makran and Arabian Coasts is the "Convergence Cloud Line". It is usually caused by directional convergence in the low-level flow. The convergence may be augmented by terrain channeling or by the land breeze component (or both).

Figure 5-7. DMSP visual image illustrating cloud patterns associated with movement of a cold front down the Persian Gulf. The surface front is passing through the Strait of Hormuz. Strong thunderstorm cells have formed in the conditionally unstable areas preceding the front. Wave patterns in the clouds in the lee (northeast) of the southeast tip of the Arabian Peninsula also show conditional instability in the frontal zone. The fan-shaped plume over the Makran Coast indicates a backing with height of the upper-level winds (from west to southwest). Parallel cloud lines are forming over the northern Persian Gulf behind the cold front. Cloud lines of this type are common during cold air surges over warm water. This condition is typical of the Winter Shamal when northwesterly winds of 20 kt or more persist. The absence of clouds over the northern Arabian Sea indicates generally weak flow. The weak cloud lines near the entrance to the Gulf of Oman result from convergent flow from the southeast and southwest. The cloud patterns crossing the coast of Somalia show an onshore component in the wind direction. The approximate local sun time at the center of this image is 0930 (0606Z).

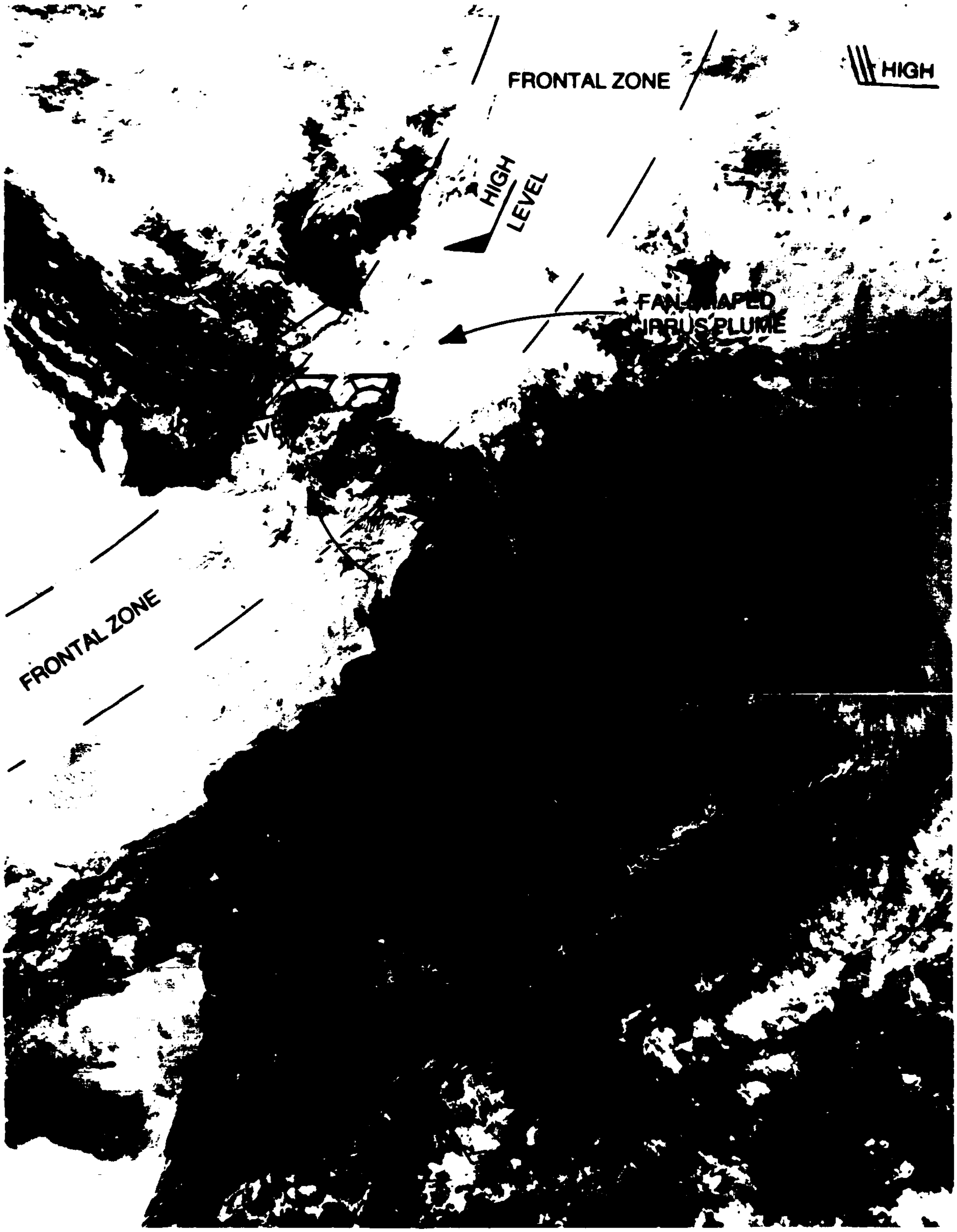

Figure 5-7. DMSP visual image recorded on December 21, 1979 showing cloud patterns typical of a cold-frontal passage during the Northeast Monsoon.

Figure 5-8 shows a prominent Convergence Cloud Line near the central axis of the Gulf of Oman and in the Strait of Hormuz. A weaker line extends southward from a point off Masirah Island. Figure 5-4 also showed weak Convergence Cloud Lines parallel to the Makran Coast and extending southward from the Arabian coast just south of Salalah.

Winds. The pressure gradient in this region normally is such that winds tend to be northerly, but are neither strong nor persistent except during the passage of extratropical disturbances. The specific direction of the prevailing winds is dependent on the geography and topography. In the northern Persian Gulf, winds average between 10 and 15 kt from the northwest. In the southern portion of the area they are lighter and generally westerly, becoming southwesterly in the western approaches to the Strait of Hormuz.

The gradient wind is usually very weak in the Gulf of Oman; surface winds are dominated by land/sea breeze effects. This results in frequent calms and considerable variability in both speed and direction. Since the land breeze is generally reinforced by the gradient wind during this period, offshore winds predominate except during the afternoon. These offshore winds tend to converge over the Gulf of Oman and result in the Convergence Cloud Lines mentioned in the previous section.

The strongest offshore winds (particularly during the early morning hours) are most likely to be found off the Iranian coast. Figure 5-8 is an excellent example of a situation with brisk offshore winds here. Low-level winds near the coast are strong enough (at least 15 kt) to raise dust at several places from the Strait of Hormuz to the northwest coast of India.

LOW-LEVEL CLOUD/WIND FORECAST RULES/AIDS.

a. Cold air advected over the Persian Gulf and Gulf of Oman by winds of 20 kt or more will result in convective cloud lines parallel to the wind. Sharpness and proximity of the lines is directly correlated with wind speed. (These are not the same as "Convergence Cloud Lines" due to converging surface winds).

b. Cloud-free coastal regions usually indicate offshore flow; cloud lines extending across the coast line indicate onshore flow.

Figure 5-8. DMSP image illustrating typical cloud features during the Northeast Monsoon: "Convergence Cloud Lines" in the Gulf of Oman, a weak front across the Arabian Sea and numerous clear coastal areas due to land breezes. Notice that the parent vortex over the Himalayas is well developed and that there is an area of suppressed cloudiness in the Central Arabian Sea south of the frontal band (probable area of anticyclonic flow). Closed cellular structure farther to the south indicates an upward slope of the inversion. Farther equatorward, some active convective clouds are seen in the northern Near Equatorial Trough. Cloud conditions over the Indian Coast south of the front and over Sri Lanka provide additional low-level wind information. Offshore flow is indicated along the Indian Coast by a clear, dry zone that terminates in a weak cloud line about 50-100 miles offshore. This clear zone is a common feature off the west coast of India during the Northeast Monsoon season. North of the front where the large-scale Northeast Monsoon flow has been replaced by the northwesterly flow behind the frontal band, the clouds appear to be continuous across the coast line from the ocean to the land. Large-scale northeasterly flow is reflected over Sri Lanka by the fine cumulus cloud lines. The basic direction is indicated by two features: the orientation of the lines and the marked drying (lack of clouds) to the west of the high terrain in central Sri Lanka. The approximate local sun time at the center of this image is 0915 (0425Z).

Figure 5-8. DMSP visual image produced from data recorded on January 1, 1980 showing a weak frontal band over the Arabian Sea, "Convergence Cloud Lines" over the Gulf of Oman and the eastern Arabian Coast and the effect of land breezes on cloud cover (time is 0830 local).

c. Surface winds are likely to be the most variable in or near "Convergence Cloud Lines".

d. Southeast or southerly winds with increasing cloudiness usually signal the approach of an extratropical disturbance with eventual shift to northwesterly or northerly winds known as "Shamal" winds.

Visibility Restrictions

Visibility is generally good during the Northeast Monsoon season except during the passage of extratropical disturbances. Strong Kaus or Shamal winds will raise dust to high levels in the same manner as the summer Shamal, but the duration is much less. Whitehead (1980) described a particularly intense sand/dust storm experienced by the USS Midway.

Restrictions to visibility due to dust are more common along the Arabian side than along the Iranian side of the Persian Gulf, but the Iranian coasts of the Gulf of Oman and the Arabian Sea are more likely to experience dust than the Arabian side. This is due to the brisk offshore flow which is common along the Makran Coast -- particularly following the passage of a cold front (see Figure 5-8).

During periods of settled weather (i.e., light winds), fog occasionally occurs in Persian Gulf coastal areas in the early morning, but it is dissipated rapidly by solar heating.

5.3.4 India

Figure 5-8 is typical of morning conditions over the Indian Peninsula during this season. Dry offshore northeasterly flow supresses low cloudiness along the Indian Coast. The offshore flow is not strong (usually less than 15 kt), particularly near the coastline, but is very persistent from December through February. In Figure 5-8 a dissipating cold front is located just north of Bombay. It illustrates the principal cause of cloudiness during this season, transient extratropical disturbances. North of Bombay, these disturbances can cause winds to shift to a southerly direction and heavy clouds and precipitation to occur over northwestern India, but the frequency of these conditions is low.

Prevailing wind directions and speeds are influenced by land/sea breeze effects, particularly late in the season. During March, surface winds are often

northwesterly due to strong heating which causes pressure falls inland as well as an enhanced sea breeze component. The southern tip of the Indian Peninsula sometimes is close enough to the Near-Equatorial Trough to experience more cloud cover than Indian coastal areas farther north. Rainshowers should be anticipated.

5.3.5 Atlantic Approaches

During the Northeast Monsoon, the southern Indian Ocean is generally dominated by a tradewind regime with associated clouds and wind patterns. The principal hazard to transiting vessels is from tropical cyclones. Figure 5-9 shows the mean frequency of occurrence of tropical cyclones with maximum winds greater than 33 kt for the period December through March. The axis of greatest frequency extends from a point just south of Diego Garcia west-southwestward across Madagasgar. A branch recurves southward, with the maximum frequency occurring between Albatross Island and Mauritius. Availability of satellite data from central sites for this area is limited, and ships tend to avoid tropical cyclone areas; therefore, warnings of tropical cyclone position and intensity tend to be less reliable than in the Atlantic and Pacific Oceans. An intense tropical cyclone such as the one shown in Figure 5-1 near 16°S, 72°E would be a serious threat to vessels heading for Diego Garcia. Although the Joint Typhoon Warning Center (JTWC) on Guam has access to some satellite data for the Indian Ocean, the quality and timeliness are generally inferior to that available in the western Pacific Ocean. Onboard satellite data receiving equipment (if available) is the best source of current position and intensity information.

5.3.6 Pacific Approaches

The Northeast Monsoon flow does not penetrate as far southward in the Bay of Bengal as it does in the Arabian Sea. This leads to the formation of dual Near-Equatorial Troughs, one between 10° N and the Equator and the second between 5°S and 15°S. The entire area between 5°N and 10°S generally has weak pressure gradients so that winds are not persistent and tropical convective activity is common. The southern Near-Equatorial Trough is usually the stronger and annually breeds a number of tropical cyclones. All transits from the Pacific

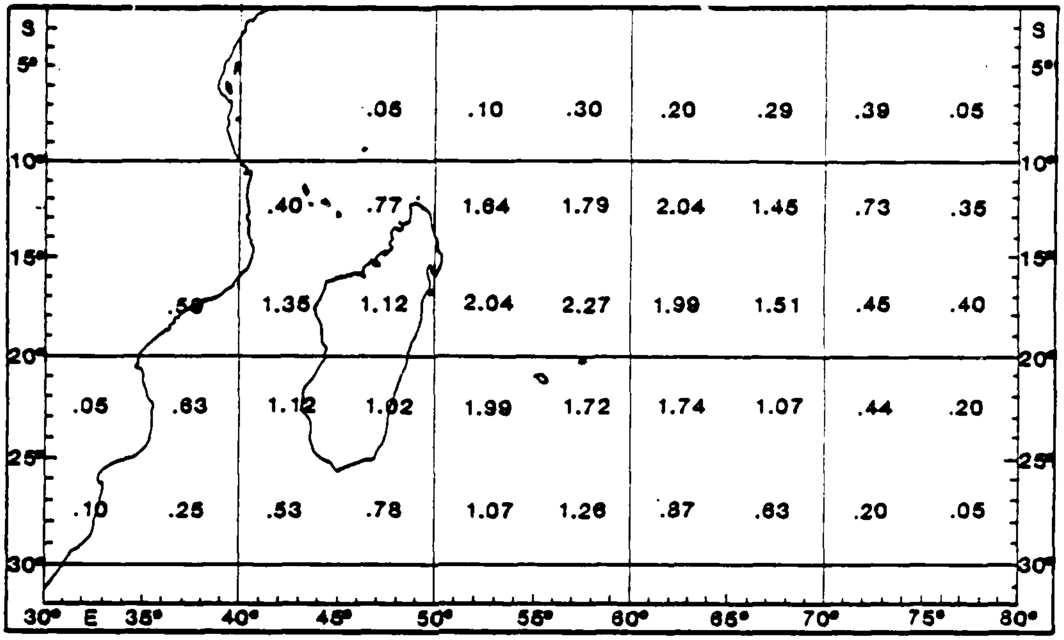

Figure 5-9. Mean frequency of occurrence of a significant tropical cyclone (maximum winds > 33 kt) in each 5° latitude-longitude rectangle for the season from December through March (adapted from Naval Weather Service Detachment, Asheville, 1974). For example, the 5° rectangle over northern Madagasgar experiences an average of 1.12 significant tropical cyclones each season (Dec.-Mar.).

Ocean (i.e., Strait of Malacca, Selat Sunda and Australian ports) should expect to encounter moderate to strong convective activity (most common south of the Equator). Interviews of Naval Oceanography Command personnel who had transited this area usually revealed comments on the severity of the convective activity frequently encountered here. Although the large scale winds are usually light, local winds from thunderstorm cells were occasionally a hazard to flight operations. If the operational scenario permits it, these areas should be avoided.

Figure 5-10 illustrates a period of strong convective activity late in the season (March). It shows that all transits from the Pacific would pass through areas of strong convective activity (but no tropical cyclone in this case). Figure 5-1, on the other hand, showed that the route via the Strait of Malacca is

Figure 5-10. DMSP visual image illustrating the heavy convective area in the Pacific Approaches to the Arabian Sea during the Northeast Monsoon. Severe thunderstorms, such as the ones shown in this image, frequently occur due to dual east-west low pressure troughs which are common in this area. These two troughs tend to cause a broad area of light winds in which the convective cells are imbedded. Strong, gusty winds are likely in the vicinity of the cell clusters. Cirrus streaks indicate that relatively strong easterly winds exist in the upper troposphere near the Equator veering to southerly toward the north and backing to northeasterly toward the south. A weak cold front (shear line) extends from the coast of Burma into the south-central Bay of Bengal. Weak Convergence Cloud Lines off the northeast Indian coast indicate a land breeze effect converging with westerly or southwesterly flow from an anticyclone centered over the Bay of Bengal. Cloud lines in the gray shade area to the southwest over the water continue inland in response to southerly flow over that region. The relatively clear skies, and probable light winds, over most of the Bay of Bengal are consistent with an anticyclone center in that region. The approximate local sun time at the center of this image is 1100 (0457Z).

Figure 5-10. DMSP visual image of the northeastern Indian Ocean during the Northeast Monsoon recorded on March 15, 1978.

relatively clear, but that tropical cyclones threaten southern hemisphere routes (particularly from Australia).

Although none of the forecasters interviewed had a close encounter with a tropical cyclone in the Pacific Approaches, the probability of such an encounter is significant. Atkinson (1971), based on data collected from 1962 to 1967, estimated that an average of more than 6 cyclones of tropical storm intensity or greater are generated each year in the southeast Indian Ocean during the December-March period. Since meteorological satellite technology was still in its infancy at that time, and no main shipping lanes cross the area, it is likely that the frequency of cyclones is greater than Atkinson's estimate. Furthermore, the frequency of occurrence of tropical cyclones in the latitude band between 5^{o}N and 10^{o}N reaches a maximum during December. These storms are close enough to the route through the Strait of Malacca to be hazardous unless a southward diversion is taken. The area near Sri Lanka is particularly dangerous because cyclones reaching this area are often well-developed. Bay of Bengal tropical cyclone activity decreases sharply to an insignificant level in January and is absent during the month of February.

FORECASTING RULES/AIDS FOR PACIFIC APPROACHES.

a. The north-south extent of convective activity is much greater than usual due to the dual trough pattern straddling the Equator east of Sri Lanka.

b. Transits between the Arabian Sea and Australian ports are likely to encounter moderate to severe thunderstorm activity from the southern tip of India to about 15^{o}S and may encounter tropical cyclones between 5^{o}S and 20^{o}S.

c. Transits via Selat Sunda are most likely to experience thunderstorm activity but avoid encounters with tropical cyclones.

d. Transits via the Strait of Malacca are most likely to encounter tropical cyclones near Sri Lanka in December. Tropical cyclones are not a threat on this route from January through March.

e. In the absence of recent satellite imagery, ship's radar should be used to avoid thunderstorm cells.

6.0 SPRING TRANSITION (APR-MAY)

6.1 General Description

During the Spring Transition season, there is a rapid increase in incoming solar radiation as the sun's nadir moves into the Northern Hemisphere. Continental high-pressure zones at the surface weaken and become low-pressure areas (heat lows); upper-level anticyclones form over the surface heat lows as successively higher levels are warmed. Concurrently, the northern Near-Equatorial Trough tends to follow the sun's nadir northward and gradually replaces the weak low-level anticyclone over the Central Arabian Sea. As a result of these circulation changes, low troposphere winds become light and quite variable early in the period (April). By late May, the pressure gradients have reversed from the winter pattern and wind directions typical of the summer (Southwest Monsoon) season predominate. Wind speeds are generally light except near the northern African Coast where the low-level Somali Jet (see Section 3.3.1) starts to appear.

Except in the immediate vicinity of the Near-Equatorial Trough and around tropical storms, skies are generally clearer and visibilities better than during the winter. Tropical cyclones become the main severe weather producers during the Spring Transition — particularly as the Near-Equatorial Trough advances north of 5^{o}N. In May, a significant number of tropical systems move westnorthwest across the Arabian Sea toward the Arabian Peninsula.

Sea heights during the Spring Transition period are usually moderate except off the northern African Coast in late May and around the more intense tropical systems. Significant heights of 10 ft may be found off Somalia by the end of this Transition Period, and heights in excess of 15 ft are common around the tropical storms.

The mosaic cloud picture shown in Figure 6-1 reflects the generally good weather which is typical of this period. No tropical systems are occurring in the Arabian Sea, but a late-season cyclone is shown near 10^{o}S, 75^{o}E. A weak extratropical disturbance can be seen approaching the northern Persian Gulf.

Figure 6-1. NOAA visual mosaic showing a typical cloud pattern for the Spring Transition when winds are usually light and skies are mostly clear. Any cloud development seen indicates some form of disturbance. The clouds over the northern Persian Gulf and the central Arabian Peninsula are caused by a trough or weak front. The transition seasons are the favored periods for tropical cyclone development in the northern Indian Ocean, and the cloud mass in the southern Bay of Bengal is a tropical cyclone in the early stages of development. A well-developed tropical cyclone is shown in the Southern Hemisphere near 10°S, 75°E. Several areas of strong convective activity are seen in the image, e.g., over the southern slopes of the Himalayas, equatorial Africa and Southeast Asia. Weaker activity is seen over southern India and the southwestern portion of the Arabian Peninsula. Convective clouds are common over coastal mountain ranges during this season. Light wind conditions are substantiated by: (a) the weakness or total absence of cirrus plumes from the convective cloud areas (light wind conditions at upper levels), (b) the absence of low-level clouds over the water (light low-level winds), and (c) the narrow sunglint pattern over the eastern Arabian Sea (smooth seas and implied light surface winds). The northern Near-Equatorial Trough is not well-defined in this image; the convective area off the coast of Somalia probably marks the western portion. This trough is most likely to be found near a line from that point to the southern edge of the developing cyclone in the Bay of Bengal.

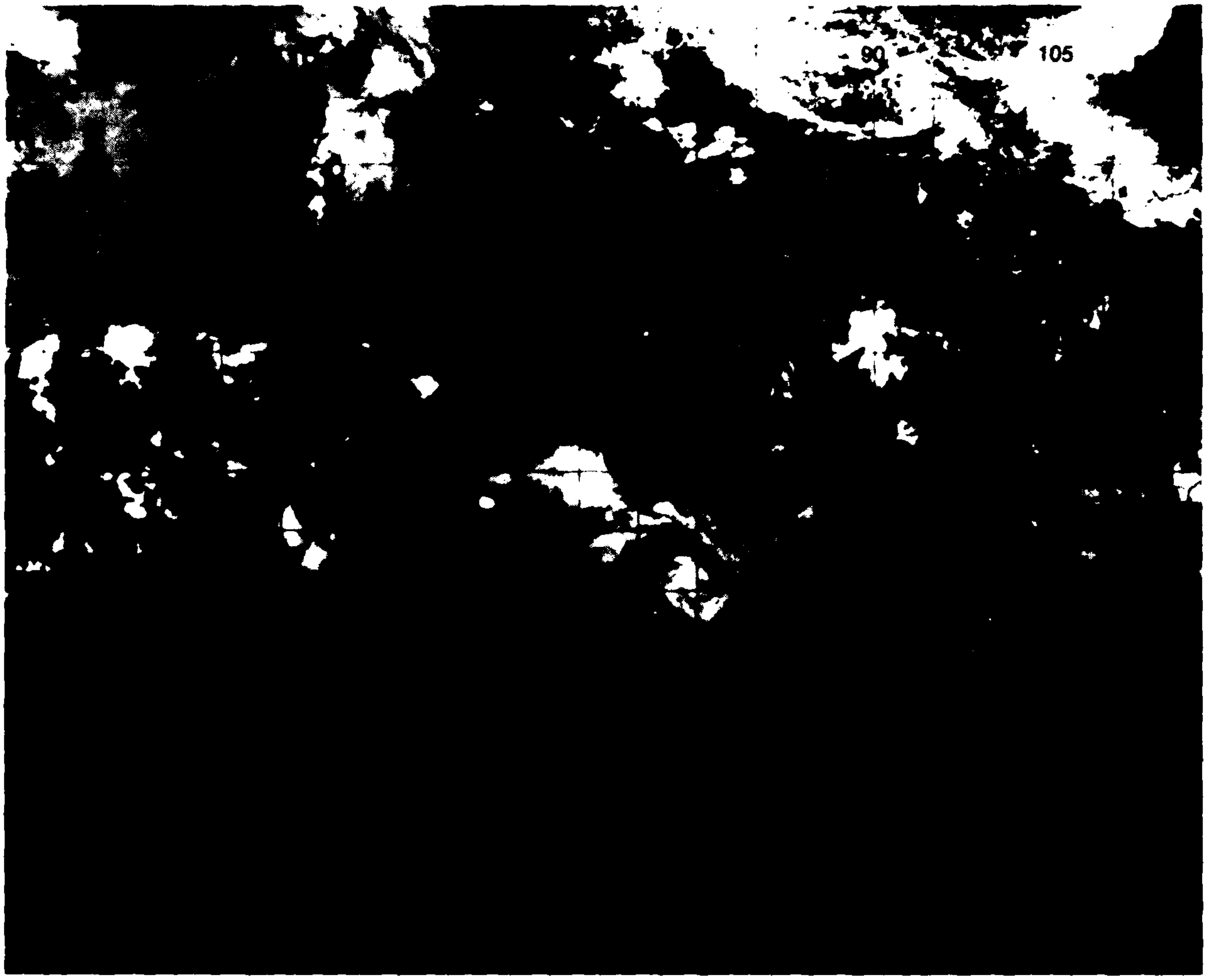

Figure 6-1. NOAA visual mosaic produced from data recorded on April 27, 1982 showing a typical cloud pattern for the Spring Transition period.

6.2 Large-Scale Circulation Features

During this period the upper-level Subtropical Ridge moves northward to a mean position between $12^{\circ}N$ and $15^{\circ}N$, and strengthens. An upper-level anticyclone forms (in the mean flow) over Indo-China. (This mean anticyclone drifts to a position over Tibet during the Southwest Monsoon.) The resulting high-troposphere flow pattern over the Arabian Sea is weak and rather variable from day-to-day. Westerlies persist north of about $15^{\circ}N$ and extratropical disturbances continue to influence the Arabian Peninsula and nearby areas. Weak cross-equatorial flow toward the Southern Hemisphere provides upper-level divergence favorable for tropical cyclone development. Weak vertical wind shear favors convective activity, and other prerequisites for tropical storm development are satisfied when the northern Near-Equatorial Trough migrates to a position north of $5^{\circ}N$. This usually occurs early in the transition period.

Low-level circulation changes of primary importance are caused by gradual intensification of heat lows over the continents bordering the Arabian Sea. The developing heat lows over the Arabian Peninsula and southern Asia gradually reverse the pressure gradient. The northward migration of the dual Near-Equatorial Troughs results in strengthening cross-equatorial flow toward the north near the equatorial east coast of Africa (Somali Jet). These changes result in a clockwise gyre of low-level flow in the Arabian Sea which is the precursor of the Southwest Monsoon. Mid-troposphere subsidence usually suppresses convection (and other cloudiness) over the Arabian Sea north of the Near Equatorial Trough until late May or early June.

6.2.1 Climatology

Naval Oceanography Command climatological publications (see Appendix A) should be consulted for information on monthly mean values of operationally significant parameters. The information which follows in Figures 6-2a through e is intended to illustrate the discussion in this section without duplicating those publications.

Of particular significance are the weakness of the winds and the low ocean waves. Although part of the reason is the averaging process, wind speeds at all levels approach an annual minimum during this season. Convective activity, whether found in the Near-Equatorial Trough or over prominent terrain, is noteworthy during the Spring Transition period. Figures 6-2c through e all reflect contour maxima related to convective cloudiness.

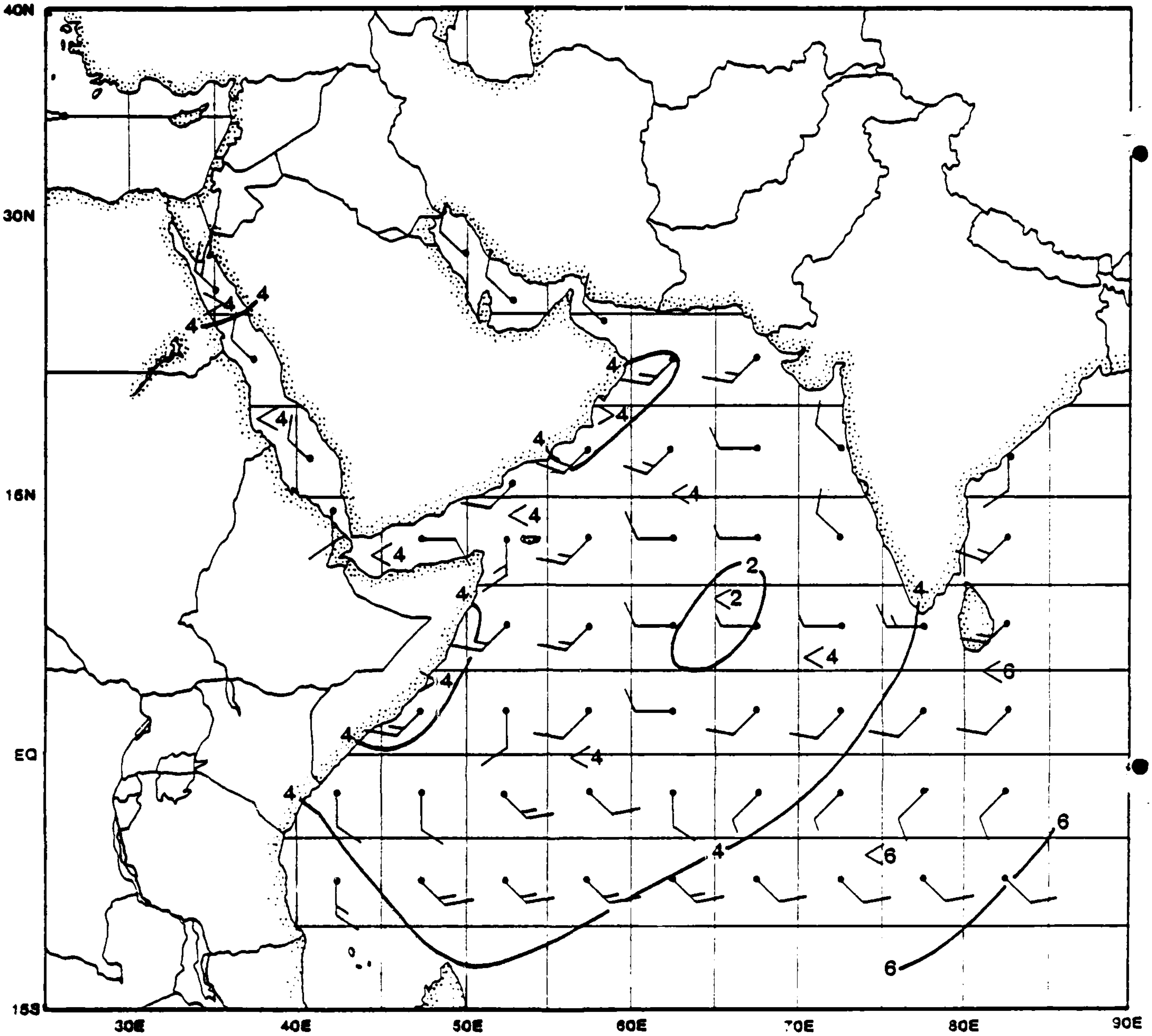

Figure 6-2a. Mean May surface winds (wind barbs) and seasonal mean significant wave heights in ft (contours) (adapted from Naval Weather Service Detachment, Asheville, 1974). The wind barbs represent the average over a 5° rectangle of latitude and longitude. Wind barbs representing the restricted waters of the Red Sea, Persian Gulf and Gulfs of Aden and Oman are plotted over the water area that they represent. The data from which the contours of significant wave height were determined represents only the highest of the observed heights when both a wind wave group and a swell group were reported.

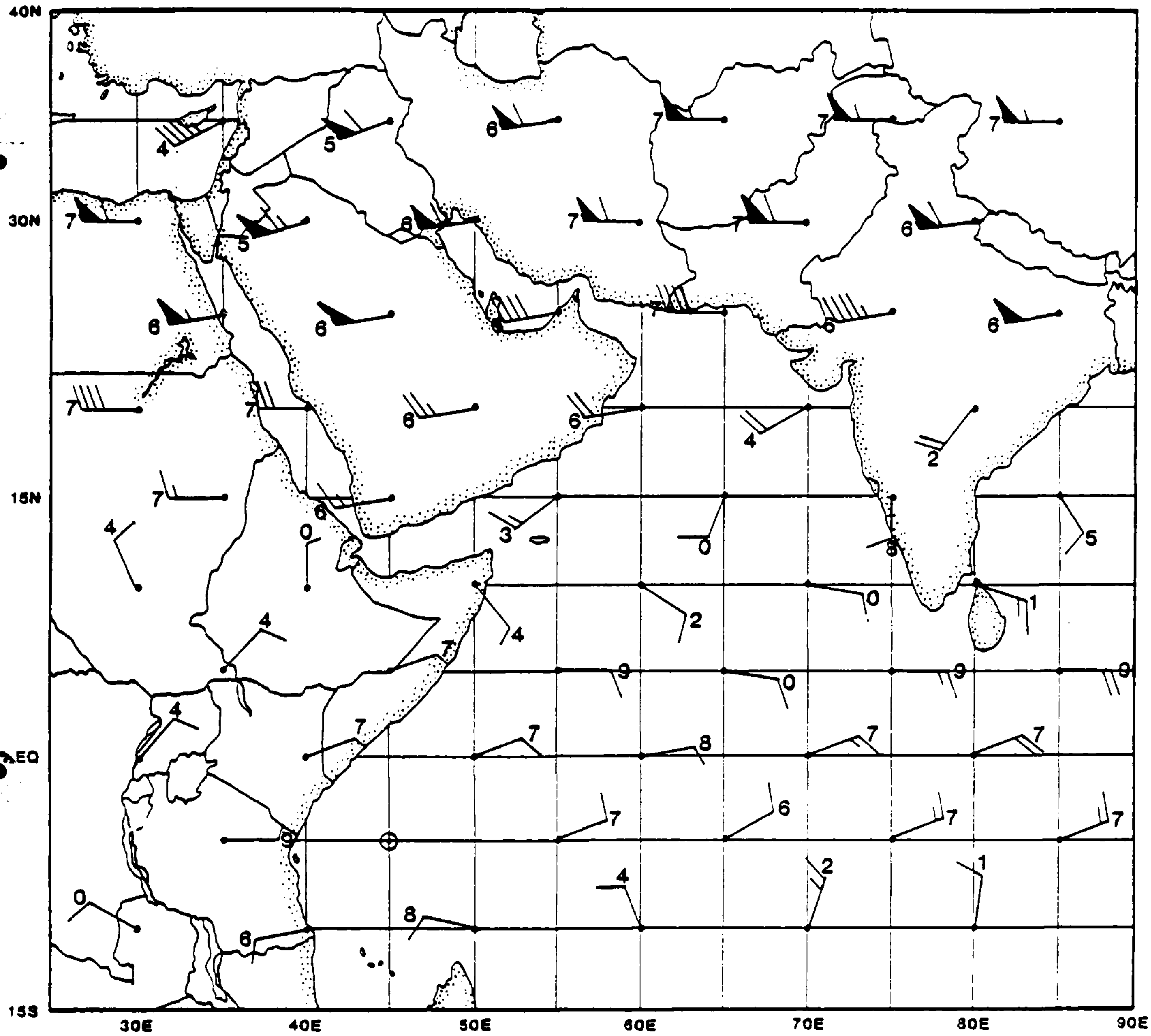

Figure 6-2b. Mean May 200 mb winds (adapted from Sadler, 1975). The numeral by each wind barb is the tens digit of direction. A circle around a latitude-longitude intersection indicates a light, variable wind. Note that westerlies persist over the Asian continent but that the Subtropical Ridge has begun to drift northward from its winter position (near 7^{o}N). Very weak cross-equatorial flow from north to south is shown, and both directional and speed divergence (favorable for tropical cyclone development) is apparent over the Arabian Sea.

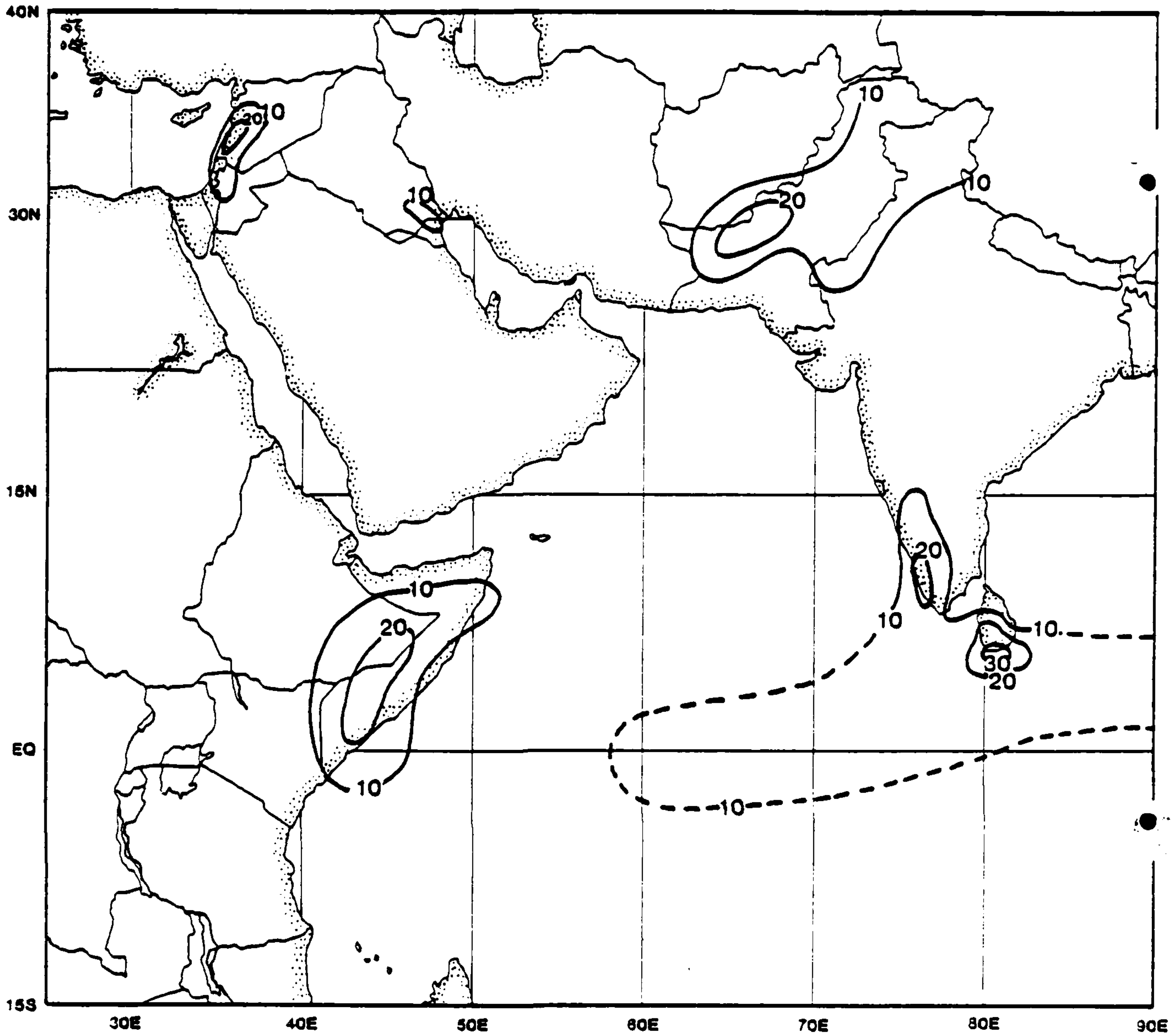

Figure 6-2c. Percent frequency of ceiling less than 1500 ft or visibility less than 3 n mi. The infrequency of adverse weather during this season is apparent in this figure. When significant contours do appear, the reason is usually due to convective rain showers. The area to the west of the southern tip of India is shown as a dashed 10% contour because observations in this region are sparse.

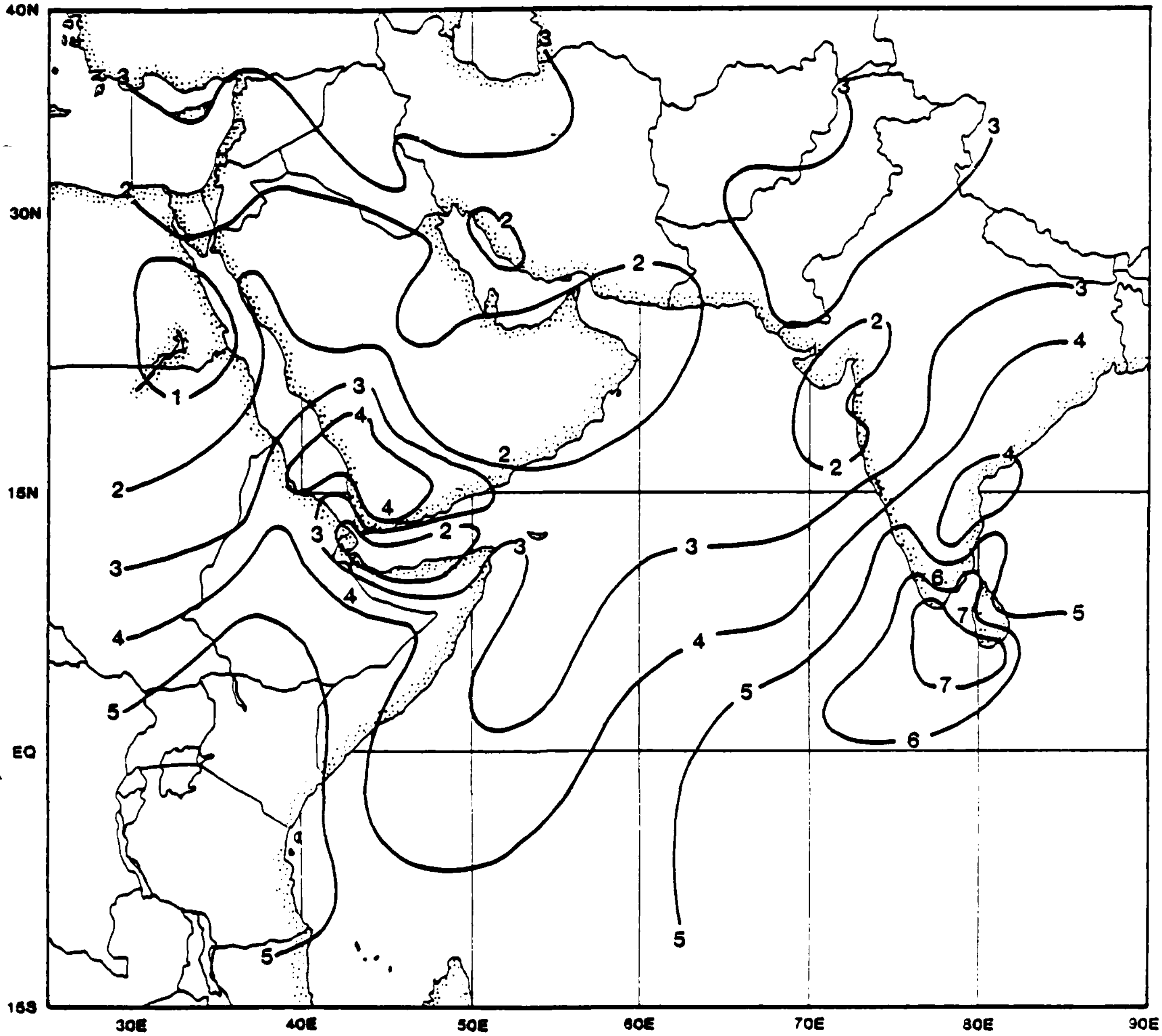

Figure 6-2d. Mean total cloud cover in tenths. The majority of the cloudiness shown is a direct result of convective activity (see Figure 6-2e).

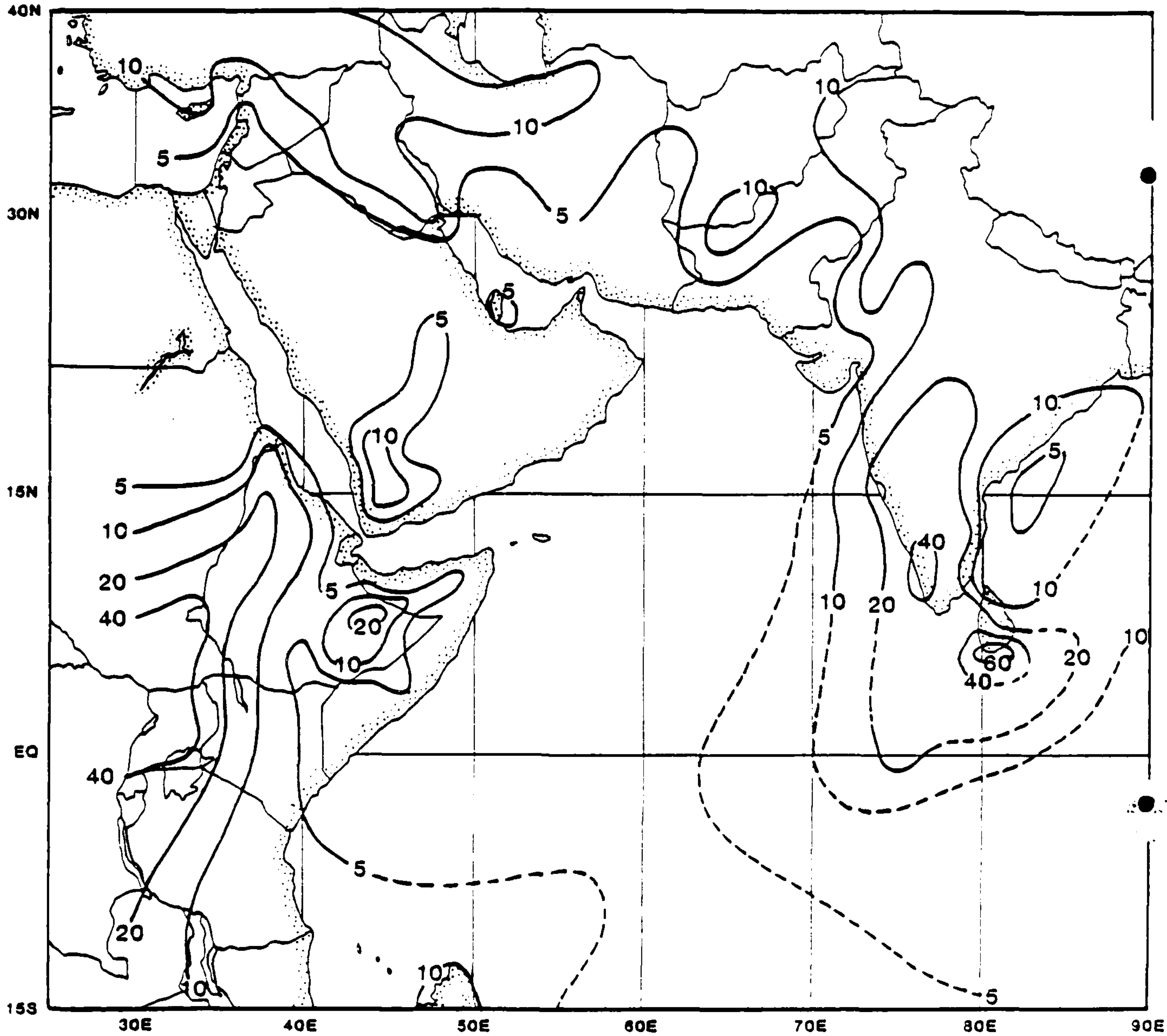

Figure 6-2e. Percent of days with thunderstorms. Light winds and strong heating result in considerable convective activity where high terrain or moist onshore flow creates instability. The thunderstorms of southern India occur primarily at night. Thunderstorm frequency in the tropical Arabian Sea and Bay of Bengal is indicated by dashed contours because the data on which it is based are very sparse.

6.2.2 Troughs and Frontal Systems

Although weak cold fronts or troughs continue to pass over the Arabian Peninsula and the Persian Gulf during this season, they are seldom strong enough to penetrate to the Arabian Coast. Figure 6-1 showed an example of an extratropical cloud system moving over the Persian Gulf in late April. Figure 6-3 shows a similar cloud system over the northern Persian Gulf on the last day of May, 1979. It is quite unusual for extratropical disturbances to occur that late in the season in this region.

The weather associated with fronts/troughs during this period is of little consequence except when local squalls are spawned. These squalls can cause moderate to severe sand/dust storms which may affect coastal areas of the Persian Gulf (see Figure 6-2e).

In response to maximum solar insolation, the northern Near-Equatorial Trough intensifies and drifts northward with the sun's nadir. It reaches a mean position near 10°N by late April and provides the conditions favorable for tropical cyclone development. Usually, migration farther northward does not occur smoothly or gradually, but rather, discontinuously; i.e., the Near-Equatorial Trough in the Central Arabian Sea disappears as the Monsoon Trough forms near the northern coastal areas.

6.2.3 Large-Scale Cloud and Wind Patterns

Arabian Sea

The Spring Transition period is one of two periods during which the meridional component of the sea-level pressure gradient reverses direction. During the northern hemisphere winter, relatively low levels of solar radiation result in the maintenance of low-level high pressure ridges over continental areas due to cooling by long wave radiation. As the sun's nadir moves into the Northern Hemisphere during the Spring Transition, incoming short wave radiation exceeds heat loss by long wave radiation. This results in the pressure gradient becoming very weak over the Arabian Sea early in the transition period, then gradually strengthening as the pressure continues to fall over the land areas. The end result is a system of continental heat lows connected by a thermal trough which extends from central India across southern Asia, the Arabian Peninsula and northern Africa.

Figure 6-3. DMSP visual image showing typical cloud conditions late in the Spring Transition period. Features of interest include the c. .vective cell clusters in the area extending southwestwar .rom the southern tip of India. These clusters have formed in the Near-Equatorial Trough. The absence of organization in the cirrus patterns associated with the convective activity reflects the light middle and upper tropospheric wind conditions typical of the transition period. The southern limit of an extratropical disturbance is evident over the northern tip of the Persian Gulf. During the transition period, these systems seldom reach the Arabian Sea. The lighter shaded north-south band in the Central Arabian Sea is sunglint. Since there is little variation in the width of the sunglint pattern, sea conditions (and surface winds) must be relatively uniform throughout the area. Furthermore, the absence of cloud lines implies weak winds. Note that cloud lines are present near the northern African Coast where moderate southwesterly flow is becoming re-established late in the transition period. Instability is apparent over northern India and Pakistan where strong convective cells are occurring in the mountains. The approximate local sun time at the center of this image is 1100 (0653Z).

Figure 6-3. DMSP visual image recorded on May 31, 1979 illustrating cloud conditions representative of the end of the Spring Transition period (about 2 weeks prior to the initial surge of the Southwest Monsoon).

The low-level circulation at this time is generally cyclonic around the heat lows but is channeled where terrain restricts flow to one of two approximately opposite directions (e.g., the Red Sea). The trough of low pressure which forms over the surrounding land masses, the strengthening of the high pressure ridge over the Central Arabian Sea and the Coriolis force reversal across the equator result in generally anticyclonic flow over the Arabian Sea. This flow is supported by the Southeast Tradewinds of the Southern Hemisphere which are channeled northward along the east coast of Africa. As this flow crosses the Equator, it is accelerated by the pressure gradient along the African Coast; eventually this process leads to the broad, persistent wind flow of the Southwest Monsoon.

As the season progresses and the effects of the solar heating over southern Asia reaches higher and higher levels, the upper-troposphere Subtropical Ridge migrates northward and strengthens. This results in easterly flow aloft south of the axis of the Subtropical Ridge (12°-15°N). Westerlies continue in the portion of the area north of 15°N but are weakening rapidly in the area south of 35°N (region of Subtropical Jet). The mean upper-troposphere winds are shown in Figure 6-2b.

Weather and winds which result from these large-scale patterns are generally moderate. Early in the period, as the pressure gradient is reversing, winds become light and quite variable, particularly in the north. Cloudiness reaches a minimum due to subsidence which prevails in the area. Coastal wind patterns are largely a result of land/sea breeze effects. Generally, the only heavy weather is associated with convective activity in the Near-Equatorial Trough or with tropical cyclones.

Near the end of the period, southwesterly winds along the African Coast and eastern portion of the Arabian Coast increase markedly. Low-level mixing causes an increase in low cloudiness which often forms in lines roughly parallel to the flow (see area off Somalia in Figure 6-3). Convective activity becomes more common over the southern Indian Coast as atmospheric stability decreases. If a low-level vortex forms in this area, and moves northward along the Indian Coast, the initial surge of the Southwest Monsoon (and the end of the Spring Transition period), can be expected in 3 or 4 days.

Red Sea and Gulf of Aden

During the Spring Transition period, the changes in the northern Red Sea are mainly related to cloudiness, but in the Gulf of Aden and the southern Red Sea, they are mainly related to the wind flow. Cloud coverage in the north, most of which is caused by extratropical disturbances, gradually diminishes during the transition period as the disturbances become weaker and less likely to penetrate south of the Mediterranean. Increasing air temperature also reduces low-level cloudiness over water areas.

The wind direction reversal usually does not occur in the Gulf of Aden until late May or early June. Winds do become weaker, however, and more subject to land/sea breeze effects. In the Red Sea, the Convergence Zone Cloud Band (CZCB) gradually retreats southward during the period, then disappears as the wind reversal occurs in the Gulf of Aden. Northwest flow follows the retreating CZCB. Gale force winds are rare during this season.

Persian Gulf and Gulf of Oman

The effects of extratropical disturbances (e.g., cloudiness, southerly winds, etc.) generally disappear in the Persian Gulf during this season. The low-level winds, though quite light, blow more persistently from a northerly direction. Land/Sea breeze effects are apparent, but the strong daytime heating causes the sea breeze to be much stronger and more persistent than the land breeze. This is particularly true along the Iranian coast.

Although light winds and settled weather are the rule, squalls can occur in the western two-thirds of the Persian Gulf. These squalls are accompanied by blowing sand/dust and result from evening thunderstorms (see Figure 6-2e). Tropical cyclones are possible near the eastern approaches to the Gulf of Oman, but are rare.

India

During the Spring Transition period, most of western India experiences a gradual change from winter to summer conditions. As the heat low develops, onshore wind directions tend to become more common than offshore components.

The resulting increase in moisture in the coastal zone leads to cloud coverage increases and stability decreases. Thunderstorm activity reaches its peak for the year, becoming very common along the southern Indian Coast (see Figure 6-2e). Sea breezes are enhanced and land breezes inhibited by the warmth of the land. Winds are generally weak except near convective activity.

The most significant change is the recurrence of conditions favorable to tropical cyclone formation. Beginning in late April, the incidence of vortex formation off the Indian Coast rises sharply. Convective cloud clusters such as the one near Minicoy Island in Figure 6-3 (lower, right edge) should be watched closely for indications of vortex formation.

SPRING TRANSITION FORECAST RULES/AIDS.

a. The sunglint pattern over the Arabian Sea provides information on relative wind speed; a narrow (in east-west direction) pattern indicates weak surface winds; widening patterns indicate increasing surface winds.
b. The continental heat lows are very shallow; anticyclonic flow occurs at 850 mb.
c. Land breezes are very weak and occasionally absent; sea breezes are more persistent than during other seasons.
d. If southwesterly flow is established along the African Coast, tropical cyclone formation and northward movement along the Indian Coast indicates the end of the transition period and the beginning of the Southwest Monsoon.
e. Cold, high pressure cells moving into the South Indian Ocean from Africa usually result in a strengthening of the southerly flow along the African Coast.
f. If extratropical disturbances penetrate to the Arabian Sea late in the period, the transition period will be extended (and the onset of the Southwest Monsoon will be delayed).

6.2.4 Tropical Cyclones

The weakening of the winds (and vertical shear) at all altitudes, the intense solar radiation and the migration of the Near-Equatorial Trough northward to the southern Indian Coast, all lead to a second maximum in the monthly frequencies

of tropical cyclones. According to Sadler, et al. (1973), the probability of a significant tropical cyclone in the Arabian Sea is not substantial for the April-May period (average of one every four years), but a threat does exist and should not be discounted.

According to past records the favored area of formation is centered near 10°N, 70°E. Favored tracks are generally northwestward toward the Arabian Coast. About 25% of the cyclones move toward the north approximately parallel to the Indian Coast, then recurve and make landfall over northwestern India. In May, the majority of the cyclones cross the Arabian Sea and make landfall along the Arabian Coast. April cyclones usually dissipate or recurve before reaching the Arabian Coast. Only one storm in 80 years of records entered the Gulf of Oman and none were recorded in the Gulf of Aden. (See the discussion of the "Onset Vortex" in Section 3.2.3).

Atlantic and Pacific Approaches

Bay of Bengal tropical cyclones are not a threat to ships on a direct route from the Strait of Malacca to the Arabian Sea (see Cuming, 1973, for a discussion of Bay of Bengal weather). In April, tropical cyclones have occurred in the South Indian Ocean between Australia and the Arabian Sea, but the frequency of occurrence is very low. The principal threat occurs in the South Indian Ocean just east of Madagasgar during the month of April. Figure 6-4 shows occurrence and movement statistics for the months of April (a) and May (b). Ships on direct routes from either WESTPAC or Diego Garcia to the Atlantic Ocean will more or less parallel the favored track. Appropriate caution should be exercised on any transit of this area prior to early May.

TROPICAL CYCLONE FORECAST RULES/AIDS DURING THE SPRING TRANSITION.

a. Strong convective cloud clusters near 10°N, 70°E should be watched closely for indications of vortex formation.
b. If initial movement is toward the northwest, forecast northwest movement to continue.
c. If initial movement is northward, forecast northward movement to continue with recurvature and landfall near the Kathiawar Peninsula.
d. In April, northwesterly moving cyclones usually dissipate or recurve northeastward before reaching the Arabian Coast.

a. April

TROPICAL STORM TRACKS

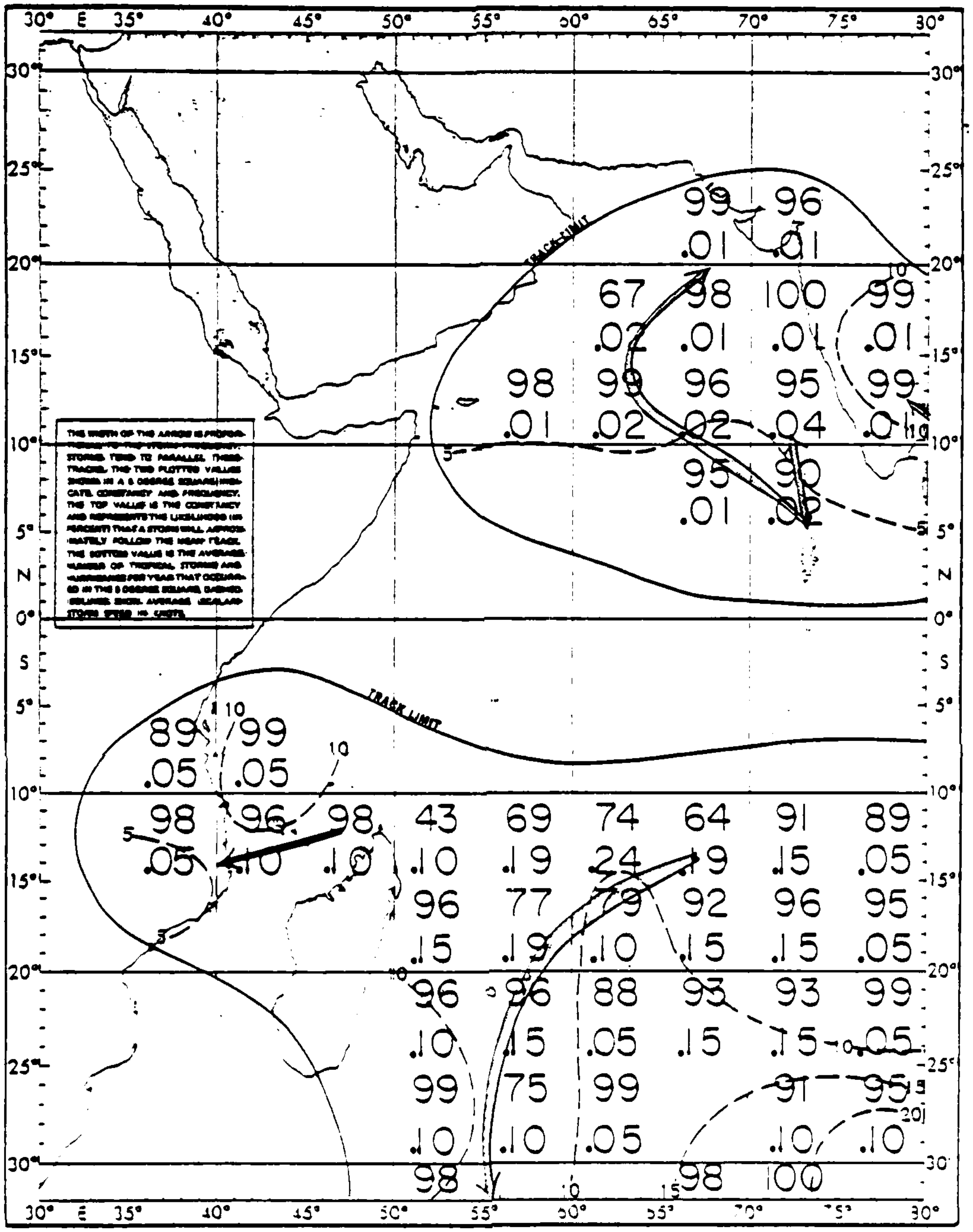

Figure 6-4a. Frequency of occurrence (lower number), probability of movement nearly parallel to the mean track (upper number) and average speed of movement in kt (dashed contours) of tropical cyclones with maximum winds greater than 33 kt (from Naval Weather Service Detachment, Asheville, 1974).

b. May

TROPICAL STORM TRACKS

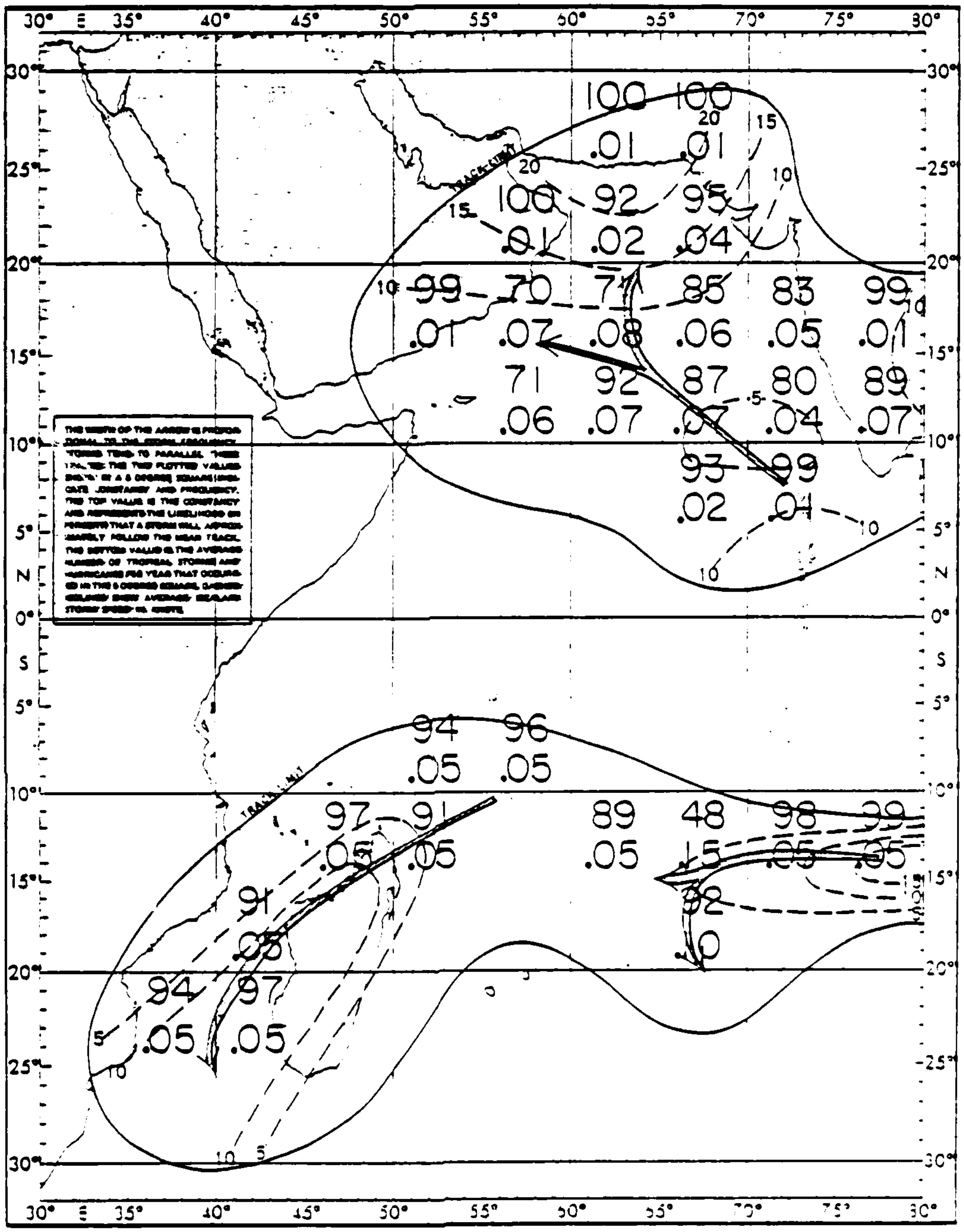

Figure 6-4b. Frequency of occurrence (lower number), probability of movement nearly parallel to the mean track (upper number) and average speed of movement in kt (dashed contours) of tropical cyclones with maximum winds greater than 33 kt (from Naval Weather Service Detachment, Asheville, 1974).

7.0 SPECIAL FORECAST RULES/AIDS

The previous sections of this Handbook discussed phenomena of interest to Navy forecasters by monsoon regimes (seasons) and geographical areas. Forecast rules and/or aids were presented as they applied to a particular phenomenon. Cruise (deployment) reports as well as interviews with geophysical officers and aerographers reveal that there are some forecast problems which are generally troublesome and are more mission or tactical-evolution oriented. This section, entitled SPECIAL FORECAST RULES/AIDS, addresses these special problems. In some cases, new material (charts, text, rules/aids) is presented; if a forecast rule/aid given in earlier sections is particularly important, reference is made to the original discussion.

7.1 ASW Operations

Navy forecasters are not usually directly involved in the preparation of acoustic propagation forecasts for support of ASW operations; however, they can expect to provide inputs concerning environmental effects. Since subsurface thermal structure changes in monsoonal flow regimes are different from those found in other naval operating areas, this section summarizes these changes.

The primary factors which influence subsurface temperature/salinity structure (and therefore sound speed profiles critical to acoustic propagation) are: (a) thermal mixing due to radiative cooling, (b) mechanical mixing due to wave action, (c) advection/upwelling due to large-scale current structure, (d) frontal formation due to large and small-scale current structure and (e) salinity changes due to current structure and evaporation. In the area covered by this Handbook, all of these factors are important; however, the upwelling patterns resulting from the monsoon wind reversal, the large negative water budget due to an excess of evaporation over precipitation and the intense solar heating produce an unique density distribution, particularly in the Red Sea and the Persian Gulf.

Figures 7-1a through f present a series of seasonal mean temperature profiles to illustrate the subsurface structure which influences ASW acoustic propagation conditions in selected areas. The user must realize that these are mean conditions based upon analysis of large numbers of soundings (Nansen cast, BT, XBT etc.) from an extended area. Individual soundings may vary greatly depending upon exact location within the area as well as particular time within any monsoon regime.

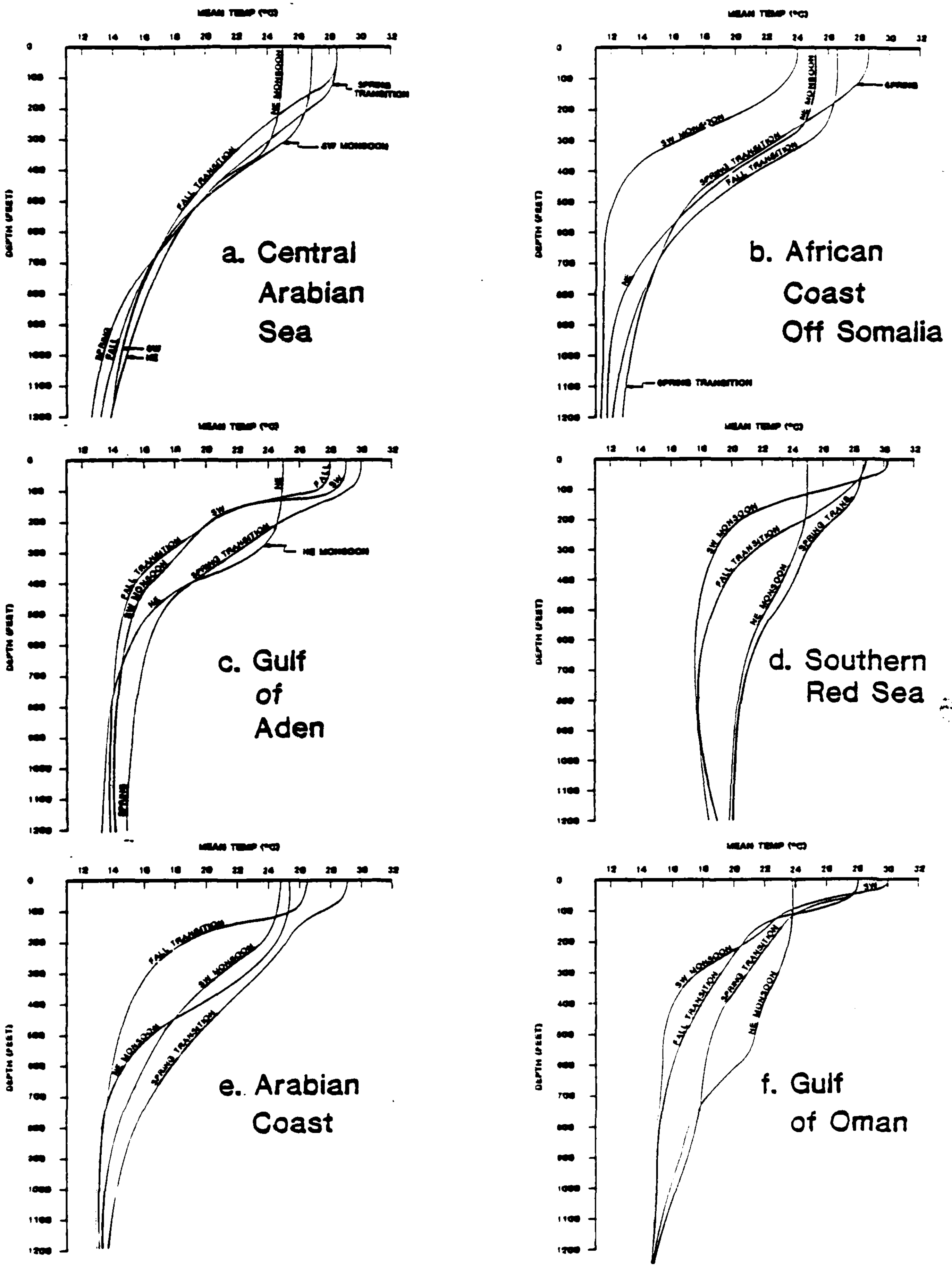

Figure 7-1. Mean subsurface temperature profiles representative of each season.

Figure 7-1a shows seasonal mean temperature profiles for the Central Arabian Sea (see Figure 2-1 for general location). Notice that temperatures below about 300 ft are nearly constant throughout the year. Near surface structure is nearly the same in both transition periods with the upper mixed layer about 100-120 ft deep. During the Northeast Monsoon, thermal mixing forces the MLD down to about 300 ft, while mechanical mixing (by stronger winds and higher waves) gives a mean MLD of about 200 ft in the Southwest Monsoon heating season.

The strongest surface flow parallel to the African coast occurs off Somalia during the Southwest Monsoon (see Section 3.3.1). This flow causes very strong upwelling along this coast. Figure 7-1b shows mean seasonal temperature profiles for the northern portion of the African Coast area defined in Figure 2-1. Notice that mean surface temperatures are warmest during the Spring Transition and coldest during the Southwest Monsoon (local temperatures along the northern Somali coast can be several degrees Celsius colder than the mean during the Southwest Monsoon). The entire water column from the surface to about 900 ft undergoes very strong cooling between spring and summer due to upwelling.

Figure 7-1c shows mean subsurface temperature profiles in the Gulf of Aden. Notice that a significant change occurs just around the corner of the horn of Africa. Whereas the Somali coast had the coldest water during the Southwest Monsoon, the Gulf of Aden has the coolest surface water during the Northeast Monsoon. During the Northeast Monsoon, the surface layer appears to be well mixed down to about 250 ft; the remainder of the year, the mixed layer depth is less than 100 ft. Thermocline gradients during the Southwest Monsoon and Fall Transition are particularly strong in this area causing very rapid sound ray refraction; however, it appears a significant sound channel can be expected near 600 ft with good conditions for deep listening.

Mean profiles for the southern Red Sea are shown in Figure 7-1d. Notice that the profiles are significantly different from those in the Gulf of Aden. The differences are due to: (a) shifts in direction of surface wind flow through the entrance from summer to winter, (b) deeper flow across the sill which separates the Red Sea from the Gulf of Aden and (c) the extreme evaporation which influences salinity (density) structure in the Red Sea. The profiles show that temperatures actually increase with depth below 650 ft during the Southwest Monsoon and Fall Transition; this indicates that salinity structure plays an

important role in column stability (and therefore in sound propagation conditions).

Figure 7-1e shows mean subsurface temperature profiles for the area off the Arabian Coast (see Figure 2-1 for location). These profiles also show the results of the strong upwelling which occurs here during the Southwest Monsoon. Notice, however, that the strongest cooling at depths of 200-400 ft occurs later in the year here than off Somalia. (Monthly mean profiles computed by Colburn (1975) show that the maximum deep upwelling along the Somali Coast is found in July and August while the maximum deep cooling off the Arabian Coast occurs in September and October.)

Figure 7-1f shows mean seasonal profiles for the Gulf of Oman. Here, the warmest surface temperatures, the shallowest upper mixed layer and the most intense thermocline all occur during the Southwest Monsoon, while upper layers are the coolest and mixed to deeper depths during the Northeast Monsoon.

No profiles are shown for the Persian Gulf because the area is so shallow.

Figures 7-1a through f illustrate the strong differences in thermal structure which are characteristic of various portions of this area. ASW forces can expect large variations in sound propagation conditions from area to area and from season to season. Since ambient noise (especially high frequency noise) is influenced by wave action, ASW operators should expect significantly higher ambient noise levels during the Southwest Monsoon.

The previous paragraphs discussed large-scale thermal structure changes which influence ASW operations in this region. The profiles presented covered areas with semi-homogeneous characteristics; however, they were seasonal means for relatively large areas and therefore smoothed out local features of importance to ASW. According to Bruce, et al. (1980), distinct smaller-scale thermal structure patterns form off the coast of Africa between the Equator and the Gulf of Aden during the Southwest Monsoon. Of most importance are the anticyclonic circulation eddies which are found off the Somali coast. The most permanent of these eddies, with a diameter of 250-350 n mi occurs each year between $4^{O}N$ and $12^{O}N$. There is also evidence that a second (smaller) semi-permanent eddy is a common occurrence to the south of the "prime" eddy. These eddies result in an ocean thermal front with crescent-shaped edges around the anticyclonic eddies due to upwelling occurring at the time of formation of these

eddies. Cloud-free areas are typically associated with the cold wedges. Figure 7-2 shows a DMSP infrared image of this coast for July 5, 1979. Notice the detailed thermal structure off Somalia and the Arabian Peninsula. The eddies mentioned above are clearly shown centered near 8^{o}N, 53^{o}E and 3^{o}N, 50^{o}E.

FORECAST RULES/AIDS.

a. Forecasters should utilize satellite infrared imagery to locate areas of maximum upwelling and edges of frontal boundaries and warn ASW operators to expect anomalous propagation conditions in these locales.

b. During the heating (summer) season, forecast the depth of the upper mixed layer (MLD) to be at least 10 times the average significant wave height over the past 12 hours (e.g., 10-ft waves give MLD of at least 100 ft).

c. Remember that: (1) SST and depth determine the probability of Convergence Zone (CZ) propagation plus CZ range and CZ width, (2) MLD influences the success of surface sound channel propagation and detection of shallow targets, (3) MLD and intensity of the thermocline gradient influence detection success and best listening depths for deeper targets, and (4) occurrence of a mid-depth sound channel influences detection success on deep targets. With these rules in mind, Table 7-1 summarizes MLD (ft), mean thermocline gradient (^{o}C/100 ft), maximum thermocline gradient (^{o}C/100 ft) and probability of mid-depth sound channel shallower than 1000 ft.

d. Areas of low SST due to upwelling tend to be cloud-free and the location of the ocean front is often marked by a sharp line between clear skies and scattered to broken low clouds.

7.2 Electro/Optic Operations

Navy forecasters with experience in operations off the U.S. west coast are familiar with Electro/Optic (E/O) anomalies associated with upwelling, but they are not as familiar with the problems associated with intense evaporation. In the general region covered by this Handbook, the forecaster can expect near-surface (0-200 ft) atmospheric enhancement due to intense evaporation to increase

Figure 7-2. DMSP IR image of the Arabian Sea selected to illustrate the complexity of the ocean thermal structure off the coast of Africa during the Southwest Monsoon. Cold upwelling is clearly depicted along the African Coast. SST features along the Arabian Coast are difficult to see due to cloud contamination. Of particular interest are the anti-cyclonic eddies centered near 8^{o}N, 53^{o}E and 3^{o}N, 50^{o}E. These circulations are responsible for the crescent-shaped patterns offshore. There appears to be some thin mid-level cloud directly over the main plume of cold water extending eastward from Ras Hafun. Figure 3-8 is the corresponding DMSP visual image for the same date. The discussion opposite Figure 3-8 addresses the cloud features which can be seen in both types of satellite output; note that cloud-free patterns and upwelling patterns off Africa are correlated. The approximate local sun time at the center of this image is 1030 (0604Z).

Figure 7-2. DMSP IR image of the Arabian Sea during the Southwest Monsoon (July 5, 1979).

Table 7-1. ASW forecast aids showing MLD (ft), mean thermocline gradient (^{o}C/100 ft), mean maximum thermocline gradient (^{o}C/100 ft) and probability (Lo/Mod/Hi) of a mid-depth sound channel by areas and seasons.

Parameter & Area	Southwest	Fall	Northeast	Spring
Mixed Layer Depth (ft):				
Central Arabian Sea	310	110	300	140
African Coast (Somalia)	105	240	210	90
Gulf of Aden	80	90	250	80
Southern Red Sea	35	90	165	120
Arabian Coast	160	90	150	70
Gulf of Oman	25	50	300	40
Mean Thermocline Gradient (^{o}C/100 ft):				
Central Arabian Sea	9.8	5.8	8.2	7.3
African Coast (Somalia)	6.4	4.9	4.6	5.5
Gulf of Aden	12.2	17.0	6.7	6.1
Southern Red Sea	14.0	10.0	2.1	4.9
Arabian Coast	7.9	14.0	5.0	4.0
Gulf of Oman	15.6	15.0	1.2	8.4
Mean Maximum Thermocline Gradient (^{o}C/100 ft):				
Central Arabian Sea	14.0	7.9	13.0	11.3
African Coast	9.8	5.6	6.0	7.8
Gulf of Aden	17.0	22.9	9.5	9.9
Southern Red Sea	20.1	16.2	4.3	8.5
Arabian Coast	11.0	20.4	6.7	6.3
Gulf of Oman	23.2	22.3	2.1	13.4
Probability of Mid-depth Sound Channel:*				
Central Arabian Sea	Lo	Lo	Lo	Lo
African Coast (Somalia)	Hi	Lo	Mod	Lo
Gulf of Aden	Hi	Hi	Hi	Mod
Southern Red Sea	Hi	Hi	Mod	Lo
Arabian Coast	Lo	Hi	Mod	Lo
Gulf of Oman	Hi	Hi	Lo	Lo

* Subjective estimate based upon the shape of the subsurface thermal profile.

surface-to-surface radar, UHF communications and ESM ranges at least 34% of the time. Integrated Refraction Effects Prediction System (IREPS) analysis of climatological data indicates that near-surface (evaporation) ducting in the northern portion of the Arabian Sea and near the Arabian Coast should occur as follows (USS John F. Kennedy 1982 Pos Deployment Report):

Southwest Monsoon	-	28%
Fall Transition	-	33%
Northeast Monsoon	-	22%
Spring Transition	-	52%

IREPS analysis of Arabian Sea climatological data also indicates that temperature inversions and low-level moisture structure cause elevated trapping layers (ducts) between 2000 and 7000 ft which reduce UHF communications and ESM ranges between surface-to-air and air-to-air platforms located on different sides of the layer. Forecasters should expect elevated trapping to occur at least 43% of the time with the following seasonal distribution:

Southwest Monsoon	-	46%
Fall Transition	-	43%
Northeast Monsoon	-	49%
Spring Transition	-	33%

IREPS runs by USS John F. Kennedy based upon actual radiosonde soundings from 10 February 1982 through 30 April 1982 gave the following statistics for non-evaporation ducting:

Surface Ducts	-	47% of time
Elevated Ducts	-	65% of time
Both Simultaneous	-	24% of time

Notice that conditions which are favorable for ducting near the surface are not necessarily favorable for simultaneous ducting at some higher level. USS John F. Kennedy found that both height and strength of the ducts varied throughout the day, and that at least two radiosonde soundings per day were desirable to support E/O calculations.

The Middle East area is noted for optical anomalies (mirages, oases seen at extreme ranges etc.). Forecasters should alert operators of optical equipment to these conditions whenever the radiosonde soundings show large vertical gradients of either temperature or moisture near the surface. Such effects will be most prevalent in the Red Sea and Persian Gulf plus along the Arabian Coast in spring, summer and fall.

FORECAST RULES/AIDS.

a. Over the Arabian Sea, Red Sea and Persian Gulf expect evaporation ducting (0 to 200 ft) to increase surface-to-surface radar, UHF comm and ESM ranges at least 34% of the time with maximum occurrence in the Spring Transition period.

b. Over the Arabian Sea, expect surface or elevated ducting due to temperature inversions and moisture layers to reduce surface-to-air (and some air-to-air) comm and ESM ranges at least 43% of the time with maximum occurrence during the Southwest Monsoon, Fall Transition and Northeast Monsoon (JFK found surface ducts (below 2000 ft) about 47% of time and elevated ducts (2000 - 7000 ft) about 65% of time off the Arabian Coast from February through April 1982).

c. Expect considerable diurnal variation in the height and/or intensity of ducting. Schedule radiosonde soundings accordingly.

d. Expect strange optical propagation anomalies in the Red Sea, Persian Gulf and Arabian Coast areas during periods of strong evaporation (clear skies and high temperatures). The evaporation layer will be deeper during periods of stronger winds.

7.3 Amphibious Operations

The weather conditions which influence amphibious operations in this region (primarily low-level winds, cloud cover, dust and precipitation) have been discussed in other portions of this Handbook. Realizing that amphibious staffs carry the detailed hydroclimatological information needed to support amphibious operations, the following material discusses only general oceanographic data required to round out the Navy forecaster's basic knowledge in this area.

Surface currents in the Arabian Sea, Red Sea and Persian Gulf are strongly influenced by the monsoon wind flow. Figures 7-3a and b show the large scale current patterns for August (Southwest Monsoon) and January (Northeast Monsoon) taken from Defense Mapping Agency Sailing Directions for the Indian Ocean, Pub 170, Change 1 of 29 Nov. 1980. Notice the reversal in current direction in almost all areas and the very strong increase in current speeds off the Somali Coast during the Southwest Monsoon.

Figure 7-4 shows mean currents in the Red Sea for February (typical of the Northeast Monsoon) and August (typical of the Southwest Monsoon). Notice the reversal in the southern Red Sea and the "Convergence Zone" off Egypt. This current pattern is primarily controlled by surface wind stresses.

Figure 7-5 shows mean tidal currents for the Persian Gulf. In this area the surface currents are primarily controlled by astronomical forces, hence the single chart with flood currents shown and ebb currents implied. However, prolonged wind stress from a constant direction (particularly from the west and northwest behind a cold front) causes significant water pileup in the Persian Gulf because of the shallow depths. Wind-stress-induced water level changes up to 1.5 ft have been computed by recent Hydrodynamic Numerical (HN) model runs for this basin.

Figure 7-6 shows mean (upper number) and spring (lower number) tide ranges in feet for various locations around the Arabian Sea.

In addition to currents and tidal ranges, amphibious operations in this area may also be affected by surf action, particularly along the coast of India. The Red Sea and Persian Gulf are not open to swell from distant storms, but waves of 12-15 ft with predominant periods of 8-12 sec have been observed during periods of strong northwesterly flow. These waves do not cause the same surf problems as long-period swells (12-20 sec) in other naval operating areas; however, the

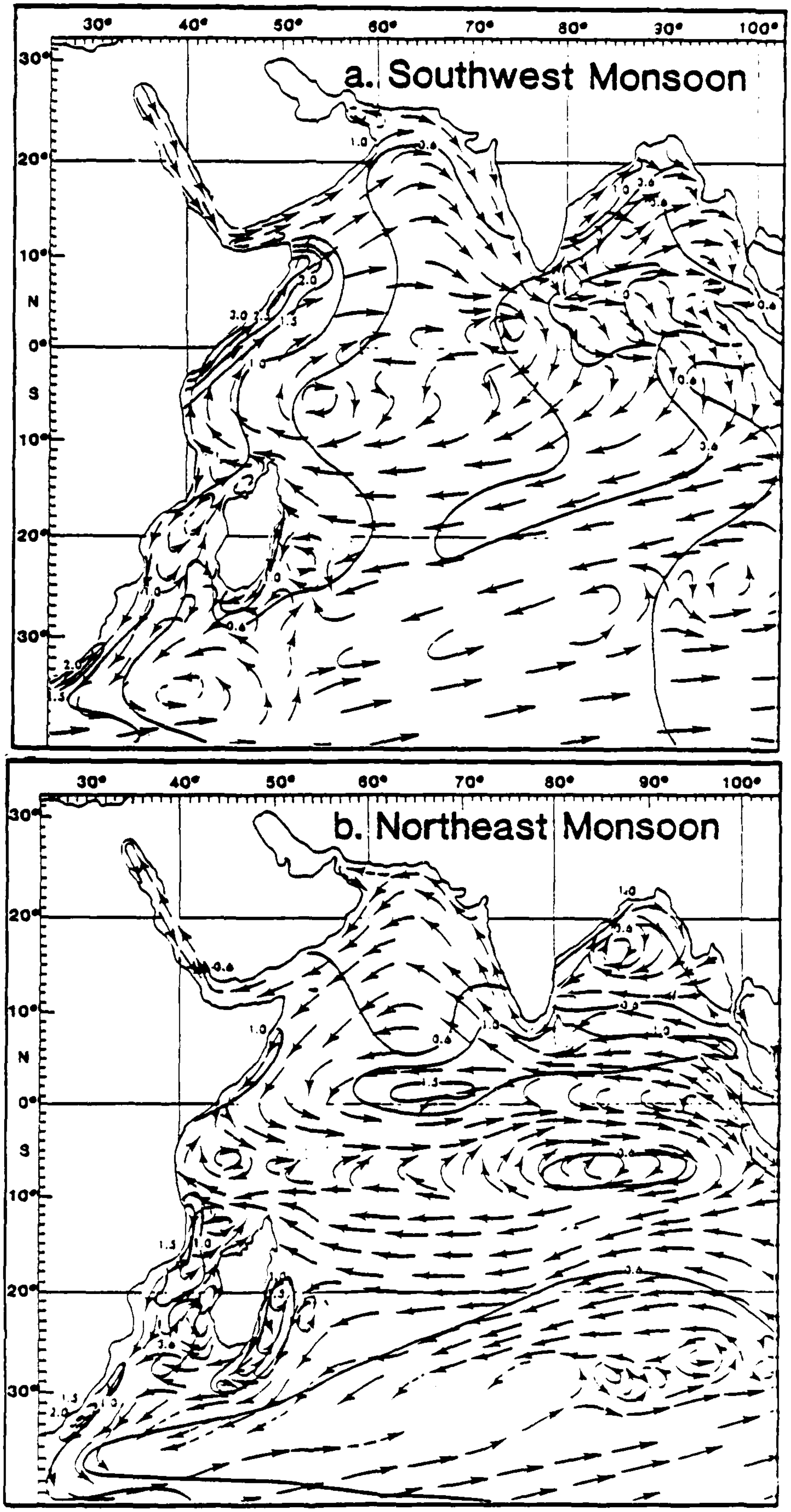

Figure 7-3. Large-scale current pattern (arrows) and speeds (contours in kt) in the Indian Ocean (from Defense Mapping Agency, 1980).

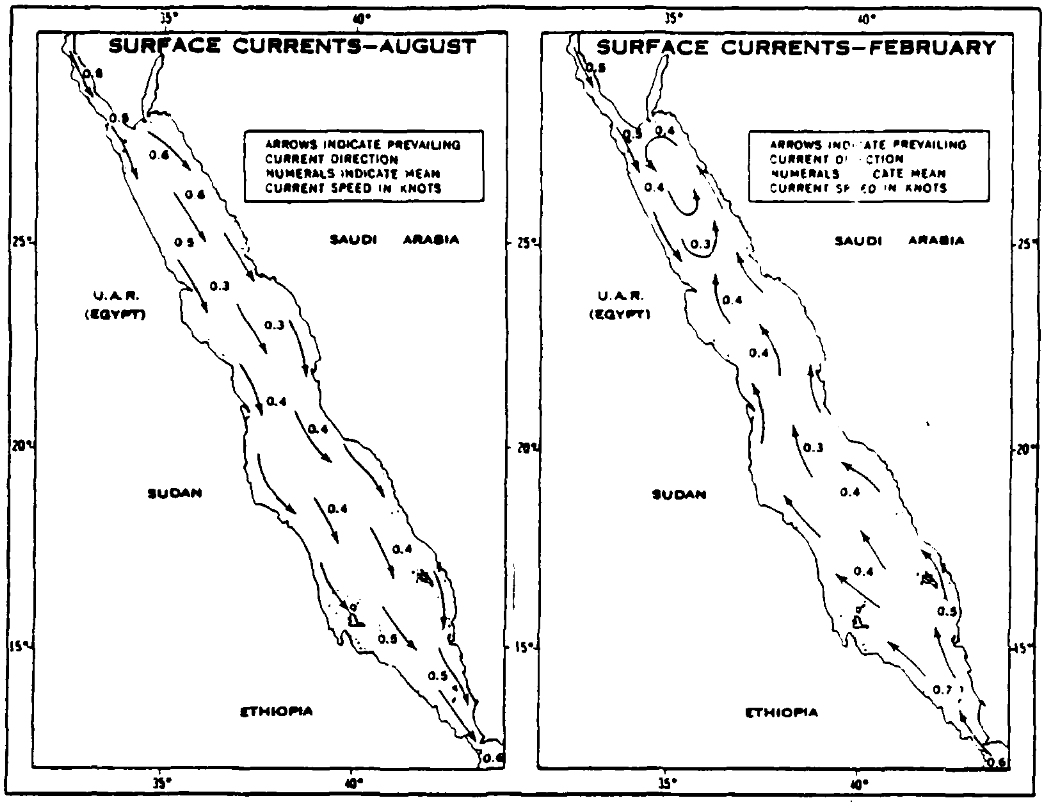

Figure 7-4. Mean surface currents in the Red Sea during the Southwest Monsoon and the Northeast Monsoon (from Defense Mapping Agency, 1980).

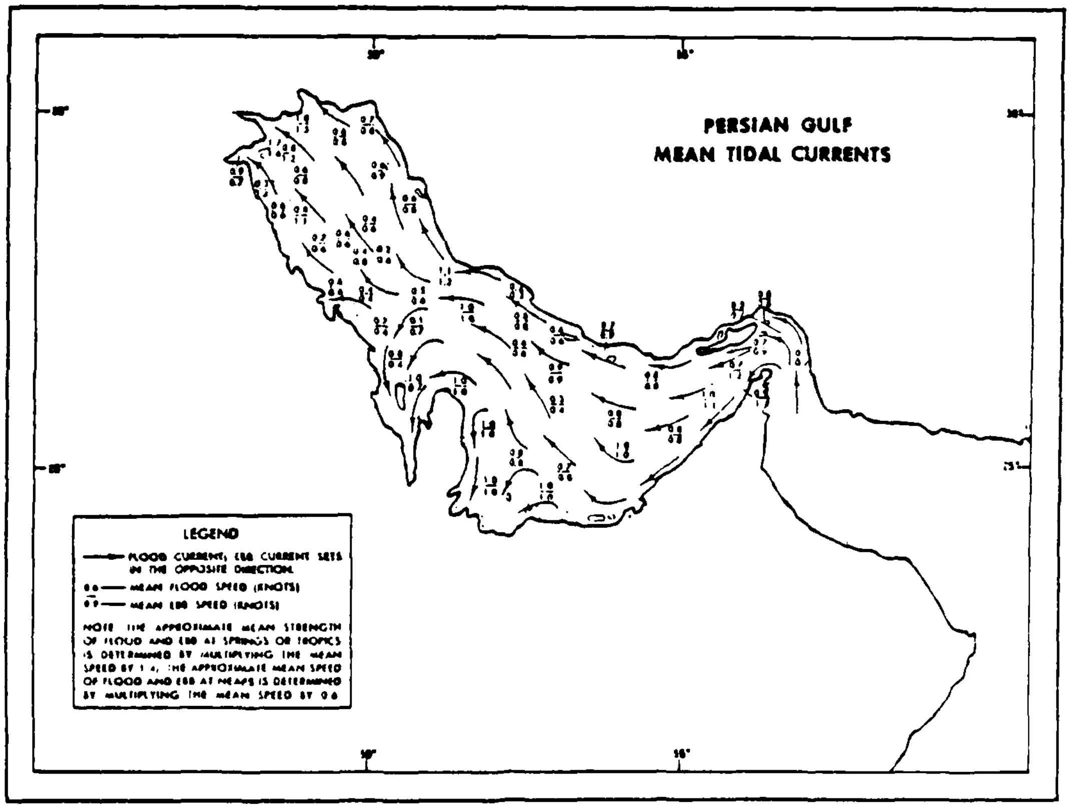

Figure 7-5. Mean tidal currents in the Persian Gulf (from Defense Mapping Agency, 1980).

Tide Ranges

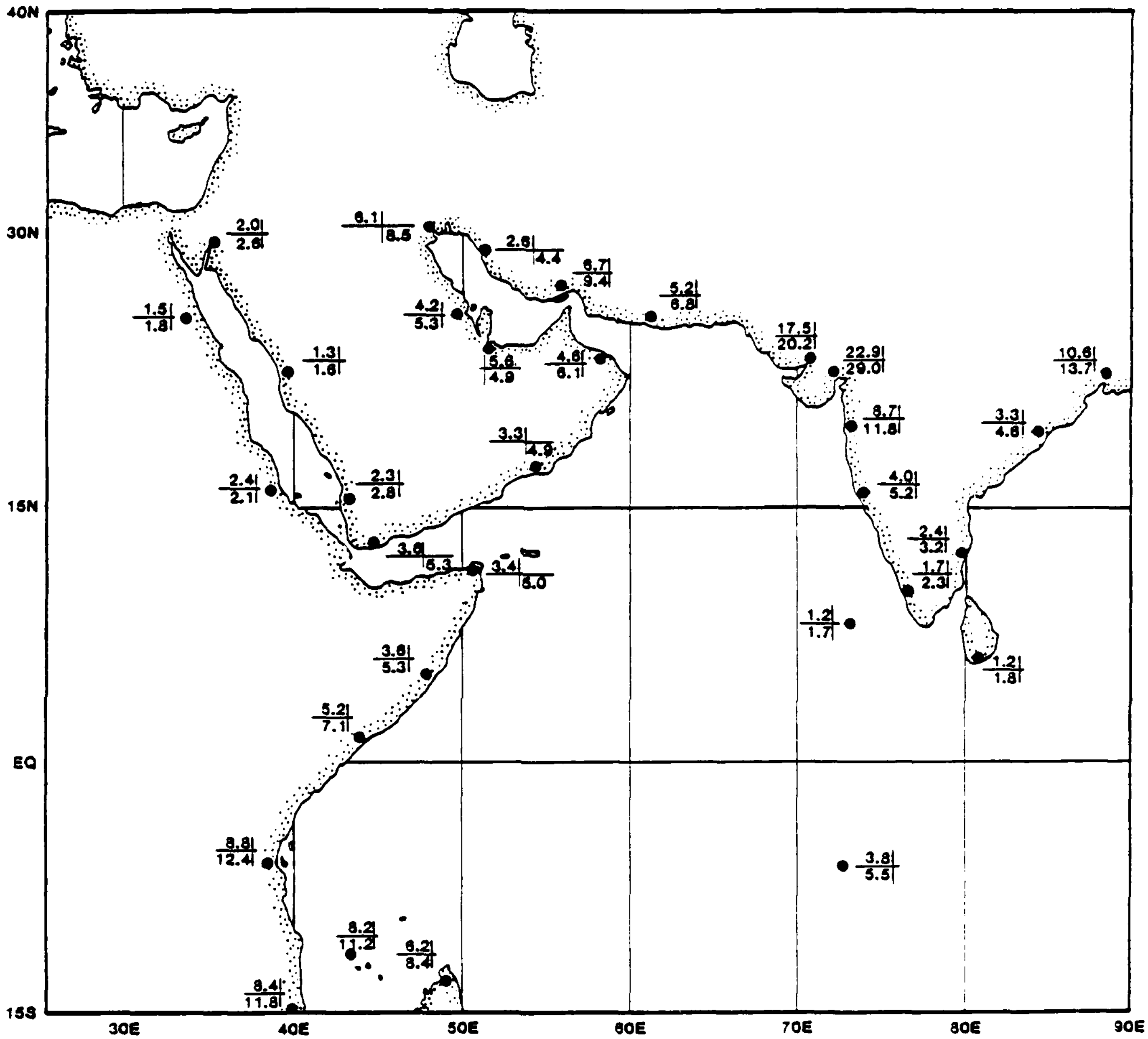

Figure 7-6. Mean (upper number) and Spring (lower number) tide ranges (ft) (adapted from Defense Mapping Agency, 1980).

predominance of shallow coral reefs in these basins means that forecasters should consider surf from any wave train having predominant periods longer than 8-10 sec. The speed of movement of swell trains (in knots) is 1.5 times the predominant period (in seconds); a swell train having a predominant period of 10 sec will propagate at 15 kt in deep water. For waves with a period of 10 sec, forecasters can expect surf 1.4-2.0 times the deep water wave height for normal beach slopes.

Problems associated with dust storms during the Iranian hostage rescue attempt attest to the fact that dust can cause serious problems in amphibious helicopter operations (and probably in boat and land vehicle operations due to engine fouling). Other sections of this Handbook discuss dust storms in the various areas and seasons. The general rule is that dust starts to become a problem in any dry Middle East area when surface winds exceed 15 kt. Most dust storms of any extent show up in satellite imagery.

See appropriate portions of Sections 3.0 through 6.0 for discussions of low-level winds, cloud cover and precipitation.

FORECAST RULES/AIDS.

a. Most areas covered by this Handbook experience a reversal in surface current direction during the transition periods between Southwest Monsoon and the Northeast Monsoon. The strongest currents occur off the African (Somali) Coast in summer (greater than 3 kt).

b. Tidal ranges vary from less than 3 ft in the Red Sea to more than 20 ft at a few points on the west coast of India. Predominant tidal types can be "diurnal", "semidiurnal" or "mixed" depending upon location.

c. The Red Sea and Persian Gulf do not experience severe surf due to limited fetch. However, forecasters should consider surf for all wave trains with predominant periods of 10 sec or longer. Move swell trains at speeds (in knots) of 1.5 times the swell period (in seconds).

d. Dust storms can seriously impact amphibious operations through engine clogging. Dust starts to become a problem over dry areas when winds exceed 15 kt. Satellite imagery should be used to monitor dust storms (see appropriate discussions in Sections 3.0 through 6.0 of this Handbook).

e. Vehicular traffic will loosen soil and lower the wind speed threshold for raising dust.

7.4 Carrier Air Operations

This Section addresses several wind forecast problems of special interest to carrier air operations.

Airlift Across the Arabian Sea

Forecasters unfamiliar with operating in an area dominated by monsoonal flow need to be especially aware of rapid changes in wind structure at the onset of the Southwest Monsoon. Winds between the northern Arabian Sea and Diego Garcia, for example increase suddenly at all levels in the few days between the end of the Spring Transition and the passage of the "Onset Vortex" which often signals the start of the Southwest Monsoon. At this time of year, do not expect reported winds from the last logistic flight to be valid for the same flight route 2-3 days later.

Forecasters should also be alert to the relatively sudden increase in the intensity of the Somali Low-Level Jet at the start of the Southwest Monsoon.

Night Operations in the Persian Gulf in Summer

From early June to mid-July, low-level winds in the Persian Gulf are characterized by what is known as the "Summer Shamal" or "40-day Shamal" (see Section 3.3.3). Low-level winds blow steadily from the northwest parallel to the axis of the gulf. Synoptic and terrain features combine to strongly enhance the flow along the southern shore -- particularly below 5000 ft. It is not uncommon to have winds in excess of 50 kt at 1000 ft. On clear nights with strong outgoing radiation, a "nocturnal low-level jet" forms where surface winds may be 15 kt but 1000 ft winds may exceed 50 kt in a narrow zone along this coast.

Navy aircraft planning night landings in this area during the "Summer Shamal" should utilize the nomogram contained in Figure 7-7 (after Membery, 1983) to forecast height and intensity of this low-level nocturnal jetstream.

Launch/Recovery Winds

Post-deployment reports of cruises in this area frequently indicate that insufficient wind speed across the deck during launch and recovery is a major

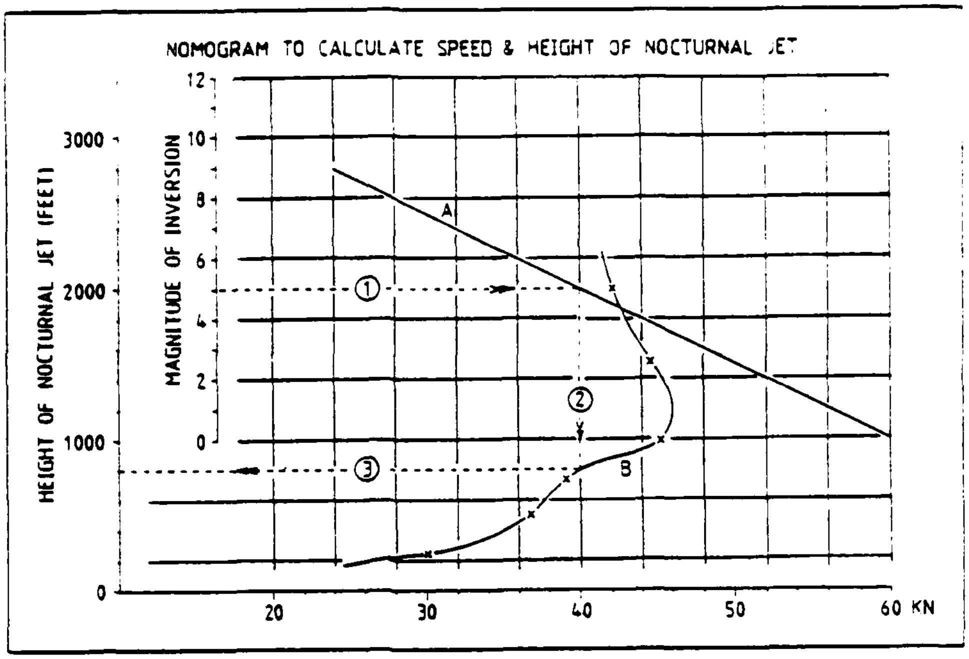

Figure 7-7. Nomogram for forecasting speed and height of low-level nocturnal jet in the Persian Gulf area during the "Summer Shamal" (adapted from Membery, 1983). To use the nomogram, use the following procedure:

1. Forecast the magnitude of the nocturnal inversion from the nearest daytime sounding (e.g., Dhahran; 40416). Compute the difference between the temperature (°C) at about 1000 ft and the forecast nocturnal surface temperature (e.g., 5°C).

2. Enter the nomogram on the "magnitude of inversion" scale with the temperature difference determined above and proceed horizontally to the sloping line labeled "A". Read the estimate of the maximum speed off the lower scale (e.g., 40 kt).

3. Proceed downward to an intersection with curve "B". Read the height of the maximum wind from the left margin height scale (e.g., 800 ft).

Notes:

1. The maximum speed determined in step 2, above, should be approximately equal to the maximum low-level wind which occurred on the previous day.

2. This nomogram is valid for inversion magnitude between 3°C and 9°C.

3. If more than one intersection with curve "B" occurs, use the height of the lower intersection.

4. If the maximum wind speed is > 46 kt (no curve "B" intersection), forecast height of maximum wind to be 1200 ft.

problem -- particularly in some operating areas. Forecasters should consult the climatological charts in Sections 3 through 6 to get a general idea of potential light wind areas. During World War II, carrier meteorologists were frequently beset with the same problem and developed techniques to find and utilize local areas of slightly higher winds.

Shear-line Enhancement. If winds to support launch and recovery are marginal, the carrier should move toward areas of convective cloud activity. If a line of convective clouds can be found, steam upwind along the left side of the cloud line because shear considerations indicate speeds on that side should be higher if the cloud band is to be maintained. Even a 5-kt differential across the band(line) is worth exploiting in marginal situations.

Land/Sea Breeze Enhancement. Around the Arabian Peninsula, field studies (Steedman and Ashour, 1976) indicate the maximum onshore sea breeze (during hot season) occurs at about 1500 local time with a normal component speed of about 14 kt, while the maximum offshore land breeze (during cool season) occurs at about 0500 local time with a mean component speed of about 12 kt. If water depths and tactical considerations permit operating within 5 n mi of shore, forecasters should search for and use the edge of the sea breeze surges when they enhance the gradient wind. On the other hand, if the sea/land breeze component opposes the gradient wind, operation farther to seaward would be advised. This is particularly true in the case of early morning flight operations (land breeze regime) since land breezes seldom extend more than about 10 n mi seaward.

Natural Wind Oscillations. Carrier operations experience and field studies indicate that there is evidence of natural wind speed oscillations at the surface with periods of 15-30 min. Carrier forecasters have found that in marginal wind speed situations it is worthwhile to load the launchers and wait for one of these oscillations. The wind speed should be monitored closely prior to scheduled launch time to determine whether such oscillations are occurring.

CARRIER AIR OPERATIONS FORECAST RULES/AIDS.

a. Expect route winds to Diego Garcia and Somalia to increase suddenly in the few days between the end of the Spring Transition and the appearance of the "Onset Vortex" which often signals the start of the Southwest Monsoon.

b. In the Persian Gulf during the "Summer Shamal" (early June to mid-July) expect a low-level (below 5000 ft), "nocturnal" jetstream along the southern coastline. Use Figure 7-7 to forecast height and speed. Be alert for dangerous shear at night between the surface and 1000 ft — especially on clear nights.

c. Use satellite imagery, aircraft reports or visual observations to locate areas of convective cloud activity. If a line (band) of convective clouds can be found, steam upwind along the left edge of the cloud band (northern hemisphere) to enhance relative wind speed.

d. If the carrier can operate within 5 n mi of the beach, expect an onshore sea breeze component up to 14 kt at about 1500 local time and an offshore land breeze component up to 12 kt at about 0500 local time. This applies to most areas around the Arabian Peninsula on relatively clear days, but varies with the season (maximum sea breeze during hot season; maximum land breeze during cold season). These components will be in addition to the gradient wind vector.

e. If <u>mean</u> wind speeds are within 5 kt of those required for launch, an increase to acceptable speeds can be expected within 15-30 min at least 80% of the time (WWII carrier launch rule).

Refer to the "Low-Level Wind" portions of Sections 3 through 6 for other pertinent rules/aids.

REFERENCES

Atkinson, G. D., 1971: Forecasters' Guide to Tropical Meteorology. Air Weather Service (MAC) Tech. Report 240.

Brand, S. and J. W. Blelloch, 1978: Typhoon Havens Handbook for the Western Pacific and Indian Oceans. NAVENVPREDRSCHFAC Tech. Paper 5-76; Change One.

Brody, L. R. and LCDR M. J. R. Nestor, 1980: Regional Forecasting Aids for the Mediterranean Basin; Handbook for Forecasters in the Mediterranean, Part 2. NAVENVPREDRSCHFAC Tech. Report TR 80-10.

Brody, L. R., 1977: Meteorological Phenomena of the Arabian Sea. NAVENVPREDRSCHFAC Applications Report AR 77-01.

Brody, L. R., 1972: Monsoon Meteorology by Colin S. Ramage: A Digest for Africa and Adjoining Indian Ocean Waters. ENVPREDRSCHFAC Tech. Paper No. 12-72.

Brown, O. B., J. G. Bruce and R. H. Evans, 1980: Evolution of Sea Surface Temperature in the Somali Basin During the Southwest Monsoon of 1979. Science, 209, 595-597.

Bruce, J. G. and G. H. Volkman, 1969: Some Measurements of Current Off the Somali Coast During the Northeast Monsoon. Jour. Geophys. Res., 74, 8, 1958-1967.

Cadet, D. and M. Desbois, 1981: A Case Study of a Fluctuation of the Somali Jet During the Indian Summer Monsoon. Monthly Wea. Rev., 109, 1, 182-187.

Central Intelligence Agency, 1976: Indian Ocean Atlas.

Colborn, J. G., 1975: The Thermal Structure of the Indian Ocean. Indian Ocean Expedition Oceanographic Monographs Number 2, University Press of Hawaii.

Cuming, LCDR M. J., 1973: Handbook for Forecasters in the Bay of Bengal. ENVPREDRSCHFAC Tech. Report TP 7-73.

Defense Mapping Agency, 1980: Sailing Directions (Planning Guide) for the Indian Ocean. DMA Publication No. 170, Change 1.

Defense Mapping Agency, 1978: Sailing Directions for the Red Sea and the Persian Gulf. DMA Publication No. 172, 1st Ed., Change 1.

Defense Mapping Agency, 1978: Sailing Directions (Enroute) for India and the Bay of Bengal. DMA Publication No. 173, 1st Ed., Change 1.

Environmental Technical Applications Center, Air Weather Service, 1974: U. S. Naval Weather Service World-Wide Airfield Summaries, Middle East. Vol. II, Part 1 (Revised) and Part 2 (Revised), National Technical Information Service (NTIS), Springfield, VA, 22151.

Environmental Technical Applications Center, Air Weather Service, 1974: U. S. Naval Weather Service World-Wide Airfield Summaries, Africa (Northern Half). Vol. IX, Part 1, National Technical Information Service (NTIS).

Fett, R. W., et al., 1983: Indian Ocean Weather Analysis and Forecast Applications. Navy Tactical Applications Guide, Vol. 5, NAVENVPREDRSCHFAC Tech. Report 83-03.

Findlater, J., 1971: Mean Monthly Airflow at Low Levels Over the Western Indian Ocean. Geophys. Mem., 115, 1-53.

Findlater, J., 1969: A Major Low-Level Air Current Near the Indian Ocean During the Northern Summer. Quart. J. R. Met. Soc., 95, 362-380.

Flohn, H., 1964: Investigations on the Tropical Easterly Jet. Met. Inst., Univ. of Bonn, Final Report No. 1, Contract No. DA-91-591-EVC-2781.

Gurunadham, G., 1971: Clouds Over Arabian Sea During Winter. Indian J. Met. Geophys., 22, 429-432.

Huschke, R. E., 1959: Glossary of Meteorology. Boston: American Meteorological Society.

Kirshnamurti, T. N., P. Ardanuy, Y. Ramanathan and R. Pasch, 1981: On the Onset Vortex of the Summer Monsoon. Mon. Wea. Rev., 109, 2, 344-363.

Kuo, W. S., 1965: A Study of Weather Over the Arabian Peninsula. Taiwan Weather Bureau Meteorological Bulletin, 11, 2, 25-35.

Membery, D. A., 1983: Low Level Wind Profiles During the Gulf Shamal. Weather, 38, 1.

Meteorological Office, Air Ministry, London, England. 1940-44: Weather in the Indian Ocean to Latitude 30S and Longitude 95E Including the Red Sea and Persian Gulf. NAVENVPREDRSCHFAC Tech. Bulletin TB 80-02, Vol. I and II.

Miller, F. R. and R. N. Keshavamurthy, 1968: Structure of an Arabian Sea Summer Monsoon System. I.I.O.E. Met. Monographs No. 1, East-West Center Press, Honolulu.

National Oceanic and Atmospheric Administration/Naval Oceanography Command, 1981: Worldwide Marine Weather Broadcasts. U.S. Government Printing Office.

Naval Oceanography Command Detachment, Asheville, 1982: Climatic Study of the Near Coastal Zone; Red Sea South and Gulf of Aden. Commander Naval Oceanography Command.

Naval Oceanography Command Detachment, Asheville, 1980: Climatic Study of the Near Coastal Zone; Persian Gulf and Gulf of Oman. Naval Oceanography Command.

Naval Weather Service Detachment, Asheville, 1974: Climatic Summaries for Major Indian Ocean Ports and Waters. Naval Weather Service Command Publication NAVAIR 50-1C-63.

Naval Weather Service Environment Detachment, Asheville, 1978: Study of Worldwide Occurrence of Fog, Thunderstorms, Supercooled Low Clouds and Freezing Temperatures. Director, Naval Oceanography and Meteorology Publication NAVAIR 50-1C-60 CH-1.

Naval Weather Service Environmental Detachment, Asheville, 1973: Climatic Summaries for Major Seventh Fleet Ports and Waters. Naval Weather Service Command Publication NAVAIR 50-1C-62.

Naval Weather Service Environmental Detachment, Diego Garcia, 1977: U. S. Navy Local Forecasters Handbook for Diego Garcia. Naval Weather Service Command.

Perrone, T. J., 1979: Winter Shamal in the Persian Gulf. NAVENVPREDRSCHFAC Tech. Report TR 79-06.

Rama, 1969: Monsoon Circulation from Observations of Natural Radon. Collected Reprints of the International Indian Ocean Expedition, VIII, 623, 402-428.

Ramage, C. S., 1969: Indian Ocean Surface Meteorology. Oceanographic Mar. Biol. Ann. Rev., 7, 11-30.

Ramage, C. S., 1966: The Summer Atmospheric Circulation Over the Arabian Sea. Jour. of Atmos. Sc., 23, 2, 644-650.

Ramamurthy, K. M., 1972: On the Activity of the Arabian Sea Monsoon. Indian J. Met. Geophys., 23, 1, 1-14.

Raman, C. R. V., Y. P. Rao and S. M. A. Alvi, 1980: The Role of Interaction with Middle Latitude Circulation in the Behaviour of the Southwest Monsoon of 1972 and 1979. Curr. Sci., 49, 4, 123-129.

Reiter, E., 1975: Handbook for Forecasters in the Mediterranean. ENVPREDRSCHFAC Tech. Paper 5-75.

Reiter, E. R., 1969: Atmospheric Transport Processes, Part 1: Energy Transfers and Transformations. AEC Critical Review Series, USAEC Report TID-24868.

Sadler, J. C., 1975: The Upper Tropospheric Circulation Over the Global Tropics. Dept. of Meteorology, Univ. of Hawaii, UHMET-75-05.

Sadler, J. C. and R. E. Gidley, 1973: Tropical Cyclones of the North Indian Ocean. ENVPREDRSCHFAC Tech. Paper No. 2-73.

Schumann, E. H. and C. P. Duncan, 1976: High Waves in the Agulhas Current. Mar. Wea. Log, 20, 1.

Shambaugh, H. S., Undated: Local Forecasting Studies December January February. Unpublished Report.

Siedler, G., 1969: General Circulation of Water Masses in the Red Sea. Woods Hole Oceanographic Institution Contribution No. 2184.

Steedman, R. A. and Y. Ashour, 1976: Sea Breezes Over Northwest Arabia. Tellus, XXVIII, 4.

Swallow, J. C. and J. G. Bruce, 1966: Current Measurements Off the Somali Coast During the Summer Monsoon of 1964. Deep-Sea Research, 13, 861-868.

Verma, R. K., 1980: Importance of Upper Tropospheric Thermal Anomalies for Long-Range Forecasting of Indian Summer Monsoon Activity. Mon. Wea. Rev., 108, 1072-1075.

Whitehead, M. E., 1980: Sandstorm in the Arabian Sea. NAVENVPREDRSCHFAC Tech. Bulletin TB 80-07.

Williams, R. O., 1979: ARAMCO Meteorological and Oceanographic Data Book for the Eastern Province Region of Saudi Arabia. Arabian American Oil Co.

Williams, R. O., 1979: ARAMCO Tide Tables, Hourly Tide Level Predictions, Daily High and Low Waters, 1980. Arabian American Oil Company.

______, 1952: Local Forecasting Study Dhahran, Saudi Arabia for January, February and March. Unpublished Report.

______, Undated: Local Forecasting Study Dhahran, Saudi Arabia for June, July and August. Unpublished Report.

APPENDIX A

Recommended Ships' Publications Library

The following is a bibliography of publications which are highly recommended for every ship's library and for study by all forecasters:

Brand, S. and J. W. Blelloch, 1978: Typhoon Havens Handbook for the Western Pacific and Indian Oceans. NEPRF Tech. Paper 5-76; Change One.

Brody, L.P., 1977: Meteorological Phenomena of the Arabian Sea. NEPRF Applications Report AR 77-01.

Cuming, M.J., 1973: Handbook for Forecasters in the Bay of Bengal. NEPRF Tech. Report TP 7-73.

Defense Mapping Agency, 1978: Sailing Directions for the Red Sea and the Persian Gulf. DMA Publication No. 172, 1st Ed.; Change One.

Environmental Technical Applications Center, Air Weather Service, 1974: U.S. Naval Weather Service World-Wide Airfield Summaries, Middle East. Vol. II, Part 1 (Revised) and Part 2 (Revised), National Technical Information Service (NTIS), Springfield, VA, 22151.

Environmental Technical Applications Center, Air Weather Service, 1974: U.S. Naval Weather Service World-Wide Airfield Summaries, Africa (Northern Half). Vol. IX, Part 1, National Technical Information Service (NTIS).

Fett, R. W., et al., 1983: Indian Ocean Weather Analysis and Forecast Applications. Navy Tactical Applications Guide, Vol. 5, NEPRF Tech. Report 83-03.

Meteorological Office, Air Ministry, London, England, 1940-44: Weather in the Indian Ocean to Latitude 30S and Longitude 95E Including the Red Sea and Persian Gulf. NEPRF Technical Bulletin TB 80-02, Vol. I and Vol. II (Parts 1-5).

National Oceanic and Atmospheric Administration/Naval Oceanography Command, (year): Worldwide Marine Weather Broadcasts. U.S. Government Printing Office.

Naval Oceanography Command Detachment, Asheville, 1982: Climatic Study of the Near Coastal Zone; Red Sea South and Gulf of Aden. Naval Oceanography Command.

Naval Oceanography Command Detachment, Asheville, 1980: Climatic Study of the Near Coastal Zone; Persian Gulf and Gulf of Oman. Naval Oceanography Command.

Naval Weather Service Detachment, Asheville, 1974: Climatic Summaries for Major Indian Ocean Ports and Waters. Naval Weather Service Command Publication NAVAIR 50-1C-63.

Naval Weather Service Environmental Detachment, Asheville, 1973: Climatic Summaries for Major Seventh Fleet Ports and Waters. Naval Weather Service Command Publication NAVAIR 50-1C-62.

Perrone, T. J., 1979: Winter Shamal in the Persian Gulf. NEPRF Tech. Report TR 79-06.

Sadler, J. C., 1975: The Upper Tropospheric Circulation Over the Global Tropics. Dept. of Meteorology, Univ. of Hawaii, UHMET-75-05.

APPENDIX B

Summary of Weather Broadcast Sources

Marine weather broadcasting stations, types of broadcasts and call signs are summarized in this appendix. The information was extracted from the joint NOAA/NOC publication, "Worldwide Marine Weather Broadcasts", which is available from the U.S. Government Printing Office. This publication lists contents, schedules, and frequencies of the various broadcasts and contains descriptions of forecast areas, code forms and English/French/Spanish translations of common terminology.

If a broadcast type is listed for a station, an entry is made in that column. (Absence of an entry indicates that the broadcast type is not listed for that station.) If known, the call sign applicable to each type consists of the entry. If the call sign is not known, the entry is "(UNK)". Some stations have more than one call sign listed. This is indicated by placing an "X" in the third character position (in parentheses) of the call sign, then listing each call sign in Remarks.

STATION	RATT	FAX	CW	VOICE	REMARKS
Australia:					
Adelaide			VIA	VIA	
Brisbane			VIB	VIB	
Broome			VIO	VIO	
Canberra	AXM	AXM	VIX		
Carnarvon			VIC	VIC	
Darwin	AXI	AXI	VID	VID	
Esperance			VIE	VIE	
Hobart				VIH	
Melbourne			VIM	VIM	
Perth			VIP	VIP	
Rockhampton			VIR	VIR	
Sydney			VI(X)	VIS	VIS, VIX
Thursday Is.			VII	VII	
Townsville			VIT	VIT	
Burma:					
Rangoon			XYR		
Egypt:					
Cairo		SUU			
Kosseir			SUK		
Ethiopia:					
Massawa			ETV		
India:					
Bombay			VWB		
Calcutta			VWC		
Cochin			VWN		
Goa			VWG		

STATION	RATT	FAX	CW	VOICE	REMARKS
India: (cont.)					
Kandla			VWK		
Madras			VWM		
Mangalore			VWL		
New Delhi	VVD	AT(X)			ATP, ATV
Port Blair			VWP		
Ratnagiri			VWZ		
Tuticorin			VWT		
Vishakhapatnam			VMV		
Indonesia:					
Jakarta	8BB		8BB		
Iran:					
Tehran		EPD			
Iraq:					
Basrah			YIR		
Japan:					
Tokyo	JMG	JMH	JMC		
Kenya:					
Mombasa			5ZF		
Nairobi		5YE	5YE	5YE	
Madagasgar:					
Tomatave			5RS		
Tomananarive	5ST				
Maritius:					
Bigsara	3BM		3BM		
Port Louis Harbor				3BB	
Vacoas			3BA		

STATION	RATT	FAX	CW	VOICE	REMARKS
Pakistan:					
Karachi			ASK		
Papua:					
Port Moresby			VIG	VIG	
Philippines:					
Manila			DZ(X)		DZR, DZG, DZO, DZN
San Miguel			NPO		
Saudi Arabia:					
Dammam			HZG	HZG	
Jedda	HZH		HZH	HZH	
Ra's Tannurah			HZY		
South Africa:					
Capetown			ZSC	ZSC 30	
Durban	ZSD		ZSD	ZSD	
Port Elizabeth			ZSQ4	ZSQ 7	
Pretoria	ZRO	ZRO			
Walrus Bay			ZSV	ZSV 4	
Spain:					
Rota		AOK	AOK		
Sri Lanka:					
Colombo			4PB		
Sudan:					
Port Sudan			STP		
Thailand:					
Bangkok		HSW	HS(X)		HSA, HSJ

STATION	RATT	FAX	CW	VOICE	REMARKS
USSR:					
Moscow		(UNK)			
Vietnam:					
Saigon	XVS		XVS		
Others:					
Djibuti			2JA		
Kuwait			9KK	9KK	
New Amsterdam Is.			FJY4		
Orcadas		LOK	LOK		So. Orkney Islands
Reunion	FZ(X)	(UNK)			FZR, FZS
Singapore			9VG		

APPENDIX C

Satellite Imagery Interpretation

APPROACH

Interpreting satellite imagery closely parallels making weather forecasts. There are three levels of knowledge needed in order to proceed in an organized and productive manner.

1. Regional climatology
2. Current synoptic pattern
3. Local conditions

Climatology

In both imagery interpretation and knowledgable forecasting for the area, climatology is vital. Familiarity with the typical circulation patterns, extremes, pattern evolutions and models of the dynamic and thermal structures provide the general framework within which the interpretations are made. A series of annotated images or representative case studies is needed to acquire an understanding of the climatology of a region as reflected in satellite imagery.

Synoptic Pattern

The next requirement to achieve productive interpretation is to determine the pattern and strength of today's large-scale or synoptic circulation pattern. It is necessary to identify the current synoptic-scale condition in order to determine the current range of climatological values. Generally, the synoptic pattern is clearly reflected in the large-scale cloud organization of the satellite imagery.

In the interpretation of mid-latitude satellite imagery, the familiar cloud features of jetstreams, fronts, vortices and ridges are used to establish the large-scale pattern. Features of this nature are not seen over the Arabian Sea during the Southwest Monsoon season, and only over the extreme northern

portion during the Northeast Monsoon. Forecasters responsible for this area must not only become familiar with the rather unique atmospheric conditions of the northern Indian Ocean region, but must also learn to recognize and properly interpret a new array of large-scale cloud patterns.

The following examples from the text of the Handbook illustrate a few of the large-scale cloud patterns that reflect variations of the Southwest Monsoon circulation. The "Onset Vortex" that ushers in the rapid development of the fully developed Southwest Monsoon over the Arabian Sea is shown in Figure 3-4. The cloud pattern illustrating a "weak" or inactive Southwest Monsoon period is shown in Figure 3-5, and the contrasting pattern of a "strong" or active Southwest Monsoon in Figure 3-6. Other large-scale variations of the Southwest Monsoon that would be of interest and would be reflected in the overall cloud patterns are the "break" in the monsoon and "monsoon depressions." These features are addressed in the Navy Tactical Applications Guide for the Indian Ocean Volume 5 (NEPRF Technical Report TR 83-03). Recognition of these large-scale conditions should provide the clues to generate in the "mind's eye" a general overall atmospheric structure.

Local Conditions

From an understanding of the area climatology and having established the large-scale circulation pattern, we next address the scale of local deviations. On these smaller scales, there are many features which we see in imagery over the monsoon regions that have the same cause and effect relationships as similar mid-latitude features, e.g., cloud types, barrier effects, upwelling, terrain features, etc. These small-scale features can be used both in a collective manner to develop the large-scale pattern (similar to analysis of plotted station reports), and to interpret the causative atmospheric conditions useful in making short-term forecasts. The trick is to be able to deduce the causative atmospheric conditions from the features seen in the imagery.

TECHNOLOGICAL ASPECTS

The analyst must have an awareness of the technological aspects of the satellite sensors; data transmission and reception modes and the viewing angle of

the satellite to maximize use of the data. In the following interpretive illustrations for example, Figure C-2 is an infrared image recorded with a special purpose enhancement curve. In this example, a rather restricted range was in use with 16 gray shades spread over a temperature range of 25°C (22°C to -3°C). This enhancement provides good descriptive patterns in the range of the Arabian Sea sea-surface temperatures (SST) and low-level cloud features, but quickly goes to black (22°C) over land and to white (-3°C) when cirrus clouds are present. Each gray shade reflects a temperature range of about 1.6°C (25°C divided by 16).

ILLUSTRATIONS OF IMAGERY INTERPRETATION DURING THE SOUTHWEST MONSOON

Figures C-1 and C-2 are simultaneous visual (VIS) and infrared (IR) images of the western Arabian Sea region on July 9, 1979 (approximately 1000 (0629Z) local sun time at the center of the image). They reflect a "weak" Southwest Monsoon period, one day prior to Figure 3-5. Three large-scale features are reflected and labeled with Roman numerals. The cloud pattern over the Arabian Sea (I) is generally suppressed with little convective activity, clearly in contrast to the pattern during active Southwest Monsoon flow as illustrated in the text (Figure 3-6). The cloud-free conditions over land (II) are typical of the regions occupied by the surface thermal lows that prevail throughout the Southwest Monsoon period. The upper-level Easterly Jet, as reflected by the cirrus pattern (III), while quite evident in the IR, would be recognized as relatively weak compared to a pattern representative of an active monsoon period. The large-scale information gained from Figures C-1 and C-2, then, is this: a "weak" Southwest Monsoon flow pattern with markedly reduced convective activity, a correspondingly weak upper-level Easterly Jet over the Arabian Sea and typical cloud-free conditions over the land areas of the thermal lows.

A number of small-scale features can also be identified in Figures C-1 and C-2. These are labeled with Arabic numerals. The features so identified can be used both to support the large-scale interpretations (i.e., they reflect conditions typically found under these large-scale patterns), and to determine the various atmospheric conditions useful as short-range forecasting guidance.

Numeral (1); Interpretation: Dust Plume. A local dust plume is seen just northwest of the northern end of the Persian Gulf. To interpret this feature from the VIS image (Figure C-1) alone requires knowledge of the unobstructed terrain features of this area (see Figure 3-10). Close inspection of the IR image transparency shows a faint gray feature reflecting the cooler temperature of the top of the dust plume, but the photographic print (Figure C-2) fails to reproduce this feature. Seasonal thermal lows are located south and east of the area of the dust plume, resulting in persistent northwesterly surface winds. This wind pattern is known locally as the "Summer Shamal" or "40-day Shamal". Frequent large and local-scale dust storms are produced by this wind pattern. Because this is near the end of the Summer Shamal season and the dust plume is a very localized feature (probably raised from a dry lake bed), the surface winds are likely to be weaker than the average during the previous 4 to 6 weeks.

Numeral (2); Interpretation: SST Pattern. The faint gray shade seen in the IR indicates a slightly cooler SST over the northern Persian Gulf. There is no support for this condition in the VIS image, and none would be expected for weak SST gradients. However, climatology supports this observation.

Numeral (3); Interpretation: Upwelling. A relatively cold feature is noted in the IR off the coast of Oman. This area appears cloud-free in the VIS (3), therefore the IR feature is interpreted as an area of colder surface water. Other cold SST features (not labeled) can be seen in the cloud-free areas to the south of feature (3) along the Oman coast. In the Northern Hemisphere where prevailing southerly (northerly) winds parallel an eastern (western) coast, oceanic upwelling may occur. The Southwest Monsoon surface flow results in a flow pattern parallel to the coasts of Oman, Yemen and Somalia. A strong SST gradient is reflected by a crescent-shaped pattern (8) off Somalia. This pattern reflects an annual SST feature and is associated with the low-level Somali Jet (see Section 3.3.1).

Numerals (4) and (5); Interpretation: Low-level Inversion. Gravity wave-induced cloud patterns are seen over the northwestern Arabian Sea, implying a low-level inversion. This interpretation is based on the following factors: gravity waves are known to propagate along density interfaces such as strong atmospheric temperature inversions, and during the Southwest Monsoon, a low-level temperature inversion is known to persist over the western [illegible]

AD-A134 312 FORECASTERS HANDBOOK FOR THE MIDDLE EAST/ARABIAN SEA (U) OCEAN DATA SYSTEMS INC MONTEREY CALIF W E HUBERT ET AL. JUN 83 NEPRF-CR-83-06 3/3

UNCLASSIFIED N00228-82-C-6433 F/G 4/2 NL

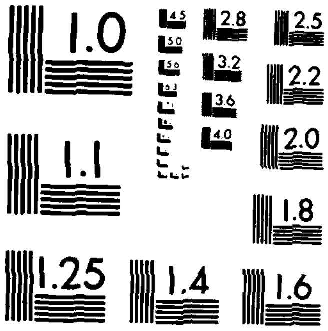

MICROCOPY RESOLUTION TEST CHART
NATIONAL BUREAU OF STANDARDS-1963-A

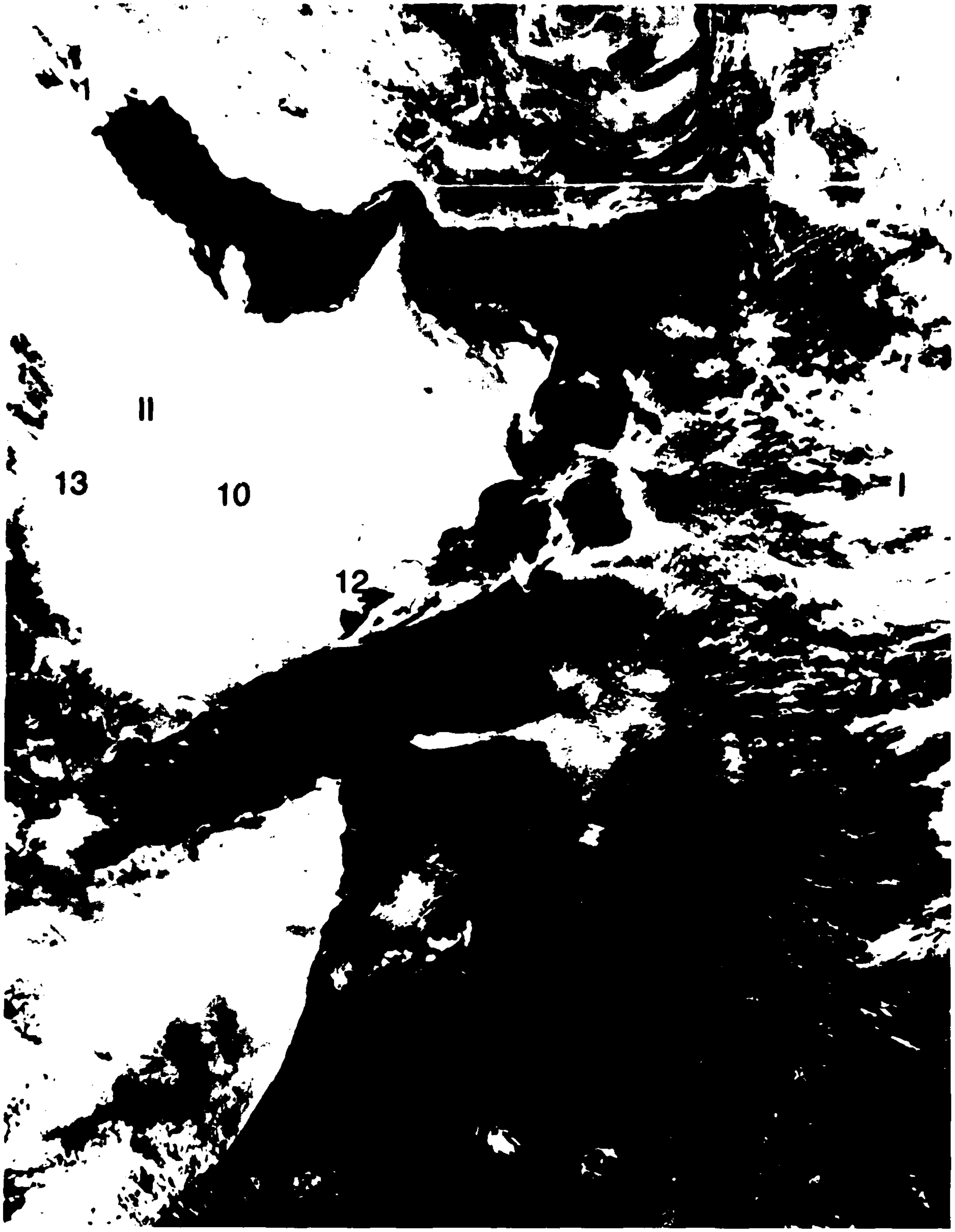

Figure C-1. DMSP visual image of the western Arabian Sea region produced from data recorded on July 9, 1979 (0629 GMT).

Figure C-2. DMSP IR image of the western Arabian Sea region produced from data recorded on July 9, 1979 (0629 GMT).

The Southwest Monsoon inversion-capped planetary boundary layer of the western Arabian Sea is so shallow, and vertical motion so restricted, that clouds typically do not form. During "weak" Southwest Monsoon periods, the inversion is lower than during "strong" Southwest Monsoon periods. Numeral (5) identifies a second cloud feature which indicates that a low-level inversion exists. Cloud formation is noted along the southern slopes of Socotra Island. The clouds do not stream over the island as would be expected if the southerly flow was perturbed upward over the island terrain. This implies a stable layer such as a low-level inversion.

Numeral (6); Interpretation: Upper-level Easterly Jet. Faint east-west oriented cirrus streamers are seen in the VIS image. Due to the restricted enhancement curve used in the IR image, all cloud tops colder than $-3^{\circ}C$ are seen as white. This IR enhancement is not intended for use in interpreting cirrus-level features. In this case, the interpretation of cirrus clouds in the IR image must be based on cloud shape plus position relative to the VIS image. From a climatological standpoint, the interpretation of this period as a "weak" Southwest Monsoon implies a weakened upper-level Easterly Jet condition. Comparison of Figures C-1 and 3-6 (active Southwest Monsoon) clearly indicates the difference in cirrus cloud characteristics during "weak" and "strong" Southwest Monsoon periods.

Numeral (7); Interpretation: Low-level Flow. Clockwise curving, low-level cloud lines are seen in both the VIS and IR image. This pattern persists throughout the Southwest Monsoon season. During active Southwest Monsoon periods, low-level cloud lines will be much better defined; however, convective and cirrus cloud formations may mask the low-level cloud patterns.

Numerals (9) and (10); Interpretation: Terrain Features. Various tonal shades are seen in the VIS image over the land regions. Cloud-free images over land areas of interest should be studied and retained to provide comparative images to aid in identifying small-scale cloud or dust features over land. In general, smooth surfaces are good reflectors, and appear lighter than rough surfaces. Terrain features vary widely in tonal shades, and provide excellent reference landmarks in satellite imagery. The light tonal qualities of desert conditions are seen in the vicinity of numeral (10).

Numerals (11) and (12); Interpretation: Clouds over Land. Clouds over light-toned land are seen in the vicinity of numerals (11) and (12). The clouds are not clearly evident in the VIS image, but are seen as washed-out white masses in the IR image. In the intepretation of visual imagery alone, there are two aids to identifying clouds over light-toned land; knowledge of the land feature as discussed above, and the appearance of shadows. Close inspection of the light features (clouds) near numerals (11) and (12) shows adjacent dark features (shadows) generally to the west. The image is from a late morning pass (0629 GMT). The use of shadows, however, is not fool-proof as is indicated by the thin, dark-toned bands to the west of terrain features near numeral (13). In general, cloud shadows can provide additional information on the relative height of cloud elements. The higher the cloud-top or the smaller the sun's elevation angle, the longer the shadow. Early morning or late afternoon satellite passes provide the clearest examples of cloud shadow patterns in the lower latitudes.

ILLUSTRATIONS OF IMAGERY INTERPRETATION DURING THE NORTHEAST MONSOON

Figure C-3 is a NOAA visual image of the Arabian Peninsula region on December 16, 1979 (approximately 0900 (0553Z) local sun time at the center of the image). This reflects a Northeast Monsoon (wintertime) condition. Four large-scale features are reflected and labeled with Roman numerals. The vortex and frontal band (I) of a migratory mid-latitude disturbance is located over Iran. A jetstream cirrus band (II) extends east-west over the southern Arabian Peninsula. The cirrus band is most clearly seen over the Red Sea and Gulf of Oman, but is faintly discernable over the land areas. This is most likely the Subtropical Jetstream, but the image alone does not clarify this point. Past history, large-scale analyses, or satellite passes on either side of this pass are needed to resolve the jetstream classification. A second mid-latitude disturbance (III) is seen over the extreme eastern Mediterranean Sea. A typical Northeast Monsoon (IV) cloud pattern is depicted over the western Arabian Sea. An active Near-Equatorial Trough (convergence area) is indicated by the convective activity over the equatorial oceanic region.

The large-scale interpretation of this image is that mid-latitude systems are being advected into the northern Arabian Sea region, suggesting that an equatorward extension of a mid-latitude long-wave trough exists at this time.

Figure C-3. NOAA visual image of the Arabian Peninsula region produced from data recorded on December 16, 1979 (0553 GMT).

Numeral (1); Interpretation: Cumulonimbus. Cumulonimbus (Cb) clouds are seen over southwestern Iran embedded in the general frontal band cloudiness. The Cb's can be identified by their point-source, fan-shaped cloud features. Additional evidence is provided by the shadows seen to the northwest of the fan-shaped features which indicate that their tops are well above the surrounding frontal cloud features. The featureless tops of these two Cb cirrus plumes indicate that they extend vertically to the tropopause. The stable layer at the tropopause restricts further vertical development, and the top of the cloud feature becomes flat and smooth in appearance.

Numeral (2); Interpretation: Wave Clouds. Wave clouds form over and downstream from terrestrial ridgelines that are aligned perpendicular to the flow at, or above the height of the ridge. In this case, the wave clouds seen over western Iran and Oman depict the lower tropospheric flow pattern associated with the migratory disturbance.

Numeral (3); Interpretation: Low-level Northwest Flow. Low-level cloud lines are seen extending southeastward over the extreme northern Persian Gulf. Cloud lines of this type typically form when cold air streams offshore over warmer water. Due to the channeling of winds by the Persian Gulf, strong, northwesterly winds locally known as the "Winter Shamal", occur frequently. The Winter Shamal sets up following the passage of a migratory low as the tight pressure gradient between the low and the following high-pressure ridge passes over the region. The cloud lines indicate the developing northwest flow over the northern Persian Gulf and the southern limit of the Shamal at this time.

Numeral (4); Interpretation: Displaced Convergence Zone Cloud Band (CZCB). The CZCB is seen south of the southern entrance to the Red Sea. This is displaced well south of its climatological norm (18-20°N) for this time of year. This implies a strong equatorward thrust of mid-latitude westerlies and correlates with the location of a migratory vortex over Iran, south of the normal storm track.

Numerals (5) and (6); Interpretation: Advection Cloudiness over the Red Sea. Cloud lines are seen over the northern Red Sea (5), implying cold air advection over the warm waters. The clouds are being advected over the

western shore (6) with nearly cloud-free conditions over the eastern Red Sea. The western coastal area is lower in elevation, and the strong downslope flow from off the Arabian Peninsula tends to advect the clouds westward. This condition of greater cloudiness over the western coast prevails in all seasons for the Red Sea region. The displacement of the CZCB, and northerly flow over the entire Red Sea provide further evidence of the strong equatorward penetration of polar air.

Numerals (7) and (8); Interpretation: Northeast Monsoon Flow. Clouds are seen along the northern and eastern coasts of Socotra Island (7), implying northeasterly low level flow. Clouds are being advected onshore along the northern coast (8) of the eastern Gulf of Aden. Both of these conditions are expected during the Northeast Monsoon season when the northeast surface winds prevail over the Arabian Sea and extend into the Gulf of Aden as easterly flow. Winds are generally light in both areas.

Numeral (9); Interpretation: Stratiform Clouds over Somalia. Smooth-edged, featureless clouds are seen over Somalia. These clouds are being advected onshore along the Somali coast. This onshore flow is an extension of the northeasterly, low-level flow over the Arabian Sea. There are no shadows seen along the edges of the majority of these clouds, indicating that they are very low. They also appear to have sharply defined edges on the upslope side along terrain features. This "contouring to the terrain" is a common characteristic of stratus and fog. The suppressed vertical motion illustrated by these clouds indicates stable conditions in the lower troposphere in this area.

Numeral (10); Interpretation: Convective Clouds over the Ocean. A band of convective activity extends eastward offshore from Somalia. This is most likely an extension of the northern Near-Equatorial Trough; additional satellite coverage to the south and east is needed for clear definition. The convective activity reflects the warm low-latitude SST with cooler air above. Weak upper-level flow is indicated by the absence of cirrus streamers such as those seen in the Southwest Monsoon examples and near numeral (1).

SUMMARY

In order to optimize the use of satellite imagery, forecasters must develop and apply skills beyond routine recognition of cloud types and patterns. A systematic interpretive approach should be developed that maximizes the information contained in satellite imagery. The approach should be directed toward a synthesis of the data so that a comprehensive three-dimensional picture of the atmosphere is formulated in the mind of the forecaster.

Interpreters must adjust their reasoning and insights relative to cloud features, to the unique perspective of satellites. Imagery must be recognized as a continuous distribution of real cloud information which is far more complete than the symbolic information of conventional surface cloud observations.

Satellite interpretation should be viewed as an extension of our basic understanding of environmental processes. Without a reasonable understanding of these processes, the images become nothing more than nice pictures. On the other hand, after developing a certain level of skill in imagery interpretation, the information conveyed by the images can provide the insights necessary to develop conceptual models of the atmospheric conditions.

Typically, the process is to acquire knowledge of atmospheric processes through study and experience, then relate this knowledge to features in the imagery. The reverse thought process, i.e., deducing the atmospheric conditions from imagery features, will develop surprisingly quickly when imagery must be relied on as a primary data source. In either approach, the recognition of the "big picture", i.e., the synoptic pattern, provides the large-scale forcing to which all smaller-scale imagery features must be related.

END

FILMED